Paleoenvironment reconstruction of the Himalayan region using stable isotopes in lake sediments

Thesis submitted to

Pondicherry University, Puducherry, India

For the award of the degree of

DOCTOR OF PHILOSOPHY

in

EARTH SCIENCES
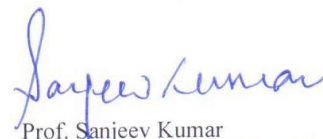
by

Abdur Rahman

Department of Earth Sciences
Pondicherry University,
Chinna Kalapet, Kalapet, Puducherry 605014

May, 2022

CERTIFICATE

This is to certify that the thesis entitled "**Paleoenvironment reconstruction of the Himalayan region using stable isotopes in lake sediments**" submitted to the Pondicherry University for the award of the degree of Doctor of Philosophy in Earth Sciences is a bonafide record of research work carried out by Mr. Abdur Rahman. The thesis or part thereof has not been submitted elsewhere for any other degree or diploma.

Prof. Sanjeev Kumar
(Supervisor)
Physical Research Laboratory
Ahmedabad, India

Place: Physical Research Laboratory, Ahmedabad
Date: 20 MAY 2022

DECLARATION

I, Abdur Rahman, hereby declare that the thesis entitled "**Paleoenvironment reconstruction of the Himalayan region using stable isotopes in lake sediments**" submitted to the Department of Earth Sciences, Pondicherry University (registration date: 28.06.2018) for the award of degree of Doctor of Philosophy in Earth Sciences is a bonafide record of research work performed by me, at Physical Research Laboratory, Ahmedabad, India during the period from July 2016 to September 2021 under the supervision of Prof. Sanjeev Kumar, Geosciences Division, Ahmedabad, India.

I also declare that the thesis represents my independent, original investigation without forming previously part of the material for the award of any Degree, Diploma or any other similar title in any University. Keeping with the general practice in reporting scientific observations, due acknowledgement has been made for technical service and laboratory facilities availed during the course of this study.

Abdur Rahman

Abdur Rahman

(Registration No. 20161110007)

Date: 24th May, 2022

Acknowledgments

I began this adventurous journey five years ago that has now come to an end. A winding road of highs and lows led me to the Himalayan lakes and kick off my scientific career as a Paleoclimatologist. Without the individuals that surrounded me, I could never have anticipated achieving my goals.

My scientific adventure began with my adviser, Prof. Sanjeev Kumar, who I would like to show my sincere gratitude for his appropriate guidance and immense patience during my PhD journey. He has created a welcoming environment in his lab where I could discuss anything at any time. I thank him for giving me the freedom to work on new ideas and encouraging me to learn new things. His positive attitude towards solving scientific problems encouraged me to probe deeper into the subject. His valuable suggestions and critical comments have helped me to improve the scientific outcomes. His constant guidance, inspiration, encouragement, and motivation during this entire period helped me at the time of research and writing of this thesis.

Further, I express my sincere gratitude towards my Doctoral Scientific Committee (DSC) members, Prof. J. S. Ray, Prof. Ravi Bhushan, Dr. Dwijesh Ray, Prof. Dependra Chakrabarty, and Dr. Nurul Absar who have always guided me during my thesis progress and provided constructive remarks to my research work. I am also thankful to the Academic Committee members for their insightful comments and encouragement during my research period. I express my sincere thanks to all the faculties: Dr. Arvind Singh, Dr. Amzad Laskar, Dr. A. D. Shukla, Prof. R. D. Deshpande, Dr. Vineet Goaswami, Prof. Neeraj Rastogi, Dr. A. K. Sudheer and staff members of the Geosciences Division for their assistance in the form of academic and administrative guidance. I express my gratitude to Dr. Navin Juyal for scientific discussions and also for providing the Pipalkoti sediment samples. I owe my thanks to Prof. Ravi Bhushan and Dr. M. G. Yadava for helping me during the radiocarbon dating. I also like to thank Dr. Raees Ahmad shah, for taking immence care of me and providing a homely environment during the Kashmir field work. I also thank to Jani sir, Sangeeta dii, Vaghela uncle and Manoj bhai for their help and support during the lab analyses.

I am very grateful to the Director, Prof. Anil Bhardwaj; Dean, Prof. D. Pallamraju; and Head of Academic Services, Dr. Bhushit Vaishnav for their constant support and assistance during

Abstract

The Himalaya provides an excellent natural laboratory to understand the interactions among different components of the environment due to its geographic and orographic heterogeneity. Despite the significant number of available studies, there remains a large gap in our understanding of the paleoenvironmental condition of the Himalayan region. This thesis attempted to understand some of the unresolved aspects of the paleoenvironmental changes in the Himalayan region, particularly in the westerlies affected central and western Himalaya, by unravelling the temporal evolution of lake biogeochemistry using stable isotopes of carbon and nitrogen.

To achieve the thesis goals, lacustrine sediment samples from five different locations, including two in the central Himalaya (Pipalkoti paleolake and Garud Lake) and three in the western (Kashmir) Himalaya (Forest Bock paleolake, Wular Lake, and Manasbal Lake) covering different time windows in the Quaternary period were analyzed. Taken together, the results obtained from the study revealed environmental and climate history during the last 45 ka of the Himalayan region. The analyzed sediment samples were dated using different dating techniques such as infrared stimulated luminescence (Pipalkoti paleolake), radiocarbon (Forest Block paleolake, Wular Lake, and Manasbal Lake), and ^{210}Pb (Garud Lake). The two paleolake sequences (Pipalkoti and Forest Block) covered 45–29 ka and 33–0.2 ka, respectively; whereas samples from the three live lakes (Wular, Manasbal, and Garud Lakes) covered 3.7–0.3 ka, 3.1–0.4 ka, and 1949–2016 AD, respectively. For the purpose of the study, C and N stable isotopic compositions along with their elemental concentrations in different components of the lake sediments were measured, which included organic carbon ($\delta^{13}C$) and bulk nitrogen ($\delta^{15}N$). Additionally, the carbon isotopic compositions of occluded organic matter within diatom frustules ($\delta^{13}C_{Diatom}$) along with carbon and oxygen isotopic compositions of authigenic carbonates were also analysed in some lake samples. In recent sediment samples, carbon isotopic compositions of black carbon ($\delta^{13}C_{BC}$) were measured to trace the recent fire history of the region.

The stable isotopic records from the central Himalaya suggested a unique wet phase during 40–32 ka, which was also reported from the China and Tibetan plateau region. The possible mechanism behind this wet phase during 40–32 ka might be due to high insolation in the Northern Hemisphere and low Mediterranean Sea surface temperature induced temperature gradient resulting in eastward moisture transport towards the Himalaya. The results obtained also provided evidence for three colder/dry events in the central Himalayan region during 45–29 ka, which coincided with the Heinrich (H5, H4, and H3) events. However, due to lack of better age constraints, the present study refrained from confirming the same in the region and recommended a high-resolution study to refute or endorse this aspect. The analysis of $\delta^{13}C_{Diatom}$ suggested the likelihood of the lake becoming CO_2 enriched during the observed cold/dry periods due to low runoff, which provided minimal bicarbonate from the catchment to the lake. The $\delta^{15}N$ and $\delta^{13}C$ data showed lower productivity during the same period with a relatively increased abundance of C4 plants in the catchment.

The stable isotopic records from the paleolake sequence in the western (Kashmir) Himalaya indicated an increase in lake productivity from the late (28–24 ka) to early (24–19 ka) Last Glacial Maxima, which was due to the weakening of the westerlies. The weakening of the westerlies has been reported due to an increase in the obliquity of the Earth, which decreased the strength of the meridional insolation gradient between northern mid and high latitudes. Additionally, evidence for two colder/drier events were noticed at ~ 29 and ~ 11 ka from this sequence that coincided with the Heinrich (H3) and Younger Dryas events, respectively. During the cold periods, the surface of this high altitude lake was partially covered with ice, resulting in a limited exchange of atmosphere-water CO_2 and nutrient supply, as documented by higher $\delta^{13}C$ and $\delta^{15}N$. During the weakening of westerlies, the temperature of the region enhanced, melting the ice cover, which resulted in the resumption of atmosphere-water CO_2 exchange and nutrient input to the lake surface from the catchment and the hypolimnion.

The stable isotopic records from the live lakes in the western Himalaya indicated two distinct climate phases in the Kashmir region during the late Holocene. These phases included largely drier conditions during 3.7–1.5 ka and wetter conditions during 1.5–0.3 ka. During the dry phase between 3.7 and 1.5 ka, a relatively drier period

during 2.8–1.8 ka with an extreme dry episode at 2.5 ka was noticed through the $\delta^{13}C$ and $\delta^{15}N$ records of the Wular Lake sediment samples. The stable isotopic records of the Manasbal samples also showed drier conditions during 2.8–1.8 ka with no carbonate precipitation around an extreme dry episode of 2.5 ka, which was quite intriguing. Within the wetter phase, a relatively drier event was noticed in the stable isotopic results of both the lakes at ~ 0.6 ka, which coincided with the "Little Ice Age" (LIA). The observed dry and wet phases noticed in the western Himalaya during 3.7–1.5 and 1.5–0.3 ka coincided with the negative and positive North Atlantic Oscillation phases, respectively. The extreme dry episode at 2.5 ka and the LIA also showed a coherency with the North Atlantic Oscillation.

The stable isotopic compositions and elemental ratios of the recent sediment samples from the central Himalaya showed lake biogeochemical evolution under natural and anthropogenic stresses during 1949–2016 AD. A consistent increase in differences between the measured and Suess effect corrected $\delta^{13}C$ of organic matter from the early 1970s to 2016 AD indicated the increased utilization of fossil fuel-induced atmospheric CO_2 by the lake biota. Also, a sudden shift in $\delta^{13}C_{BC}$ in the early 1970s showed an increase in fossil fuel-induced black carbon in the region during that time. Overall, a comparison of the current study with other lakes in the region revealed the effect of land-use change and population growth on the lake biogeochemistry, which was clearly recorded in the stable isotopic records. However, the overall response of each lake depended on the location (distance from the city) and the size of the catchment.

Contents

List of Figures

List of Tables

Abbreviations

‰: Per mil

^{10}Be: 10-Beryllium

^{137}Cs: 137-Caesium

^{14}C: Radiocarbon

^{210}Pb: 210-Lead

^{3}He: 3-Helium

C: Carbon

CO_2: Carbon dioxide

DIC: Dissolve inorganic carbon

GC: Gas chromatography

HCO_3^-: Bicarbonate

IAEA: International Atomic Energy Agency

IRMS: Isotope ratio mass spectrometer

LGM: Last Glacial Maxima

LIA: Little Ice Age

Ma: Mega annum (million year)

MIS: Marine Isotope Stages

N: Nitrogen

NAO: North Atlantic Oscillation

NO_3^-: Nitrate

NH_4^+: Ammonium

TN: Total nitrogen

TOC: Total organic carbon

YD: Younger dryas

$\delta^{13}C$: Carbon isotopic composition of organic matter

$\delta^{13}C_{AC}$: Carbon isotopic composition of the authigenic carbonate

$\delta^{13}C_{BC}$: Carbon isotopic composition of the black carbon

$\delta^{13}C_{Diatom}$: Carbon isotopic composition of the occluded organic matter within diatom

$\delta^{15}N$: Nitrogen isotopic composition of bulk sediment

$\delta^{18}O$: Oxygen isotopic composition

$\delta^{18}O_{AC}$: Oxygen isotopic composition of authigenic carbonate

Chapter 1
Introduction

1.1   Paleoenvironment

Paleoenvironment is simply a study of the past environment of the Earth preserved in various archives such as rocks, sediments, tree rings, and speleothems. In other words, the paleoenvironment refers to the diverse interactions between climate forcings and ocean-land-atmosphere-biosphere-cryosphere dynamics in the past (Mörner, 1995; Jansen et al., 2007; An et al., 2012). Among the external climate forcings, the astronomical cycle was the longest in the timescale that controlled the incoming solar radiation on the Earth and provided the chronometer for the successive major glacial (cold) and interglacial (warm) episodes in geological history (Kershaw et al., 2007; Fernández-Donado et al., 2013; Mörner, 2013). A wide range of internal variabilities arises from climate forcing feedback and responses (Marotzke and Forster, 2015). For example, the melting/retreating of the polar ice sheets affects atmospheric and ocean circulation and modulates the global and regional climate systems. Changes in the environment can also be caused by a variety of factors, including continental positioning, mountain-building episodes (which affect air circulation, atmospheric composition, and provide upland areas for the spread of aerosols in the atmosphere), and changes in atmospheric chemistry, particularly greenhouse gases (Pagani et al., 2005; DeConto et al., 2008; Zachos et al., 2001, 2008). Many processes within the terrestrial biosphere and upper ocean operate over years, decades, and centuries.

Environment-dependent natural processes that incorporate a measure of this dependency into their systems will have a more comprehensive view of climate variability. This natural occurrence serves as a proxy record for the environment and is the foundation of the paleoenvironment. The likelihood of learning the causes and mechanisms of climatic change improved as more detailed and reliable proxy databases of paleoclimate fluctuations were set up. Lake and ocean sediments, tree rings, wind-blown (aeolian) deposits, coral, ice cores, speleothems, and historical records are used

as potential natural repositories for paleoenvironment studies (Choudhary et al., 2012; Dixit et al., 2018; Ali et al., 2020; Amir et al., 2020; Ghosh et al., 2020; Shah et al., 2020). It could be possible to synthesize various records into a detailed explanation of past environmental and climatic fluctuations and their potential triggers using current proxy data (Currás et al., 2012; Bracegirdle et al., 2019).

According to marine and terrestrial proxies, the Quaternary (2.58 Ma – present) was a time of significant environmental change (Kar et al., 2001; Nakamoto et al., 2021), possibly more so than any other time in the previous 60 million years (Ma)(Mudelsee et al., 2014). The marine sedimentary records (particularly oxygen isotopic composition (δ^{18}O) of foraminifera) provide a fascinating glimpse of climate fluctuations such as alternate cold (glacial) and warm (interglacial) climate conditions during the last 2.6 Ma of Earth's history (Imbrie et al., 1984; Imbrie et al., 1993). These cold and warm periods are called the Marine Isotope Stages (MIS). Based on δ^{18}O of shallow downwelling planktonic species of foraminifera (*Globigerinoides sacculifer* and *Globigerina bulloides*) that recorded global climate change, Imbrie et al. (1984) evaluated the Pleistocene ice age orbital theory. It is quite clear that marine proxies from the open ocean majorly provide the global climate information of the past. However, the coastal and terrestrial sediment deposits, which incorporate high sedimentation rates, are better archives to understand the high-resolution global as well as regional climate changes. Because of the distribution of landmasses (topography and geography), the consequences of climate change may not always be observed globally, making climate dynamics more complicated to comprehend. For example, mountainous regions, such as the Himalaya, which are characterised by heterogeneous orography, may or may not record global events throughout their entire stretch, or may be affected by strong regional phenomena. Therefore, to fully comprehend the paleoenvironment in regions like the Himalaya, terrestrial archives such as lake sediments are indispensable.

In the context of the Indian sub-continent, paleoenvironment and paleoclimate studies have been extensively carried out using marine and terrestrial archives (e.g., Krishnaswami et al., 1992; Chauhan et al., 2003; Shekhar et al., 2010; Krishna et al.,

2016; Goes et al., 2020). The trace element geochemistry, stable isotopic composition of carbon and nitrogen ($\delta^{13}C$ and $\delta^{15}N$) and $\delta^{18}O$ of foraminifera in marine sediments from the two adjacent basins, i.e., the Arabian Sea (Altabet et al., 1999; Yu et al., 2019; Lathika et al., 2021) and the Bay of Bengal (Rashid et al., 2011; Achyuthan et al., 2014; Kumar et al., 2018; Kangane et al., 2021) have been widely used to decipher the past monsoonal variabilities in the sub-continent. However, a terrestrial climate system is also strongly influenced by geography and orography. Therefore, marine archives may not provide adequate details about spatial climate heterogeneity. Hence, paleoenvironmental studies using terrestrial archives and proxies from the sub-continent have been carried out to advance our understanding of the regional climate settings (Sinha et al., 2007; Raza et al., 2017; Shah et al., 2020; Rawat et al., 2021; Dhyani et al., 2021). Furthermore, in the mountainous regions like the Himalaya, the heterogeneous orography affects the regional climate and environment, which is documented in many archives such as cave deposits, tree rings, lake sediments, geomorphic features, and sedimentary rocks since its origin around 65 Ma ago. Despite numerous studies, our grasp of the paleoenvironmental condition of the Himalayan region remains less than adequate. In particular, there are limited studies using robust geochemical and isotopic proxies. In this thesis, an attempt has been made to understand some unresolved aspects of the Himalayan past environment, particularly in the western and central Himalaya, at different time scales [MIS 3 (60–30 ka) to present] using stable isotopes in lake sediments. In this context, a brief introduction to the Himalaya, a review of relevant paleoenvironmental studies in the Himalaya, the usefulness of lake sediments in deciphering paleoenvironmental conditions, as well as general lake carbon (C) and nitrogen (N) pools and cycling are discussed below.

1.2 The Great Himalaya

The Himalaya is one of the largest mountain ranges in the world, spanning 2400 km in length and 250–300 km in breadth (Valdiya, 1998). The Himalaya is also home to some of the tallest mountain peaks in the world. Bounded by major faults or thrusts, the Himalayan range has been divided into a few longitudinal zones (from south to north), which are as follows (Fig. 1.1; Gansser, 1981): the Sub-Himalaya between the Main

Frontal Thrust and Main Boundary Thrust, the Lesser Himalaya between the Main Boundary Thrust and Main Central Thrust, the Higher Himalaya between the Main Central Thrust and the South Tibetan Detachment System, and the Tethyan Himalaya between the South Tibetan Detachment System and Indus-Tsangpo Suture Zone. Although not defined strictly, the Himalaya can also be divided into three geographical zones, i.e., the western, central, and eastern Himalaya.

Due to its location and altitude, the Himalaya contains a massive amount of freshwater in a form of ice (glacier) and is also known as the water tower of the southern Asia. Essentially, it acts as a water source to millions of people in India, Bangladesh, and Pakistan. The great Himalaya and Tibetan Plateau are regarded as the Earth's third pole (Bahadur, 1993). They play a crucial role in influencing the weather and climate of the southern Asia and China as well as the global climate system. Both the Himalaya and Tibetan Plateau have long been held as heat source and sink during summer and winter, respectively, which creates cross-equatorial pressure and temperature gradient driving the direct thermal circulation of the Asian monsoon (Yanai et al., 1992; Liu et al., 2012). Two atmospheric circulations, i.e., Indian summer monsoon and westerlies, play a significant role in the Asian monsoon system (Fig. 1.2; Kotlia et al., 2015). The westerlies, which are essentially controlled by the North Atlantic Oscillation, carry heat and moisture from the Mediterranean Sea and the Atlantic Ocean to the Tibetan Plateau and Himalayan region covering western China and northwest India (Lide et al., 2005). In contrast, the Indian summer monsoon carries the Indian Ocean moisture to the peninsular India (Pathak et al., 2017). The central Himalaya experiences the interplay of the Indian summer monsoon and westerlies, depending on the strength of the circulation system (Benn and Owen, 1998; Kotlia et al., 2015).
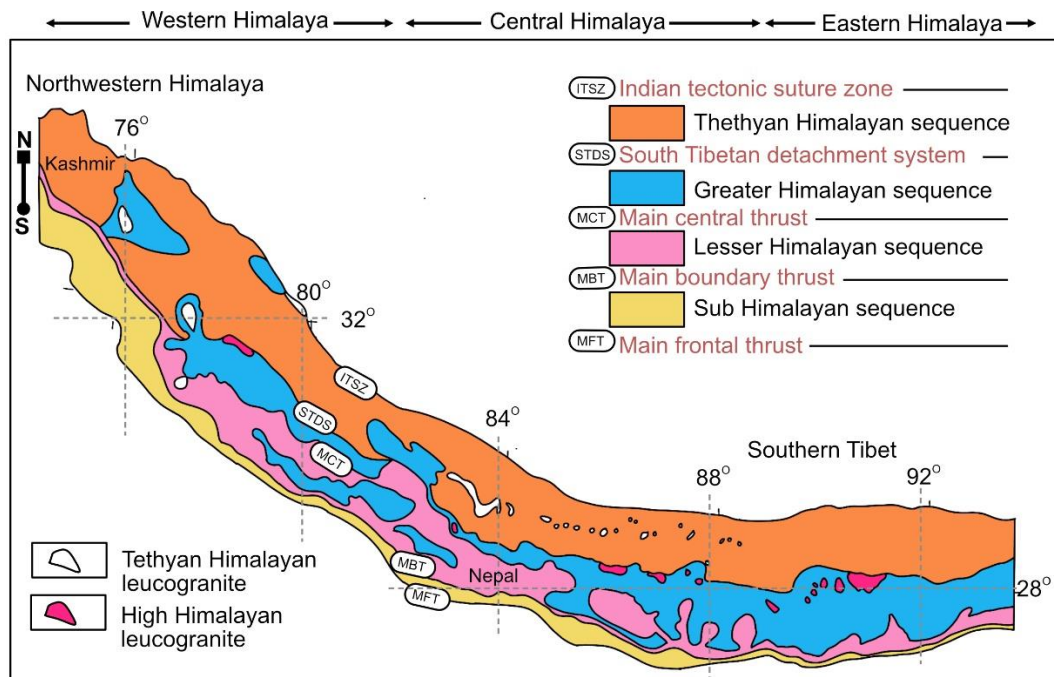
Figure 1.1 Simplified geological map combined with the cross section of the Himalaya.

Digging into the past, various impacts/events have been experienced at different time scales in the Himalayan region due to the direct or indirect impact of climate change. In the past, the Himalaya supported the establishment of various civilizations in the vicinity of their glacial-fed rivers. Also, the Himalaya is currently one of the world's most important biodiversity hotspots, supporting a diverse range of life forms (Mehraj et al., 2018). As mentioned above, the Himalaya is a primary climate driver and exerts an important control on the atmosphere-hydrosphere (cryosphere)-biosphere coupling. Recent and past climate change in the Himalaya is associated with glacial advancement and retreat (Kothyari et al., 2017), changes in vegetation and ecology (Phadtare, 2000; Mampuku et al., 2008; Ali et al., 2020), and montane lake chemistry and biology (Khan et al., 2018; Shah et al., 2020).

1.3   A brief review of the paleoenvironment study in the Himalaya during MIS 3 to present

The teleconnection between global climate and the Himalayan environment has been extensively studied using terrestrial archives and proxies like geomorphic features, lake and soil sediments, loess sediments, tree rings, and speleothems (Ramesh et al., 2013; Ronay et al., 2019; Sun et al., 2020; Banerji et al., 2020; Shah et al., 2020). Based on speleothems $\delta^{18}O$ record, a coherence between the Northern Hemisphere Summer Insolation and Indian monsoon variability during 150 ka of the Himalayan climate history has been reported (Kathayat et al., 2016).

Quaternary climate studies from the Himalaya suggested extensive glacial and enhanced moisture conditions during MIS 3 (60–30 ka) (Phillips et al., 2000; Richards et al., 2001; Owen et al., 2002; Finkel et al., 2003). It has been suggested that the MIS 3 was a period of high insolation and a strong South Asian summer monsoon that penetrated further into the Himalaya (Owen et al., 2002). On the other hand, the geomorphic investigations revealed deglaciation, which was preserved as outwash gravel in the eastern Himalaya (Sarchu Plain) during the pluvial MIS 3. It has also been suggested that glaciers in the path of the westerlies are found in phase with northern latitude glaciation (Sharma et al., 2016). A geomorphic feature-based study from the northwest Himalaya (Baspa valley) suggested humid and wet conditions during the middle stage of MIS 3 followed by intense precipitation in the region during the end phase, which blocked the river course through rock avalanches and imposed lacustrine conditions, which recorded sedimentation until the beginning of Holocene (Dutta et al., 2018). Another study in the central Himalaya (Pindari valley) suggested stage-1 glaciation (out of 5 glaciation stages) during the cold and wet MIS3/4 (Bali et al., 2013). Geochemical proxies-based reconstruction from loess deposits in the Kashmir valley, on the other hand, suggested a warm and dry climate (stadial condition) during MIS 3 (Ali and Achyuthan, 2020); however, this study had very poor age resolution. Taken together, available studies from the western and central Himalaya have shown MIS 3 climate to be largely wet. However, the understanding towards the source of moisture

and high resolution understanding of the paleoenvironment condition of the Himalaya during MIS 3 is less than desirable.
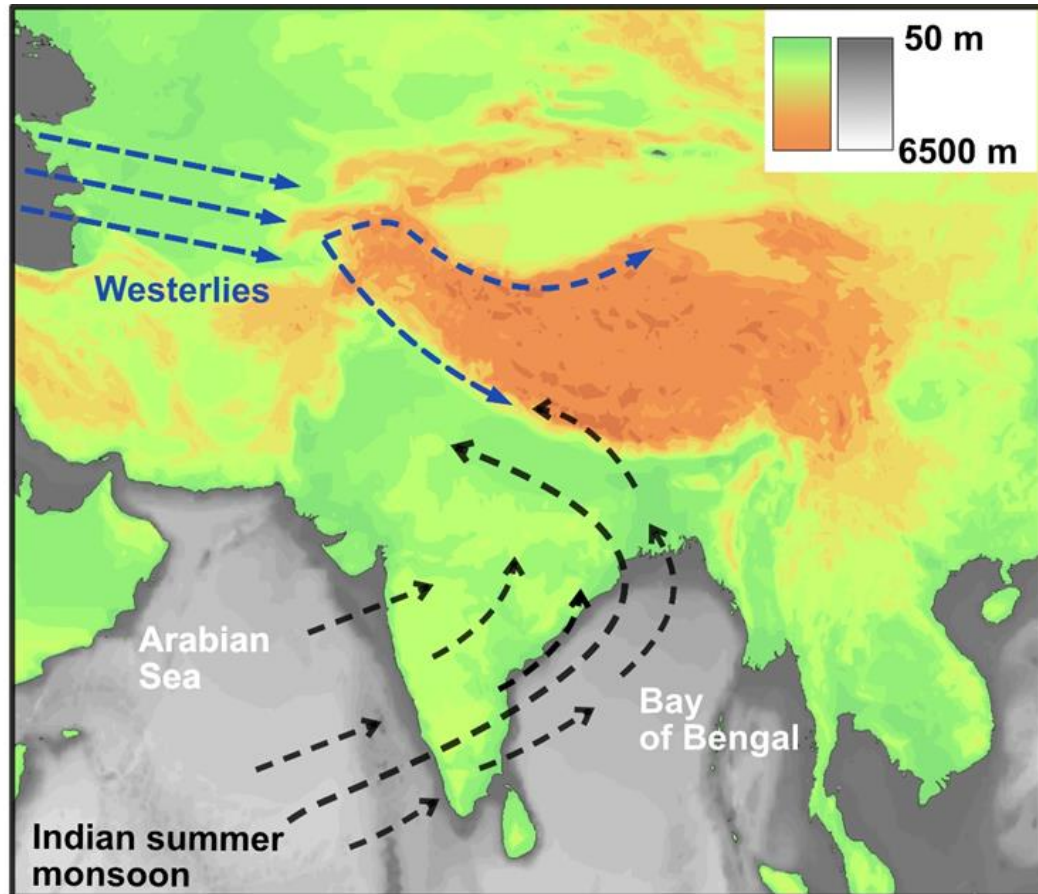
Figure 1.2 Schematic diagram showing dominant atmospheric circulations (westerlies and Indian summer monsoon) in the Indian region, including Himalaya.

Following warming during MIS 3, evidence of a global cooling event, i.e. the last glacial maxima (LGM; 26.5–19 ka), was observed in various parts of the Himalayan region during MIS 2 (29–14 ka). A lag from the globally reported LGM has been noticed in the Himalayan region, leading to debate on the duration and role of moisture sources for glaciation. Also, studies have shown different time ranges of glacial advancement in different parts of the Himalaya. A decrease in insolation was responsible for the low temperature and precipitation in the form of snow in the high-altitude Himalayan region, leading to glacier advancement (Owen et al., 2002). By combining extensive ^{14}C, ^{10}Be, and ^{3}He data, it has been suggested that the growth of the ice sheet was at its maximum between 33.0 and 26.5 ka in the Northern Hemisphere

due to the response of climate forcing caused by a decrease in the northern summer insolation, tropical Pacific sea surface temperature, and atmospheric CO_2 (Clark et al., 2009). After 26.5 ka, almost all ice sheets were at the LGM position up to 19–20 ka. In the Himalayan region, glacial advance from the Annapurna valley has been dated at 28 ± 3 ka using [10]Be; whereas investigations of the Khumbu Himalayan moraine revealed its age to be 25–18 ka (Richards et al., 2000; Zech et al., 2009). Other studies focused on glacial moraines in the Himalaya showed an LGM time range of between 25 and 15 ka (Dortch et al., 2013; Nawaz Ali and Juyal, 2013; Shukla et al., 2018). Speleothems $\delta^{18}O$ records have shown the weakening of atmospheric circulation during the LGM (Kathayat et al., 2017). On the other hand, the $\delta^{13}C$ record of a fluvial-lacustrine section from the Kashmir Himalaya suggested warm and moist conditions at around 25 ka due to the intensification of the Indian summer monsoon (Sanwal et al., 2019). Another study by Juyal et al. (2009) showed moderate to strengthened monsoon conditions around 25.5–22.5 ka, 22–18 ka, 17–16.5 ka, and 14.5–13 ka. A study from China during the LGM period found strong westerlies during 26.5–19 ka and reported extreme climate periods and glacial extensions (Cheng et al., 2021).

In the post-glacial (MIS 2) period, there was an increase in global temperature, which was recorded worldwide in marine and terrestrial archives. However, various extreme and abrupt cooling periods were reported from the Himalayan region during the Holocene (11.7 ka – present), including at 12 ka (Younger Dryas; YD), 8.2 ka, 4.2 ka, 2.8 ka, and the "Little Ice Age (LIA)" (Ali et al., 2013, 2018; Kotlia et al., 2015; Bohra et al., 2017; Ranhotra et al., 2018; Rawat et al., 2015, 2021). A study based on changes in geochemical proxies in a lacustrine trench sediment from the western Himalaya during the Holocene suggested abrupt climate events (cold) in the Kashmir valley during 9–8 ka and 5–4 ka, which was also taken as an indication of lake level fluctuation. Another study related to paleolimnology of a lake in the Kashmir valley showed changes in the lake environment due to the strengthening and weakening of westerlies during the last 6 ka (Lone et al., 2020). A recent study from Ladakh in the western Himalaya has highlighted the interplay of the Indian summer monsoon and westerlies during 4.1–0.26 ka and suggested that the region was dominantly controlled

by westerlies during 4.1–2.6 ka, whereas the Indian summer monsoon was largely controlled from 2.6 to 0.26 ka (Phartiyal et al., 2021). The strength of the Indian summer monsoon and westerlies in the Himalaya during the Holocene period has been extensively studied (Babeesh et al., 2019; Amir et al., 2020; Joshi et al., 2020; Lone et al., 2020; Ghosh et al., 2020; Ali et al., 2020). However, due to orography-induced climatic heterogeneity, the Himalayan regional climate and environment are highly unclear, necessitating comprehensive spatial and temporal paleoenvironment research.

Paleoclimate of the Himalaya has been prominently studied using lake sediments based on magnetic properties of sediments, geochemistry, pollen, diatom, and mineral composition with limited studies using stable isotopes. The C isotopic composition (δ^{13}C) and C/N records from the Mansar Lake sediments, Lesser Himalaya, suggested biogeochemical changes in the lake due to warm and wet climate regime during the early Holocene with cold and dry during the late Holocene period (Das et al., 2010). The geochemical, mineral composition, and aquatic pollen records in the Tso Kar lake sediments (Ladakh, India) revealed maximum glacial advance during LGM and 15 ka with relatively moist summer monsoon around 12.5 ka and during 11.5–8.6 ka (Wünnemann et al., 2010). The lake level started to increase around 11.8 ka followed by a maximum extent between 8.5 and 7.0 ka under warm-moist climate conditions. Afterward, the lake shrank due to weakening in the summer monsoon after 8.0 ka, and it observed its lowest level around 4.2 ka. The δ^{13}C, total organic C (TOC), and pollen analysis in peat-lake sediment sequence from the Chandra valley, Lahaul, northwest Himalaya, revealed the weakening of Indian summer monsoon during 12.8–11.6 ka (YD event), 8.8–8.1 ka, 4.8–4.3 ka (closely preceding the global 4.2 ka cold and arid event), and 1.3–1.6 ka (LIA) (Rawat et al., 2015). The δ^{13}C, C/N, and pollen record in a paleolake sequence from Sangla, Kinnaur, Himachal Pradesh, suggested high lake level between 10 and 4.0 ka with some dry phase ~ 1 ka to finally dry at ~ 0.8 ka (Chakraborty et al., 2006). Using stable isotopes and concentrations of C, N, and S of the organic matter, studies from Kumaun Himalayan lakes showed human influence on lake ecology during the last ~ 100 years (Chaudhary et al., 2009a, 2009b, and 2013). The available studies from the Himalaya have definitely

improved our understanding of the interaction between the environment and climate during the Holocene. However, given its vast stretch, the number of studies carried out, particularly those based on robust geochemical and isotopic approaches, are miniscule and leaves many research gaps in the understanding of regional and global climate events in the region.

1.4   Lakes: potential environmental indicator

According to the most recent count, there are around 117 million lakes in the world, with ~ 5 million km^2 of non-glaciated lake area (Downing et al., 2006; Verpoorter et al., 2014). It is well known that lakes play an important role in the global C and N cycles. Despite being 2% of the world ocean surface area, lakes, along with reservoirs and peatlands, bury three times more C than the world ocean (Dean and Gorham, 1998). Carbon in lake sediment is an effective sink and is highly vulnerable to environmental change (Li et al., 2013; Reed et al., 2018; Steinberger et al., 2021). Similarly, lake organic N also contributes significantly to the global N sequestration (Fields, 2004). The C and N cycles are highly dependent on each other in terms of various biogeochemical processes and oxygen availability (Thornton et al., 2007; Couture et al., 2015). The production of greenhouse gases such as CO_2, CH_4, and N_2O also influences concentrations of C and N pools in lakes and ultimately contributes towards climate change (Elliott et al., 2005). The variation in CO_2 significantly alters the N cycle in the lake ecosystem and vice versa (Hadas et al., 2009; Liu et al., 2018). In a lake, biogeochemical cycles depend on multiple factors such as atmospheric CO_2, nutrient dynamics, catchment geology, topography of the region, and geographical location (Hadas et al., 2009; Gammons et al., 2014). Increases in reactive N, greenhouse gases, and other pollutants like black carbon in the atmosphere caused by fossil fuel combustion, land-use alteration, pesticide overuse, and deforestation have harmed the natural world in recent decades (Baron et al., 2013; Marotta et al., 2014; Heiskanen, 2015; Beaulieu et al., 2019; Wagner et al., 2019).

Lake sediments are an excellent repository for tracking biogeochemical changes as well as associated climate and environmental variabilities over an extended period

(Meyers, 2003; Watanabe et al., 2004; Fan et al., 2017 Chen et al., 2018). These sediments are a mixture of different biotic and abiotic components such as phytoplankton, macrophytes, zooplankton, terrestrially derived and soil organic matter, carbonate (authigenic and biogenic), pollen, clay minerals, and black carbon. Among these components, phytoplankton, zooplankton, carbonate (authigenic) are largely produced within the lake, whereas terrestrial/soil organic matter, black carbon, pollen, and clay minerals are transported from the catchment. In principle, these various components are likely to have distinct stable isotopic signatures that have been widely employed in modern and paleoenvironmental research. Important among these components, whose stable isotopic compositions and contents have also been used during the present thesis are C isotopic composition of organic matter ($\delta^{13}C$), diatom ($\delta^{13}C_{diatom}$), authigenic carbonate ($\delta^{13}C_{AC}$) and black carbon ($\delta^{13}C_{BC}$) along with N isotopic composition of bulk sediments ($\delta^{15}N$) and oxygen isotopic composition of authigenic carbonate ($\delta^{18}O_{AC}$). The usefulness of these proxies and their controlling mechanisms are discussed below.

1.4.1 Lake carbon pools and cycling

The organic matter deposited in a lake could be terrestrially derived or *in-situ* produced (Fig. 1.3). The elemental ratios of total organic carbon (TOC) and total nitrogen (TN) of lake sediments have been used to identify the dominant organic matter source in a lake, i.e., TOC/TN > 20 for terrestrially derived (rich in cellulose) and < 10 for *in-situ* produced (rich in protein) organic matter. If the TOC/TN ratios are > 20, the lake organic matter is likely to reflect the signature of terrestrial plants, which are dominantly of two types, i.e., C3 and C4, having $\delta^{13}C$ values of -22 to $-32‰$ (average $-28‰$) and -9 to $-16‰$ (average $-13‰$), respectively (Isotope, 1989; Schulze et al., 1996). On the other hand, if TOC/TN < 10 it reflects the $\delta^{13}C$ signature of *in-sit*u produced organic matter whose values can range from -20 to $-32‰$ depending largely on the $\delta^{13}C$ of dissolved inorganic carbon (DIC). The DIC in a lake is generally a mixture of atmospheric CO_2 through the atmosphere-water exchange, CO_2 through respiration of organic C, HCO_3^- input through river runoff, conversion of CO_2 into HCO_3^- through carbonic anhydrase, and carbonate dissolution (Berman-Frank et al.,

1994; Cole et al., 1994; Simms, 2002; Gu et al., 2004; Wang et al., 2012). Mainly, all these fractions and processes control the $\delta^{13}C$ of DIC. The modern atmospheric $\delta^{13}C$ value of CO_2 is -8 to $-9‰$, whereas that of HCO_3^- is $\sim 0‰$ (Affek and Yakir, 2014; Wang et al., 2016). The respired CO_2 has the $\delta^{13}C$ value of -28 to $-45‰$ (Karlsson et al., 2007; McCallister and Del Giorgio, 2008). The CO_2 and HCO_3^- play a major role in aquatic photosynthesis and are used by autotrophs to fix C through the Calvin-Benson-Bassham (C3) cycle in the organic body (Farquhar et al., 1989). RubisCO (Ribulose-1,5-bisphosphate carboxylase-oxygenase) plays a major role in fixing the C (preferentially lighter isotope) with the isotopic fractionation of $\sim -29‰$ (Scott et al., 2004; Wilkes and Pearson, 2019). The phytoplankton prefers lighter isotopes (^{12}C) from DIC during the assimilation resulting in lower $\delta^{13}C$ values of the phytoplankton than DIC (Gu et al., 2004). The $\delta^{13}C$ of lake DIC shows a large range, which also plays a role in controlling $\delta^{13}C$ of autotrophs. Input of the terrestrially derived organic matter and soil respired CO_2 into the lake through precipitated runoff water or river stream also affect the lake C biogeochemistry and $\delta^{13}C$ of autotrophs (Jones et al., 2018). For example, terrestrial C loading controls the heterotrophic degradation and oxygen availability in the lake water column and sediment (Strauss and Lamberti, 2000).

One of the prominent C sinks in a lake is carbonate precipitation (authigenic and biogenic) due to bicarbonate super-saturation and through biological precipitation as a shell over the organisms, like gastropods and molluscs (Jin et al., 2004; Cangemi et al., 2016; Wu et al., 2018; Bini et al., 2019; Karami et al., 2019). The carbonate minerals experience great variability concerning water chemistry, catchment geology, climate, and biology of the lake (Golubić et al., 1979; Marcé et al., 2015). The $\delta^{13}C$ of carbonate in a lake, having the signature of DIC, is a valuable tracer of environmentally determined mechanisms that are essentially related to climate change (Schwalb, 2003; Jin et al., 2004).

The C isotopic composition of lake sediment organic matter also depends on the phytoplankton species in the lake, which varies with climate and nutrient conditions. Diatom is one of the prominent microalgae in the aquatic ecosystem (Rühland et al., 2015), which utilizes CO_2 and HCO_3^- as a C source for photosynthesis (Roberts et al.,

2007; Hopkinson et al., 2011; Limoges et al., 2020). Various studies have suggested that the C isotopic signature of occluded C does not alter via decomposition and diagenesis and hence can be used as a prominent proxy to understand the DIC signature of the lake (Shemesh et al., 1995; Hurrell et al., 2011; Webb et al., 2016). It has been shown that the occluded C within diatom frustules preserves the signature of the initial DIC (Crosta and Shemesh, 2002; Webb et al., 2016). The $\delta^{13}C$ of occluded C within diatom frustules ($\delta^{13}C_{Diatom}$) also has the potential to provide detailed information about the effect of geology on the lake C dynamics and the associated climate of the region (Barker et al., 2013; Webb et al., 2016). High $\delta^{13}C_{Diatom}$ has been previously reported from a lake that existed in carbonate terrain and was controlled by variation in weathering of the carbonate rocks (Webb et al., 2016). On the other hand, relatively low $\delta^{13}C_{Diatom}$ has been noticed in non-carbonate terrain. A long-term effect of climate change on $\delta^{13}C_{Diatom}$ has not been well explored. Limited studies are available for $\delta^{13}C_{Diatom}$ as a paleo-carbon biogeochemical proxy. Based on literature and present understanding, it could be hypothesised that changes in $\delta^{13}C_{Diatom}$ in a lake located in carbonate terrain would be possible due to change in climate. In a carbonate terrain, during a shift in climate, e.g., from a warmer/wetter to a colder/drier climate, it might be possible that the $\delta^{13}C_{Diatom}$ would decrease due to limited or no input of HCO_3^- in low runoff conditions and CO_2 would dominate the C pool.
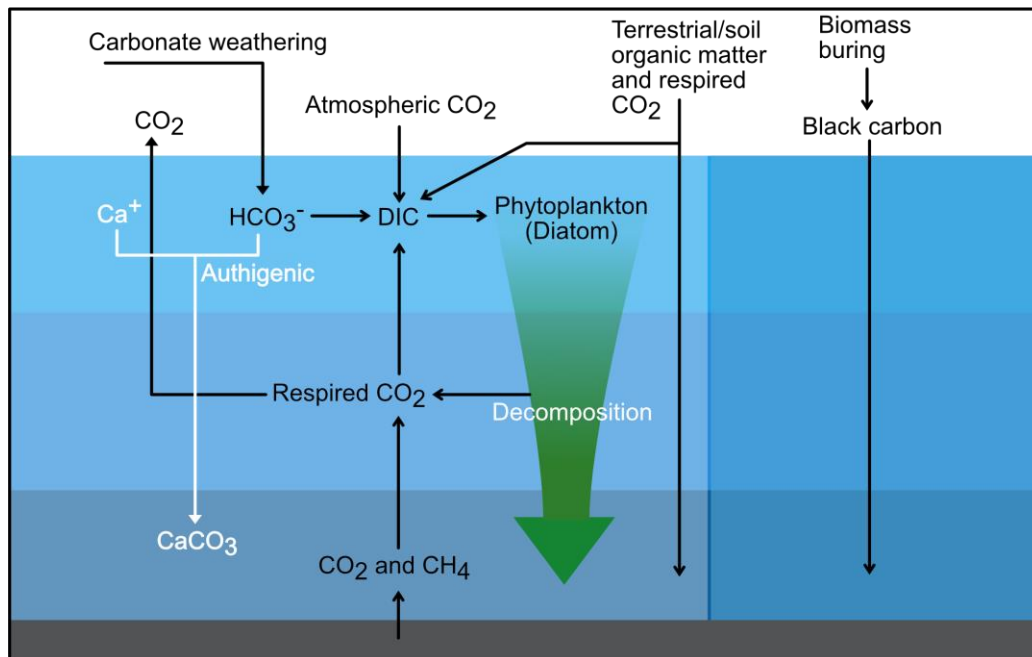
Figure 1.3 Schematic diagram representing a broad overview of various C pools and it's cycling in a lake.

Black carbon, a product of partial combustion of terrestrial biomass, is one of the air pollutants that ends up in lakes and other water bodies (pond, river, and ocean) (Wagner et al., 2018, 2019). The primary source of black carbon is forest fire which directly and indirectly affects the lake ecology and environment through the change in land cover, biodiversity of the region, and chemistry of the catchment soil. It has been reported that (dissolve) black carbon also plays a role in the lake biogeochemical processes (Wagner et al., 2018). After industrialization, the black carbon deposition in lakes has increased many-fold due to fossil fuel combustion and increased forest fire activity (Nair et al., 2013; Wagner et al., 2018). Various studies have shown a change in the depositional rate of black carbon in soils and lakes of the Himalayan and Tibetan region in the last 100 to 200 years (Wagner et al., 2018). Before the industrial revolution, the black carbon deposits in the lake mimicked the $\delta^{13}C$ signature of terrestrial plants, which largely depended on the precipitation, temperature, and atmospheric CO_2.

1.4.2 Lake nitrogen pools and cycling

Nitrogen in a lake is available in both particulate and dissolved organic and inorganic (dissolve inorganic nitrogen; NO_3^- and NH_4^+) forms (Gardner et al., 1987; Voβ and Struck, 1997; Hadas et al., 2009; Sugimoto et al., 2014). Different pools of N are linked and fluctuate over time based on the rates of biogeochemical processes (Fig. 1.4). In general, lake N chemistry is controlled by inflowing waters (which supply the nutrients to the lake), catchment vegetation, and the climate of the region (Agnihotri et al., 2011; Ahmad and Davies, 2017). The lake phytoplankton fixes the inorganic N (such as atmospheric N_2, NO_3^-, and NH_4^+) into the organic body through photosynthesis. The $\delta^{15}N$ of the phytoplankton in a lake depends on the availability of inorganic N and its isotopic composition. If N source for phytoplankton is atmospheric N_2 or soil derived nutrients (NO_3^- and NH_4^+) with low $\delta^{15}N$ contributed through runoff and rain, the $\delta^{15}N$ of the phytoplankton is likely to be low (Watanabe et al., 2004; Hadas et al., 2009; Sugimoto et al., 2014; Liu et al., 2016). On the other hand, if phytoplankton productivity is dependent on nutrient pools that have undergone nitrification and denitrification, probability of $\delta^{15}N$ of the phytoplankton being on an elevated side is relatively higher (Gardner et al., 1987; Hadas et al., 2009; Sugimoto et al., 2014). Lake biogeochemical processes mediated through biology generally result in isotopically lighter product pool, leaving the remaining pool enriched (Hadas et al., 2009; Sugimoto et al., 2014). Therefore, phytoplankton which utilizes these isotopically enriched nutrients, show higher $\delta^{15}N$. Also, in a lake, the primary producers which utilize atmospheric N_2, largely under N limiting conditions (Shatwell and Köhler, 2019) result in lower $\delta^{15}N \sim 0$‰, which is less than those produced through new and regenerated production ($\delta^{15}N \sim 4$ to 6‰) (Montoya et al., 2002; Lehmann et al., 2004).
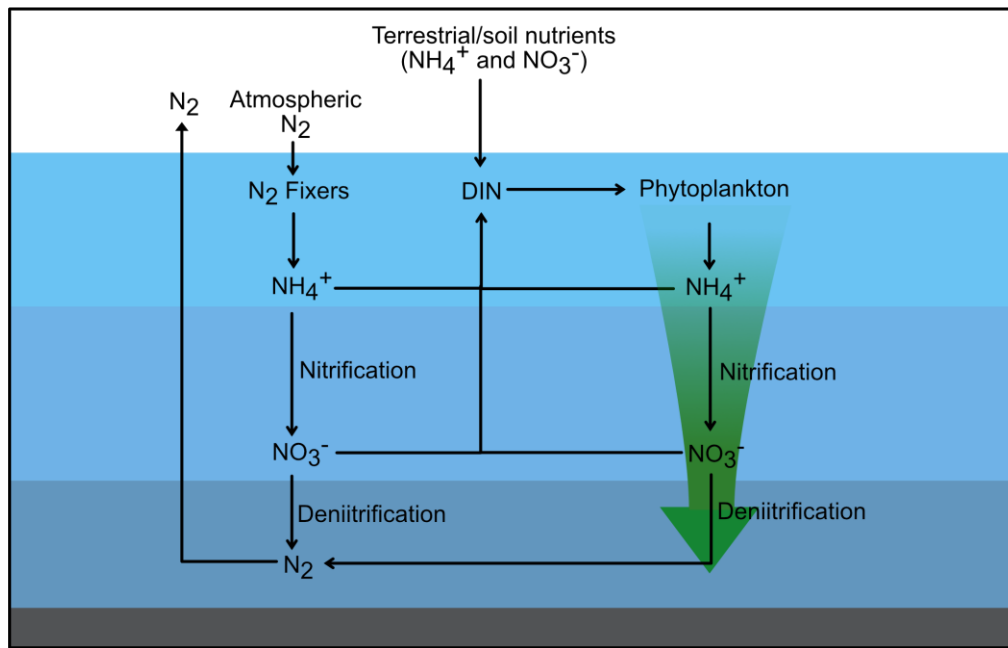
Figure 1.4 Simplified schematic diagram representing various N pools and its cycling in a lake.

The transformation of nutrients from one form to another dominantly depends on the oxygen availability in the lake water column and sediments (Strauss and Lamberti, 2000; Hadas et al., 2009). Nitrification, denitrification, anammox, and dissimilatory nitrate reduction to ammonium (DNRA) are the major biogeochemical processes that control NO_3^- and NH_4^+ concentrations and its isotopic compositions (Petersen et al., 1994; Rysgaard et al., 1994; Gardner et al., 2006). Nitrification is the process in which nitrifying bacteria convert the NH_4^+ to NO_3^- in aerated condition (Small et al., 2013). The $\delta^{15}N$ of NH_4^+ enhances with an increase in nitrification rates (Strauss and Lamberti, 2000; Hadas et al., 2009). Inversely, during the anaerobic condition (high productivity and high terrestrial organic matter input), denitrification becomes a dominant process where NO_3^- gets converted to N_2 as a final product and the lake NO_3^- pool becomes enriched in ^{15}N (Chen et al., 2012).

1.4.3 Paleohydrological reconstruction: oxygen isotopic composition of carbonate

The oxygen isotopic composition of authigenic carbonate ($\delta^{18}O_{AC}$) has the potential to provide information about the hydrological condition of a region, including lake water, evaporation, precipitation, runoff to the lake, and the moisture source of rainfall (Liu et al., 2009; Horton et al., 2016). The $\delta^{18}O$ of carbonate largely depends on the $\delta^{18}O$ of the lake water and temperature of lake surface in which carbonate precipitates. The $\delta^{18}O$ of lake water depends on the source of water which can be glacial meltwater, groundwater, and precipitation/evaporation balance in the region (Leng and Marshall, 2004; Horton et al., 2016). The precipitated water or the moisture is largely derived from evaporating ocean water transported landward through the wind originated by temperature and pressure gradient between the land and sea (An et al., 2012; Kathayat et al., 2017). During evaporation, the lighter water molecules preferentially move to the vapour phase resulting in enrichment of ^{18}O in the remaining water body (Clark, 1997). The precipitation (rainfall or snow) having low $\delta^{18}O$ lowers the $\delta^{18}O$ of the lake water, which further decreases with intense rainfall (Craig et al., 1965; Clark and Fritz, 1997). During its transport from the ocean to the high mountain ranges, such as the Himalaya, vapour mass normally undergoes several precipitation phases resulting in the lower $\delta^{18}O$ of precipitation (Clark and Fritz, 1997; Kumar et al., 2018). In addition, the glacial meltwater (low $\delta^{18}O$) also reduces the $\delta^{18}O$ of the lake water. Finally, changes in the source $\delta^{18}O$ (i.e., lake water) and signatures of associated hydrological conditions get preserved in the $\delta^{18}O$ of carbonate, which is largely used for paleoenvironmental studies worldwide (Jin et al., 2004; Leng and Marshall, 2004).

1.5   Motivation and objectives of the thesis

Using different terrestrial proxies, a significant number of studies have been carried out to understand the past climate and environmental changes in the Himalayan region (e.g., Phillips et al., 2000; Srivastava et al., 2009; Kothyari et al., 2017; Ali et al., 2020; Shah et al., 2020; Ghosh et al., 2020; Rawat et al., 2021). These studies also included understanding of glacial advance and retreat using geomorphological features (Kothyari et al., 2017), weathering conditions using the geochemical signatures of soil

and lake sediments (Bhushan et al., 2018; Rashid and Ganai, 2018; Shah et al., 2020), vegetation change using pollen assemblages and stable C isotopic composition in soil and lake sediments (Phadtare, 2000; Mampuku et al., 2008; Ali et al., 2020), lake productivity using diatom assemblages in the lake sediments (Babeesh et al., 2019; Shah et al., 2021) and their connection to global climate change. However, after all these efforts, there remains a large gap in our understanding of the paleoenvironmental condition of the Himalayan region, particularly in the central and western Himalaya which are westerlies affected regions. Specifically, these gaps include lack of robust high-resolution dataset to identify signatures of the past global climate events in the Himalayan region, change in lake trophic states due to climate change, understanding of the biogeochemical evolution of the Himalayan aquatic systems with time, and availability of paleofire data and its linkage to climate, vegetation, and human interferences. By analysing different components of lake sediments collected from the central and western Himalaya representing diverse regions and time ranges, an attempt has been made to resolve some of the outstanding questions in this thesis. Specific objectives of the thesis are to:

1. Decipher the paleoenvironment of the central Himalayan region during the late MIS 3 and explore the potential imprints of global climate events in the region during that time period.

2. Explore the role of climate and catchment geology on the central Himalayan lake C and N biogeochemistry during late MIS 3.

3. Reconstruct the paleoenvironment of the high altitude region of the Kashmir Himalaya during the last ~ 33 ka with a focus on fluctuations during the Last Glacial Maximum.

4. Understand the paleoenvironment and associated biogeochemical condition of lakes in the Kashmir Valley during late Holocene.

5. Understand the potential of stable isotopic compositions of organic matter and black carbon in modern Himalayan lake sediments as a recorder of anthropogenic footprints.

1.6   Outline of the thesis

The thesis has been divided into six chapters with following contents.

Chapter 1: Introduction

This chapter provides a brief overview about the paleoenvironment and lakes as recorder of environmental conditions. This chapter also contains a summary of previously published research on the Himalayan climate and its connection to the global climate system. Finally, broad and specific objectives of the thesis have also been outlined in this chapter.

Chapter 2: Methodology

This chapter includes a brief overview of analytical techniques and methodologies adopted in the thesis for measurement of stable isotopic compositions of various components of lake sediments (organic matter, bulk sediments, diatom, BC, and carbonate). The dating techniques, i.e., radiocarbon dating, ^{210}Pb dating, and IRSL dating, used in this thesis are also briefly discussed here.

Chapter 3: Paleoenvironment of the central Himalaya

This chapter deals with the paleoenvironment of the central Himalayan region during the late MIS 3 using one of the promising techniques, i.e., C isotopic composition of occluded organic matter within diatom frustules along with C and N isotopic composition of a paleolake sequence. Based on the isotopic signatures, an effort has been made to decipher the evidences for extreme global climatic events in the region. Effect of catchment geology and climate fluctuations on the lake biogeochemistry through time has also been explored in this chapter.

Chapter 4: Paleoenvironment of the Kashmir Himalaya

This chapter is focused on understanding the fluctuations in environmental conditions in the western Himalaya, specifically the Kashmir Himalaya, during ~ 33– 0.2 ka using stable isotopic compositions in different components of lake sediments in cores extracted from three different lakes (one paleolake and two live lakes). An attempt has also been made to decipher the past environmental conditions in the high altitude region as well as the Kashmir valley with focus on the LGM and late Holocene. The biogeochemical evolution of the lacustrine systems of the Kashmir region through time has also been discussed in this chapter.

Chapter 5: Recent environmental record from the central Himalayan Lake

This chapter deals with recent isotopic records from a central Himalayan lake where evidence for natural to anthropogenic transition has been observed using multi-proxy stable isotope systematics. Using the concentrations and isotopic composition of black carbon, the fire event history of the studied region has also been discussed in this chapter. An attempt has been made to interlink human-made changes in the region to that of the lake C and N biogeochemistry.

Chapter 6: Summary and scope of future work

This chapter highlights the significant results of the thesis along with the future scope of paleoenvironmental research in the Himalayan region.

Chapter 2
Methodology

The core objective of this thesis is to understand changes in the paleoenvironmental conditions of the Himalayan region using stable isotopes in different components (organic matter, diatom, black carbon, and authigenic carbonate) of the lake sediment. To fulfil the goals of the thesis, live– and paleo- lake sediment samples were obtained from several Himalayan locations that covered different time ranges of the Quaternary period, and by integrating them, an attempt has been made to understand the poorly understood aspects of the Himalayan paleoenvironment. In this context, a brief description of the sediment core/trench locations, method of sample collection, sample processing, stable isotopic measurements, and dating techniques employed during the thesis have been provided below.

2.1   Study regions

Sediment samples from cores/trenches from five lakes, including two paleo-lakes and three live lakes ranging in age from 45 ka to present, were obtained from different locations in the western and central Himalaya. The details of the study region are described in respective chapters. The names of the lakes from where the sediment samples were obtained, along with locations, coordinates, and altitude are mentioned in Table 2.1 and shown in Fig. 2.1.

Samples from the Pipalkoti paleolake located in the Chamoli district of the Uttarakhand state of India, which lies in the central Himalayan region, were obtained from a 1.41 m long trench of a lacustrine sedimentary sequence (Fig. 2.1). The sequence was subsampled at 1 cm interval for analytical purposes. For the work carried out in this thesis, this sequence was analyzed for $\delta^{13}C$ of organic matter and $\delta^{15}N$ of bulk sediment along with C and N contents at every 1 cm, whereas it was analyzed at every 5 cm for $\delta^{13}C_{diatom}$.

A 4.4 m long paleolake sedimentary sequence was excavated in the Forest Block region of the Gutlibag Hill located in the Ganderbal district of the Union Territory of Jammu and Kashmir, India (Fig. 2.1). The sedimentary sequence was sub-sampled at 2 cm resolution. The elemental (C and N contents) and isotopic analyses (δ^{13}C of organic matter and δ^{15}N of bulk sediment) were performed in every alternate sample.

One sediment core each from the Wular and Manasbal Lakes in the Kashmir Valley of the Union Territory of Jammu and Kashmir, India (Fig. 2.1 and 2.2) was obtained using PVC corer. The cores from the Wular and Manasbal were 2.4 and 1.8 m long, respectively, which were sub-sampled at 2 cm intervals. All the samples obtained from the Wular Lake were analysed for elemental (C and N contents) and isotopic analyses (δ^{13}C of organic matter and δ^{15}N of bulk sediment). The samples from Manasbal Lake were analyzed for δ^{15}N of bulk sediment, $\delta^{13}C_{diatoms}$, δ^{13}C and δ^{18}O of authigenic carbonate. This analytical strategy was adopted based on the location and differences in catchment lithology of the lakes.

Table 2.1 The names of the studied paleo- and live-lakes with their locations, coordinate, altitude, and annual precipitation

Lakes	Location	Coordinate (lat, long)	Altitude (m)	Annual Precipitation (mm)
Pipalkoti Paleolake	Chamoli, Uttarakhand	30°27'–30°25'N, 79°24'–79°26'E	1259	1670
Forest Block Paleolake	Ganderbal, Kashmir	30°13'46"N 74°52'07" E	3300	693
Wular Lake	Bandipura, Kashmir	30°21'57" N, 74°33'30"E	1580	693
Manasbal Lake	Ganderbal, Kashmir	30°14'48" N, 74°40'17"E	1583	693
Garud Lake	Nainital, Uttarakhand	29°21'24" N, 79°31'52"E	1370	1636

The sediment core from the Garud Lake, located in the Nainital district of the Uttarakhand state of India, was collected to study recent lacustrine records to unravel natural to anthropogenic transition in the central Himalaya (Fig. 2.1). For this purpose, a 58 cm long core was collected using hammer corer and was subsampled at every 1

cm interval. For this study, elemental (C and N contents) and isotopic analyses ($\delta^{13}C$ of organic matter and $\delta^{15}N$ of bulk sediment) were performed in every alternate sample. Analyses for black carbon contents and its isotopic compositions were performed in the same samples or samples in-between, depending upon its availability.
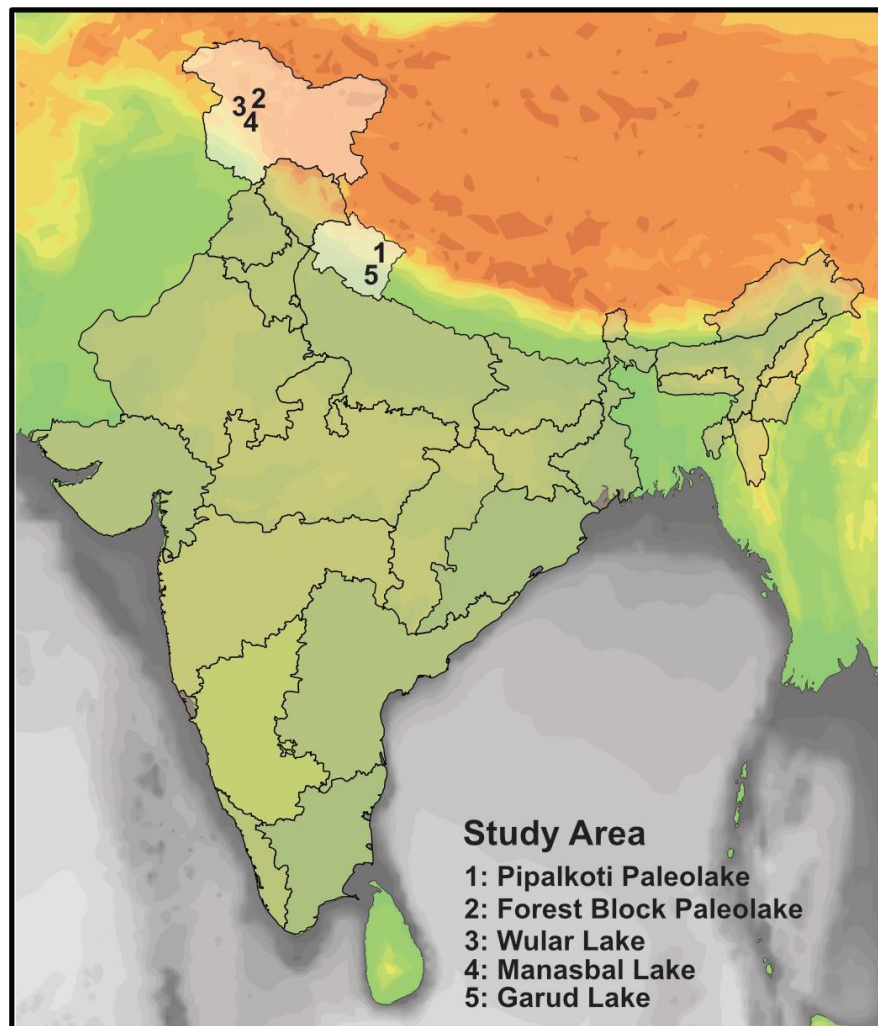
Figure 2.1 Map showing the study locations in the western and central Himalayan region.

Figure 2.2 Field photograph from the Kashmir Valley (a) Forest Block region, (b) core collection from the Manasbal Lake, (c) exploration of the Manasbal Lake for core collection, and (d) Wular Lake.

2.2   Sample processing

As stated previously, stable isotopic compositions of different components of lake sediments formed the primary tool to understand the Himalayan paleoenvironment. Before the mass spectrometric analyses for stable isotopic compositions, collected sediment samples were processed to purify for respective components/measurements following standard protocols, which are briefly discussed below.

2.2.1 Total organic carbon and total nitrogen

For TOC contents and its C isotopic compositions, sediment samples were powdered and treated with HCl at 80 °C for 24–60 h to remove the carbonates (calcite and dolomite) (Froehlich, 1980; Hedges and Stern, 1984). The treated samples were centrifuged and rinsed with ultrapure water three times at 1500 rpm to neutralize the acid. Subsequently, the samples were dried in an oven at 60 °C for moisture removal. This technique has been applied in each core for organic C purification. Measurements for N contents and their isotopic compositions were performed in bulk sediment samples without any acid treatment.

2.2.2 Diatom purification

For C isotopic composition of occluded organic matter within diatom frustules, the protocol of Morley et al. (2004) modified after Hurrell et al. (2011) was followed where samples were treated with 1M HCl to remove carbonates followed by treatment with 30% H_2O_2 and HNO_3 to remove organic matter. Subsequently, samples were sieved at 10 and 80 μm to remove large clay particles from the sediments. The sieved material was then treated with sodium polytungstate (density 2.1 g/cc) for density separation, where diatom cells floating in the sodium polytungstate solution were separated and washed for mass spectrometric analysis. This technique was used to purify the diatom from Pipalkoti and Manasbal core sediments.

2.2.3 Black carbon

The black carbon from the Garud Lake sediments was extracted following the chemical method developed by Lim and Cachier (1996). For this purpose, the lake sediments were treated with 3M HCl to remove the carbonate from the samples and then centrifuged 3 to 4 times with ultrapure water. Further, the samples were treated with 10M HF/1M HCl to remove silicates and centrifuged 3 to 4 times with ultrapure water to neutralize them. Subsequently, samples were treated with 0.1M $K_2Cr_2O_7$/2M H_2SO_4 at 55 ºC for 60 hours to remove the organic matter from the samples. The residue samples were black carbon, which included charcoal and atmospheric black carbon particles. During the chemical treatment, glass vials containing some samples broke

leading to partial loss of samples. However, in these samples, enough amount could be retrieved for isotopic analyses but exact black carbon concentrations could not be calculated.

2.2.4   Authigenic carbonate

For the carbon and oxygen isotopic compositions of authigenic carbonate in the Manasbal Lake sediments, the samples were oxidised to remove organic fraction using H_2O_2. Subsequently, the samples were washed with ultrapure water and sieved at 80 μm (Lamb et al., 2000) to remove the larger biogenic carbonate shells. The sieved samples were dried in an oven at 60 °C for 24 hours for carbon and oxygen isotope analysis.

2.3   Instrumentation

Following sample preparation, a variety of instruments, including an Elemental Analyzer (Thermo Fisher Scientific - Flash 2000) and a GasBench II (Thermo Fisher Scientific) interfaced with isotope ratio mass spectrometers (Thermo Fisher Scientific - Delta V plus and MAT 253), were utilized to determine the stable isotopic compositions of the aforementioned lake sediment components. All the analytical measurements during this thesis were performed at the Geosciences-Stable Isotopes Laboratory (GeoSIL) at the Physical Research Laboratory, Ahmedabad, India (Fig. 2.3). The brief details about these instruments are discussed below.

2.3.1   Isotope ratio mass spectrometer (IRMS)

The isotope ratio mass spectrometer (IRMS) is a widely used instrument in various disciplines. This instrument works on the principle of the measurement of mass/charge ratio and has three main components, i.e., (i) ion source, (ii) magnetic analyzer, and (iii) detector. The ion source ionizes the gases and accelerates them to the magnetic analyzer where they get deflected according to their respective mass/charge ratios. Finally, these ionized gases hit the Faraday cup and produce the electric signal to be converted into the isotopic ratios of the samples.

For mass spectrometric analyses using IRMS, samples in any form are converted into gaseous form for which several external peripherals are utilized. During this thesis, peripherals such as Elemental Analyzer and GasBench attached to IRMS were used, which are briefly described below.

Figure 2.3 Photograph of the Geosciences-Stable Isotope Laboratory (GeoSIL), Physical Research Laboratory, Ahmedabad, India. Name of the available facilities in the GeoSIL are marked in the photograph.

2.3.2 External peripherals

A. Elemental Analyzer

The contents and stable isotopic compositions of C in organic matter, diatom frustules, and black carbon, along with N contents and its isotopic compositions in bulk sediments were measured using an IRMS (Delta V plus) interfaced to an Elemental Analyzer via ConFlo IV (Fig. 2.4a).

During these analyses, known amount of samples, tightly packed in tin capsules were dropped into a quartz tube containing chromium oxide and silver cobaltous oxide to get combusted in the presence of highly pure oxygen at high temperature (1020 °C). The released gases, such as carbon dioxide and oxides of nitrogen, were then carried through by a carrier gas (Helium) into a reduction column containing pure copper

granules, where oxides of nitrogen got reduced to N_2. After passing through a moisture trap, the resultant gases were separated by the gas chromatographic (GC) column based on their retention time to be injected into the IRMS for analyses. A schematic diagram of the Elemental Analyzer and pathway of gases are shown in Fig. 2.4b.

B. GasBench II

A GasBench attached to an IRMS (Thermo Fisher Scientific MAT 253) was used for carbonate isotopic measurements (Fig. 2.5). To convert the carbonate samples into CO_2, the samples were put into Labco exetainer vials and flushed with highly pure Helium gas to avoid atmospheric CO_2 contamination. Subsequently, the flushed vials were injected with 100% phosphoric acid and heated at 72 °C for 1 hour. Afterwards, the CO_2 produced moved through the GasBench to the IRMS for C and O isotopic measurements. A brief overview of the GasBench, which has two main components, is provided below (Fig. 2.5).

I. A sample introduction system (sample tray)

The sample tray of GasBench is a cuboid-shaped container that can hold 96 samples by arranging 12 ml vials in a row and a column (8×12). The temperature of the sample tray can be regulated depending on the kind of sample (carbonate or water sample). The tray temperature for carbonate samples was set at 72 ($\pm$ 0.5) °C.

II. GasBench (GC column)

The gas that has been released or equilibrated with the samples is transported to the GasBench, which may also include water vapour, which is removed using a gastight but hygroscopic Nafion® tube. The generated dry gas is sent to the Valco 6 port loop and subsequently to the GC column. These gases eluting from the GC column enter the IRMS (MAT 253 for carbonate during this thesis) via an open split in the Nafion® guard trap.
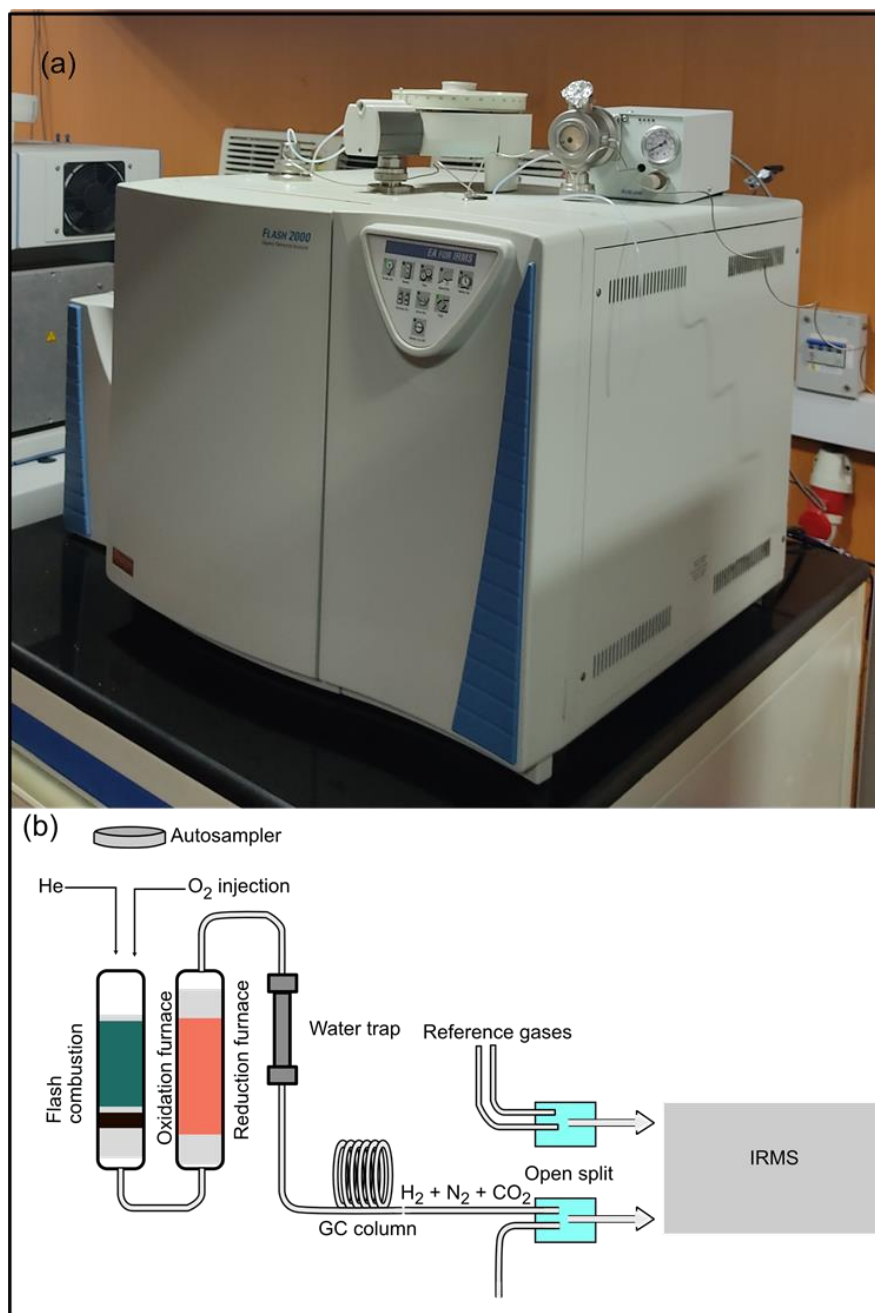
Figure 2.4 (a) Photograph of the Elemental Analyzer used for analysis and (b) simplified schematic diagram and pathways of gases in the Elemental Analyzer. Source: Thermo Fisher Scientific manual.
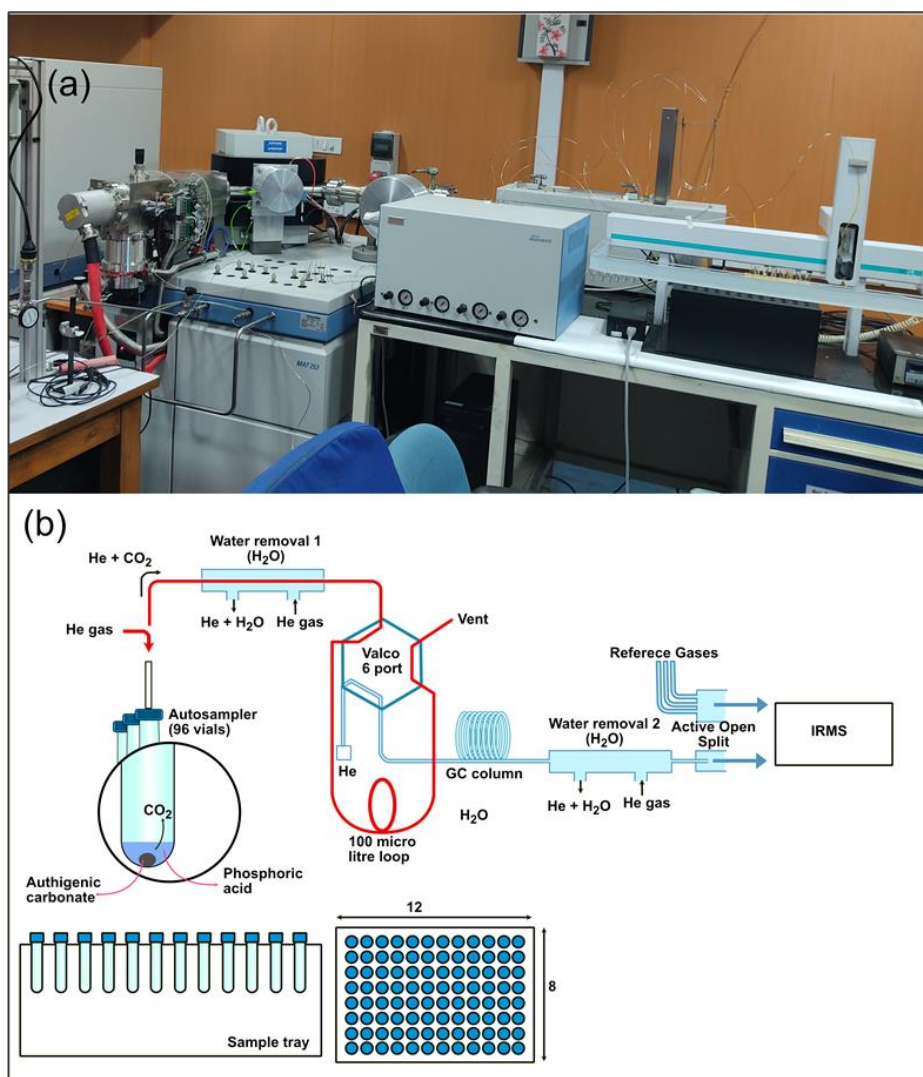
Figure 2.5 (a) Photograph of the GasBench used during the analysis and (b) schematic diagram of the GasBench and pathways of CO_2 from GasBench to IRMS. Source: Thermo Fisher Scientific manual.

2.4 Elemental and isotopic measurements and precision

The C and N contents in sediment samples were measured using standard procedure, where calibration curves were generated using known amount of C and N in standards and total area under the curve for respective masses (CO_2 and N_2) obtained using mass spectrometer (Kumar et al., 2005). For this purpose, cellulose (IAEA-CH3; C content = 44.44%), ammonium sulfate (IAEA N2; N content = 21.2%) and protein (IVA-OAS; C content = 46.5 % and N content = 13.32%) were used during this thesis. Upon generation of calibration curve, known amounts of samples were analyzed to obtain the

C and N contents, i.e., % C and % N, in samples. The analytical precisions for C and N contents for repeat measurements were better than 10%.

For C and N isotopic measurements, cellulose (IAEA-CH-3; $\delta^{13}C = -24.72 \pm 0.04‰$) and ammonium sulphate (IAEA-N2; $\delta^{15}N = 20.3 \pm 0.2‰$) were primarily used as standards. Protein (IVA-OAS; $\delta^{15}N = 5.94 \pm 0.08‰$) was also used during N isotopic analyses to track the instrumental precision. Blank correction was also performed in samples containing less than 2 micromole of N. Altogether, during this thesis work, more than 100 runs of standards were performed. The analytical precisions during each run or altogether were less than 0.1 and 0.3‰ for C and N isotopic compositions, respectively. The C isotopic compositions in this thesis are reported with respect to Vienna Pee Dee belemnite (VPDB), whereas N isotopic compositions are reported with respect to atmospheric N_2.

For carbonate C and O isotopic composition measurements in carbonate, the MMB (Makrana marble) was used as a laboratory standard. The $\delta^{13}C$ and $\delta^{18}O$ values of the MMB with respect to VPDB are $-3.9‰$ and $-10.7‰$, respectively, which was calibrated with respect to the International Atomic Energy Agency procured NBS-19 ($\delta^{13}C_{VPDB} = 1.95‰$ and $\delta^{18}O_{VPDB} = -2.20‰$). The $\delta^{13}C$ and $\delta^{18}O$ of carbonate reported in this thesis are with respect to VPDB. The analytical precisions for both C and O isotopic measurements of carbonates during this thesis work were better than 0.1‰.

2.5   Chronology

The chronology of lake sediment samples is an essential aspect of paleoclimate research as it provides the actual and relative ages of the samples through which the temporal climate and environmental information are obtained. Among various dating techniques for chronology construction, this thesis has used luminescence (Infrared Stimulated Luminescence), radiocarbon, and ^{210}Pb and ^{137}Cs dating techniques to determine the ages of lake sediment samples. The chronology for the Pipalkoti paleolake sediments in the central Himalaya was established using Infrared Stimulated Luminescence dating technique. These ages were measured by Dr. Navin Juyal of the Physical Research Laboratory, Ahmedabad, India, and one of these ages has been reported earlier (Juyal

et al., 2010). Radiocarbon technique was used for the chronology establishment of the samples from the Kashmir Himalaya, including Forest Block, Wular Lake, and Manasbal Lake. The ^{210}Pb and ^{137}Cs dating technique was used for the Garud Lake samples in the central Himalaya. The details of the above-mentioned techniques are explained below.

2.5.1 Infrared Stimulated Luminescence (IRSL) Dating

In this study, Infrared Stimulated Luminescence (IRSL) dating was used to estimate the chronology of the Pipalkoti paleolake samples. The dating was performed by Dr. Navin Juyal at the Physical Research Laboratory (PRL), Ahmedabad, India. The ages obtained are based on clay-rich lake sediment where multiple aliquots additive dose method using IRSL technique on fine-grained feldspar was employed (Singhvi et al., 2001). The general protocol used in the lab for IRSL dating is as follows.

The samples are collected in sealed metal tubes after cleaning the few cm of trench/section. The samples are kept in dark till it reaches the lab, where they are opened and processed under the subdued red light. The upper 3 cm of samples are used for moisture content and radioactivity analysis. The remaining inner portion of the samples are treated with HCl for 24 hours to remove carbonate fractions. The decarbonated samples are treated with 40% Hydrogen Peroxide (H_2O_2) for 12 hours to remove organic materials (Wintle, 1997). The samples are sieved between mesh size 90 and 150 µm. Further, between 90 and 150 µm of grain size, quartz and feldspar are separated using a Frantz® magnetic separator. After the separation of the feldspar grains, these grains are etched with 10% hydrofluoric (HF) acid for 10 minutes to remove the alpha irradiated skin (Goedicke, 1984; Porat et al., 2015; Duval et al., 2018). After HF etching, feldspar grains are treated with concentrated HCl (37%) for 30 minutes to dissolve the residual fluorides. Measurements are carried out on single grain discs in single aliquot mode. In this, feldspar grains are mounted on discs containing 100 holes. Grains are stimulated using Infrared (IR) LEDs in a Risø TL/OSL DA-20 reader (Bøtter-Jensen et al., 2003). The wavelength of IR LEDs peaks at 850 ± 30 nm. The detection of emitted luminescence is done in the blue window using BG-39 and BG-3

filter combination. The post IR-IRSL Single Aliquot regeneration (p-IRIRSL SAR) protocol is used for the estimation of paleo-dose (De) (Buylaert et al., 2009).

The concentration of Uranium (U) and Thorium (Th) nuclides are also measured using ZnS (Ag) thick source alpha counter and Potassium (K) concentration is measured using NaI (Th) gamma counter. Further, these concentrations are used to estimate the total dose rate assuming infinite matrix assumption, and secular equilibrium for all the nuclides. Using the paleodose and dose rate, age of the samples are obtained.

2.5.2 Radiocarbon dating

The age of samples using the radiocarbon dating method is estimated by measuring the concentration of radioactive carbon (^{14}C) against its known half-life (Arnold and Libby 1949; Libby et al., 1949; Hua, 2009). The principle of radiocarbon dating is the balance between continuous production of ^{14}C in the atmosphere due to high energy cosmic ray interaction with the ^{14}N and losses due to radioactive decay. The newly formed ^{14}C in the atmosphere oxidizes and produces ^{14}CO$_2$, which mixes with atmospheric CO$_2$. It is constantly transferred to the living beings of C reservoirs such as animals, plants, and microbes in various ecosystems. When these lives are severed of exchange processes from the atmosphere by death, the ^{14}C in these beings begins to degrade with a half-life of 5730 years to ^{14}N.

The current ratio of ^{14}C/^{12}C and the half-life of ^{14}C helps to determine the ages. The specific activity in pre-industrial times was 13.56 dpm (g C)$^{-1}$ (dpm represents the decay per minute), which is taken as a reference value for modern activity. To estimate the ^{14}C/^{12}C ratio in milligram level of C in samples, Accelerator Mass Spectrometer (AMS), a highly sensitive instrument is used (Bhushan et al., 2019). By using this method, the age of samples dating 50,000–55,000 (8 to 10 half-lives) years back in time can be estimated. Radiocarbon dating using AMS is carried out in the two-step process:

Graphitization

For AMS, to create a stable ion beam with negligible memory effect in the ion source chamber, C in the form of graphite (elemental C) is required. Therefore, the organic matter samples to be dated using the AMS must be transformed into graphite. To produce graphite, the organic matter must be thermally oxidized into pure CO_2. Before graphitization, the organic samples need to be decarbonated and subsequently converted to pure CO_2. During this thesis, for conversion of organic matter to pure CO_2, a specially designed glass line developed at the Radiocarbon Laboratory, Physical Research Laboratory, Ahmedabad, India, was used (Fig. 2.6). To achieve the measurable C content required for the AMS measurements, the samples were accordingly weighed and transferred to a pre-cleaned and pre-combusted (400 ℃) dry sample reaction tube and combusted in a vacuum glass line at ~ 1000 ℃ to extract CO_2 gas. The extracted CO_2 gas was purified by pasing through multiple steps in a vacuum glass line using liquid nitrogen. While the CO_2 was frozen, all other gases generated, if any, were pumped out.

For AMS dating, the extracted CO_2 was reduced to graphite by heating in the presence of catalyst iron powder (~ 4 mg) at 600 ℃ and Zn (~ 20 mg) in an adjacent connected tube at 450 ℃ to form ZnO. The CO_2 precipitated on the catalyst iron powder as elemental C (graphite form) was used for dating. The graphitization system at the Radiocarbon Laboratory used during this study is shown in Fig. 2.7.
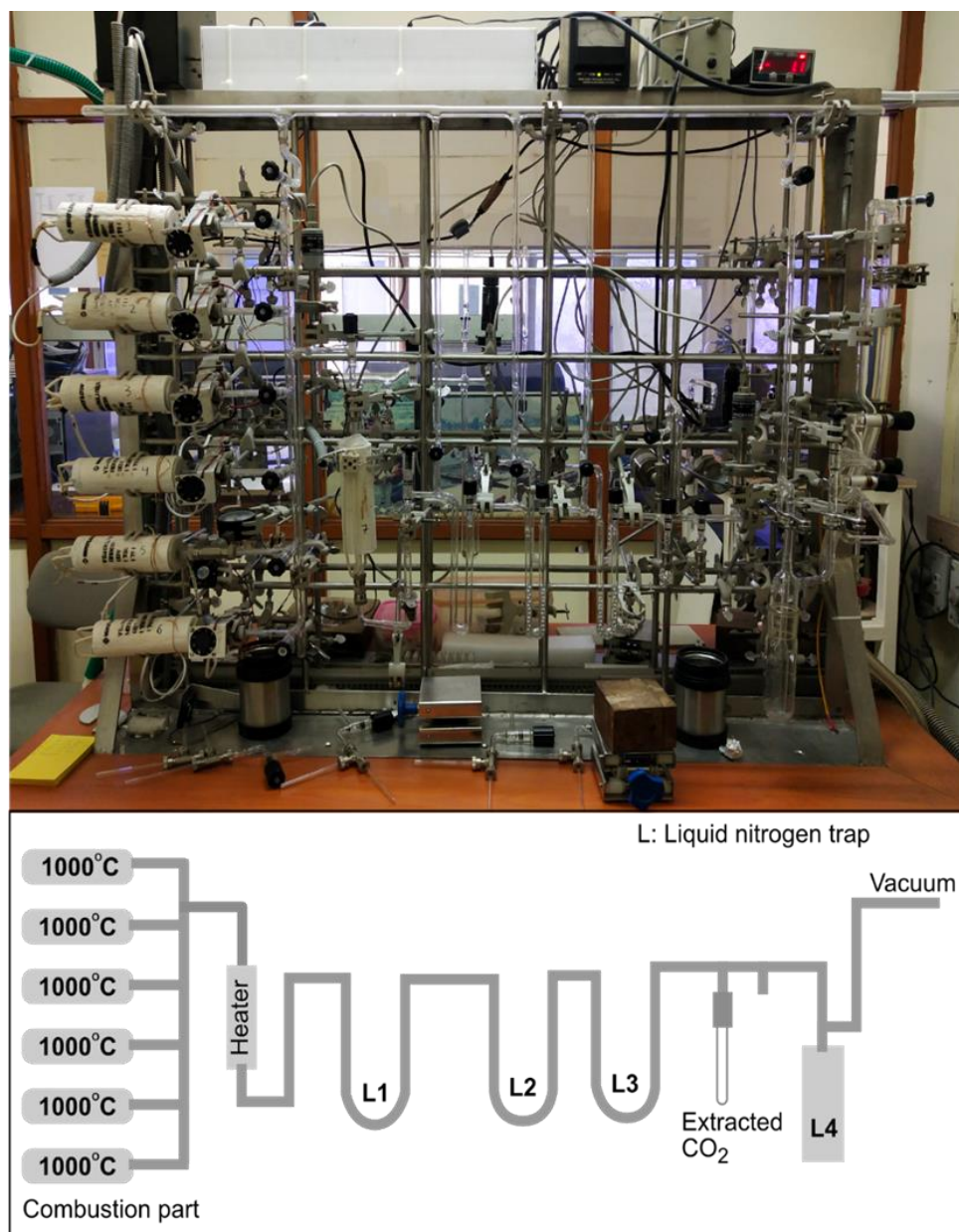
Figure 2.6 CO_2 preparation line for organic matter samples at the Radiocarbon Laboratory, Physical Research Laboratory, Ahmedabad.

Figure 2.7 Graphitization system for extracted CO_2 at the Radiocarbon Laboratory, Physical Research Laboratory, Ahmedabad, India.

^{14}C measurement by AMS

The concentration of $^{14}C/^{12}C$ (also $^{13}C/^{12}C$) in a sample is measured by the AMS. The advantage of AMS lies in the small amount of C (~ 0.3 mg to 1 mg C) required for measurements with high precision results in a reasonable time.

For the present work, the prepared graphite samples were pressed into a target (a cylindrical cavity of an aluminum holder), which were mounted in the sample carousel located in the AMS source to be evacuated later to a high vacuum level (10^{-5} to 10^{-6} mbar). In a single run during the analysis, about 50 targets can be mounted in the carousel, including targets prepared for samples and standards. The international standards [OXALIC ACID – I (OX-I) and OXALIC ACID – II (OX –II)] were used for estimating modern values. Similarly, for background, laboratory standards of anthracite and marble materials were used.

In the present study, the ^{14}C ages were calibrated using IntCal 13 atmospheric curves (Reimer et al., 2013) in OxCal v 4.3.2 (Bronk Ramsey, 2017) without any reservoir corrections or hard water correction. The age-depth model was also generated

using the same software. The unit of the radiocarbon age is expressed in Cal year Before Present (BP: 1950); however, in this thesis, to maintain consistency of age-units, the radiocarbon ages, i.e., Cal ka BP, have been reported as "ka."

2.5.3. ^{210}Pb and ^{137}Cs dating

Importance and principle

Pb-210 (^{210}Pb): The radioactive decay of ^{222}Rn and ^{210}Pb are used to estimate the age of ^{210}Pb geochronology. Because of its short half-life (22.3 years; Hohndorf, 1969), this approach is commonly employed to estimate the sedimentation rate during the last century in limnology, marine, palynological, and glaciological research (Binford and Brenner, 1986). The utility of the ^{210}Pb dating technique is maximized when used in conjunction with ^{137}Cs chronology.

The ^{210}Pb dating methodology is based on the radioactive decay principle; ^{210}Pb is a mid-product of the ^{238}U decay chain, which comprises of daughter elements of radium (^{226}Ra), radon (^{222}Rn), lead (^{210}Pb), bismuth (^{210}Bi), and ultimately a stable isotope of lead (^{206}Pb). Due to the short half-life of ^{210}Pb and its production in the atmosphere and the Earth along with its availability in all sediments and close sedimentary environment, this dating approach is almost indispensable in Quaternary geochronology.

The atmospheric production of ^{210}Pb involves ^{222}Rn (specifically gas) with a half-life of 3 days. The ^{222}Rn is produced in the Earth and escapes to the atmosphere, where it undergoes decay through four daughter products, including solid ^{210}Pb. The solid ^{210}Pb settles from the atmosphere through dry deposition or scavenging by rainwater to the lake and marine systems, where it bounds with the organic matter and deposits. The ^{210}Pb produced in the atmosphere and deposited in the lake is known as supported ^{210}Pb (Goldberg, 1963). After deposition, ^{210}Pb is assumed to be immobile and spontaneously decays to ^{210}Ra. On the other hand, the ^{210}Pb is also produced by in situ decay of ^{222}Rn gas within the sediments, which is referred to as unsupported ^{210}Pb (Goldberg 1963).

Caesium-137 (^{137}Cs): Over the last few decades, ^{137}Cs has been extensively used for estimation of age in soils, lakes, and marine sediments (Ritchie and McHenry, 1990).

The ^{137}Cs is an artificial radionuclide with a half-life of ~ 30.2 years, most of which was produced by the above-ground thermonuclear weapon testing in the 1950s and 1960s (Zapata, 2002). The ^{137}Cs was ejected to the stratosphere and circulated globally. The ^{137}Cs fallout on the land surface was first recorded in the early 1950s and was primarily associated with precipitation (Ioannidou and Papastefanou, 2006). Due to more atmospheric nuclear testing in the northern hemisphere, the ^{137}Cs fallout was greater there, with the greatest effect in the lower latitudes. A peak of fallout in 1963 was reported from a different regions of the world (Norris and Arkin, 1996). Afterward, apart from the Chernobyl accident in 1986, a negligible amount of ^{137}Cs fallout has been observed since the mid-1980s (Norris and Arkin, 1996). Due to its strong association with surficial sediments, the ^{137}Cs is widely used for dating and tracing purposes.

^{210}Pb and ^{137}Cs dating method

During this thesis, the sedimentation rate in the Garud Lake was estimated using ^{210}Pb and ^{137}Cs. For this purpose, ~ 3 gm of dried and powdery homogenized sediment samples were packed and sealed in plastic vials and stored for 20 days to allow the production of ^{222}Rn and ^{226}Ra without its loss to the atmosphere. The activities of ^{210}Pb, ^{137}Cs, and ^{226}Ra were measured in the high purity germanium (HPGe) coaxial 16×40 mm well type detector following the method described in Somayajulu et al. (1999). The non-destructive techniques were used to assay the ^{210}Pb, ^{137}Cs, and ^{226}Ra of the sediment samples (Cutshallet et al., 1983). To determine the activities of ^{210}Pb, ^{137}Cs, and ^{226}Ra, samples were counted for ~ 3 days. It is the unsupported ^{210}Pb that decays, whereas supported ^{210}Pb being in secular equilibrium with its parent ^{226}Ra remains constant. The activity of excess unsupported lead (^{210}Pb$_{xs}$) was calculated by subtracting the activity of ^{226}Ra from the total activity ^{210}Pb. The sedimentation rate was determined by applying the constant rate of supply (CRS) model of ^{210}Pb-dating (Appleby and Oldfield, 1992).

Chapter 3
Paleoenvironment of the central Himalaya during 45 to 29 ka: study from Pipalkoti paleolake

3.1 Introduction

The Marine Isotope Stages (MIS), defined based on oxygen isotopic composition of the ice cores and deep marine foraminifera, were the warm (interstadial) and cold (stadial) phases in the Quaternary period of the Earth history (Imbrie et al., 1984; Wright, 2000; Lisiecki and Raymo, 2005; Andersen et al., 2006). From which, the period between 60 and 30 ka, characterised by a warm and humid interstadial phase, is known as MIS 3 (Vam Meerbeeck et al., 2009; Weber et al., 2018). Within the MIS 3, there were four Ice Rifted Debris (IRD) or Heinrich events reported at approximately 29, 39, 45, and 61 ka, which were essentially rapid extreme cold events experienced globally due to partial collapse of the polar ice sheets (Heinrich, 1988; Bond et al., 1992; Rabassa and Ponce, 2016). In addition, within the MIS 3, a unique warm and wet phase has been reported from the western China, Tibetan Plateau, and northern India for the period of 40–30 ka. This gradual warming over the Tibetan Plateau and northwest China has been noticed using various terrestrial proxies (Kezao and Bowler, 1986; Pachur et al., 1995; Yang et al., 2004; Zhang et al., 2004, 2008 Herzschuh, 2006; Yang et al., 2010; Yang et al., 2011). Studies from the northwestern India also showed humid phase during late MIS 3 (40–30 ka), which has been suggested to be due to strong Indian summer monsoon (Tandon et al., 1997; Andrews et al., 1998; Singh et al., 1999; Juyal et al., 2000; Chahal et al., 2019). This unique warm and wet period over western China, Tibetan Plateau, and northern India is in contrast with the Greenland GRIP (Greenland ice core project), SPECMAP (Spectral mapping project), and Vostok ice core δ^{18}O records, which show a decrease in sea surface temperature and stepwise increase in global ice volume (Imbrie et al., 1993; Petit et al., 1999). The decreasing trend in δ^{18}O of foraminifera record from the northern Indian Ocean also suggested the lowering in sea surface temperature in the Arabian Sea and Bay of Bengal, which coincided with

polar $\delta^{18}O$ records (Reichart et al., 1998; Kudrass et al., 2001; Kumar et al., 2018). Since the paleoclimate record of this interesting phase (40–30 ka) from the Himalayan region is scarce, this study aimed to explore the paleoenvironment and cycling of C during this phase using a stable isotope approach on sediment samples collected from a paleolake sequence in the central Himalaya.

3.2   Study area

The samples for this study were collected from the Pipalkoti paleolake, named after the Pipalkoti village located in the Alaknanda basin, south of the Main Central Thrust. It lies in the transition zone of the lesser and higher Himalaya (Fig. 3.1 and Fig. 3.2). Pipalkoti village (30° 27′–30° 25′ N, 79° 24′–79° 26′ E) is located in an asymmetrical valley having a western slope of $\sim 45°$ and eastern slope of $\sim 35°$(Juyal et al., 2010). As the lake sequence is located on one of the terraces of the Alaknanda River (Fig. 3.3), it has been suggested that the lake was fed by the Alaknanda River, which flows from the Satopanth and Bhagirath Kharak glaciers in the Himalaya. The river has a drainage basin size of 10,237 km^2 and runs 230 km before entering the Bhagirathi River near Devprayag (Pal, 1986).

The catchment of this paleolake is dominated by the Cambrian carbonate rocks with a subordinate amount of gneisses, phyllites, quartzite, sericite-biotite schist and slates (Fig. 3.2; Gaur et al., 1977; Singh et al., 1998). The $\delta^{13}C$ of the carbonate rocks in the region has been reported to be around $-$ 0.7 to 1‰ (Singh et al., 1998). The lithology of the studied sequence is shown in Fig. 3.4.
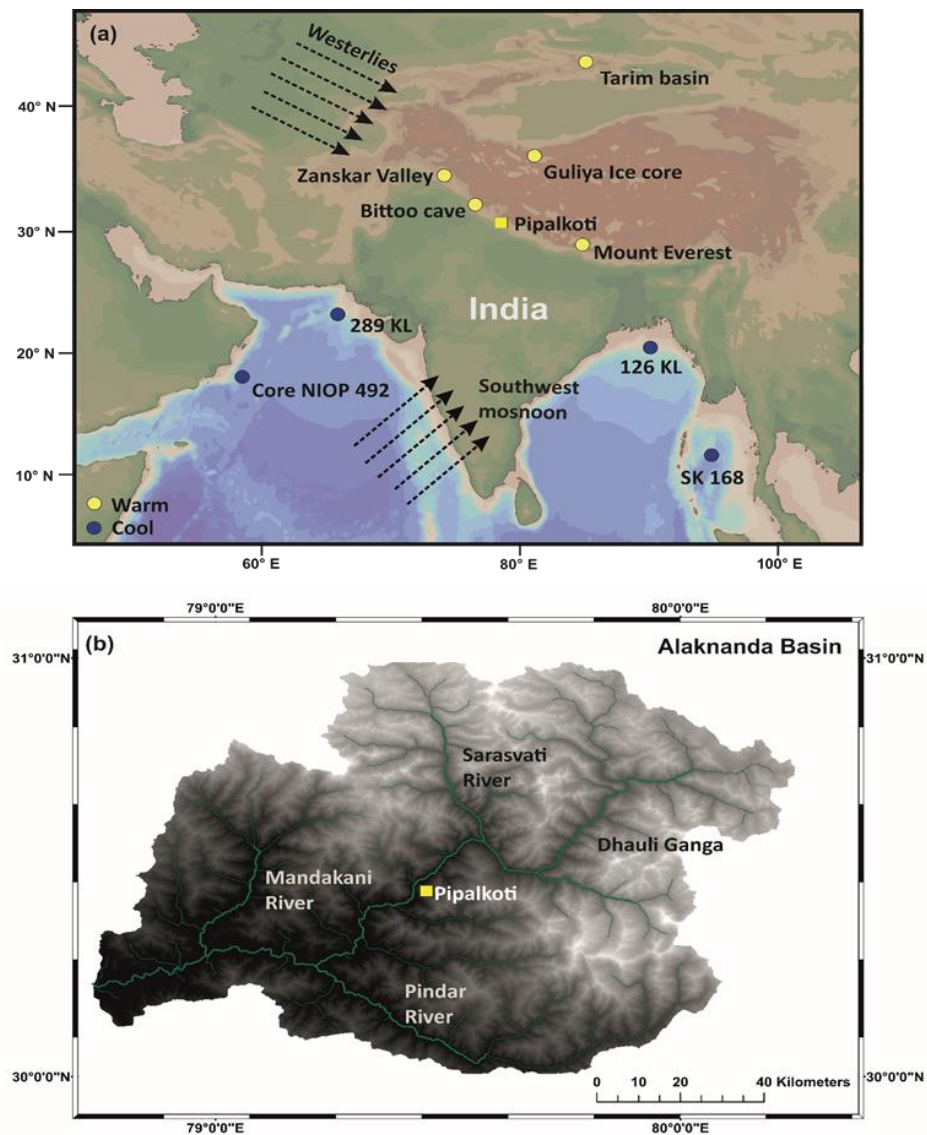
Figure 3.1 Schematic diagram showing (a) location of the study area (square) and (b) detailed map of the basin in which the study area is located. Locations of the previous studies covering period 40 to 30 ka in the region are also shown Zanskar valley: Chahal et al. (2019); Bittoo cave: Kathayat et al. (2016); Tarim basin: Yang et al. (2004); Yang et al. (2006); Mount Everest: Finkel et al. (2003); Guliya ice core: Thompson et al. (1997), Core NIOP 492: Reichart et al. (1998); 289KL: Deplazes et al. (2014); 126 KL: Kudrass et al. (2001); SK168: Kumar et al. (2018). Yellow circles in (a) represent studies advocating the wet period during 40–30 ka, and blue circles represent studies supporting weak Indian summer monsoon during late MIS 3.
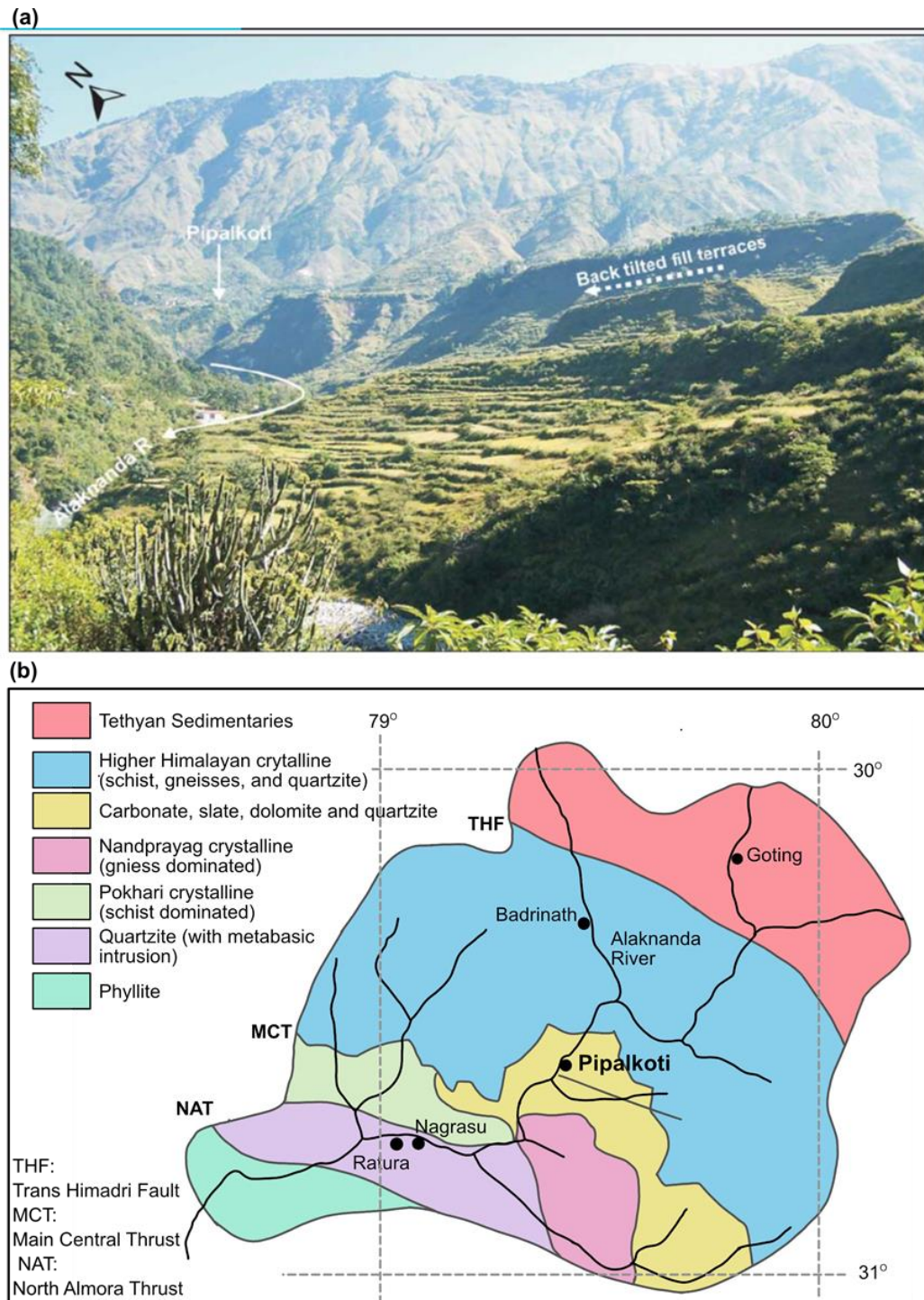
Figure 3.2 (a) Field photograph showing back tilted terraces around Pipalkoti. Direction of tilt is shown by white dotted arrow [photograph taken from Juyal et al., (2010)] and (b) generalised lithological and structural map of the Alaknanda catchment (modified after Gaur et al., 1977; Srivastava and Ahmed, 1979; Valdiya, 1980).
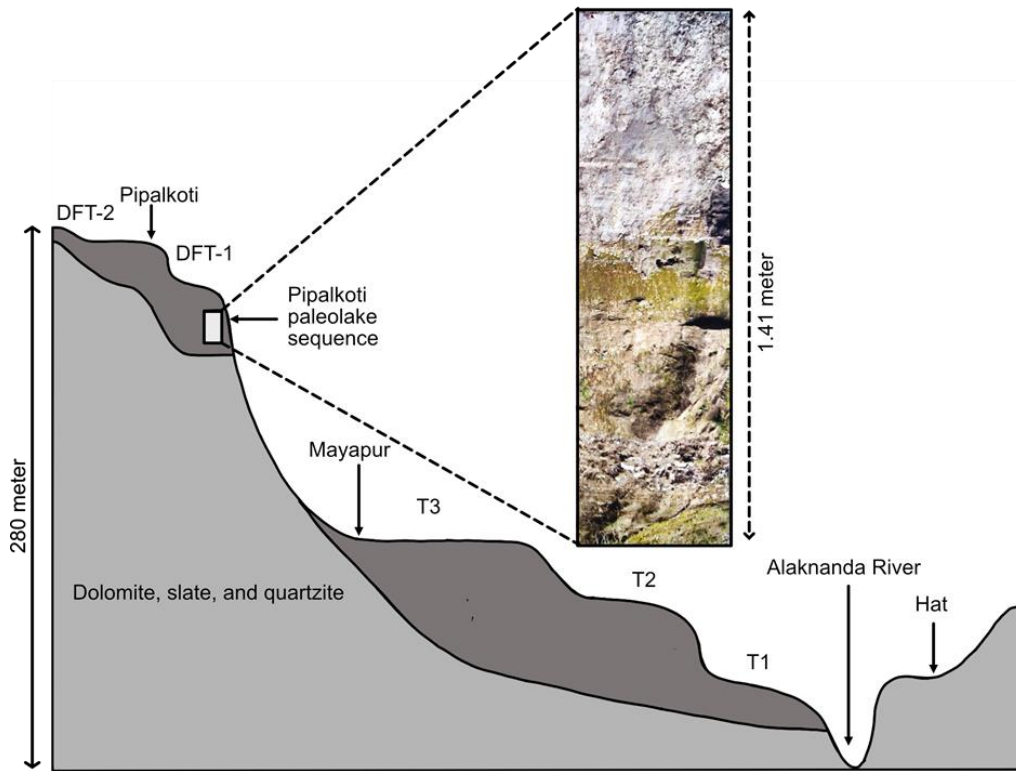
Figure 3.3 Schematic diagram showing the upper Debris Flow Terraces (DFT) and Lower Valley Fill Terraces in Alaknanda basin near Pipalkoti village (T3–T1). Pipalkoti paleolake sequence was found in one of the Debris Flow Terraces (DFT-1). Photograph showing the Pipalkoti paleolake sequence.

3.3   Chronology

As mentioned in the methodology, Infrared Stimulated Luminescence dating technique was used to constrain the chronology of the studied Pipalkoti paleolake sequence. The dates obtained for the sequence are mentioned in Table 3.1 and shown in Fig. 3.4. The two top ages of the sequence are quite close to each other despite significant sediment thickness between them. This may be due to landslide leading to the dumping of huge sediment load in the lake from the surrounding region, eventually resulting in vanishment of the lake. Following Zhang et al. (2015), linear age-depth (depth/age) model was used to establish a better chronology, especially for the depth where isotopic patterns change (Fig. 3.5). For this, a linear regression was performed between age and

depth. The slope and intercept of the regression line were used to calculate the ages for different depths.

Table 3.1 Details of radioactivity, dose rate (DR), equivalent dose (Ed), and ages obtained using multiple aliquot additive dose method.

Sample No.	U (ppm)	Th (ppm)	^{40}K (%)	DR (Gy/ka)	Ed (Gy)	Age (ka)
PKT-1	1.60 ± 0.04	5.50 ± 0.10	0.82 ± 0.01	1.79 ± 0.20	53 ± 3	29 ± 4
PKT-43	1.50 ± 0.03	5.10 ± 0.10	0.50 ± 0.00	1.47 ± 0.10	41 ± 2	28 ± 4
PKT-49	2.48 ± 0.04	8.20 ± 0.10	1.70 ± 0.08	3.00 ± 0.50	98 ± 3	32 ± 4
PKT-141[a]	2.00 ± 0.40	6.60 ± 0.15	1.02 ± 0.01	2.18 ± 0.30	98 ± 7	45 ± 6

[a]Sample no.: PKT-1, Table 1 (Juyal et al., 2010)

3.4   Results: stable isotopic variation in the paleolake sequence

The temporal variations in $\delta^{13}C$, TOC/TN ratios, $\delta^{13}C_{Diatom}$, and $\delta^{15}N$ are shown in Fig. 3.5. The $\delta^{13}C$ in the lake sequence varied from -24.6 to -19.7‰ with an average of -21.6‰ (Fig. 3.5). The $\delta^{15}N$ showed a large variation ranging from 1.4 to 9.3‰ with an average of 4.5‰ (Fig. 3.5). The TOC and TN contents ranged from 2.5 to 5.1% and 0.01 to 0.14%, respectively (shown in Fig. 3.5 in terms of ratios). No correlations were noticed between $\delta^{13}C$ - TOC and $\delta^{15}N$ - TN.

The $\delta^{13}C_{Diatom}$ in the sequence varied from -25.0 to -20.3‰ with a mean of -22.6‰ (Fig. 3.5). In general, values for $\delta^{13}C_{Diatom}$ were lower than $\delta^{13}C$ with a maximum difference of 5.1‰. Interestingly, four significant negative excursions in $\delta^{13}C_{Diatom}$, with values around -25.0‰, were noticed at ~ 45, ~ 40, ~ 35, and ~ 30 ka (Fig. 3.5).

An increasing trend in $\delta^{13}C$ was noticed during 45 to 41 ka, whereas TOC/TN ratios and $\delta^{15}N$ during this period did not follow any specific pattern (Fig. 3.5). Decreasing trends in $\delta^{13}C$ and $\delta^{15}N$ were noticed along with increase in $\delta^{13}C_{Diatom}$ and TOC/TN ratios between 40 to 32 ka (Fig. 3.5). The sediment sequence showed an increasing trend in $\delta^{13}C$ with a lowering in TOC/TN ratios and $\delta^{15}N$ from 32 to 29 ka (Fig. 3.5).
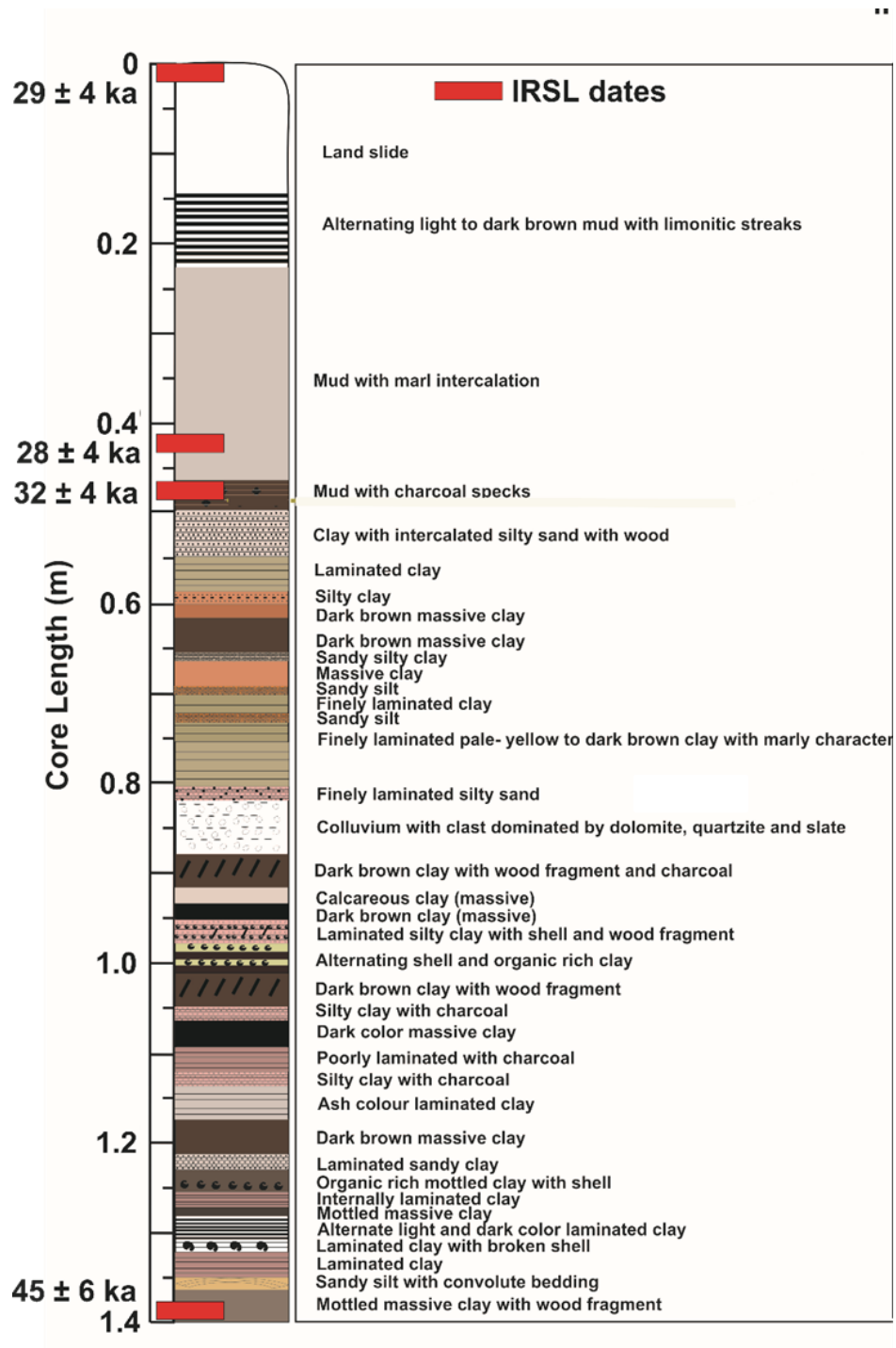
Figure 3.4 Litholog of the Pipalkoti trench section with four IRSL dates at different depths. Red boxes show the sample depths of IRSL dates.
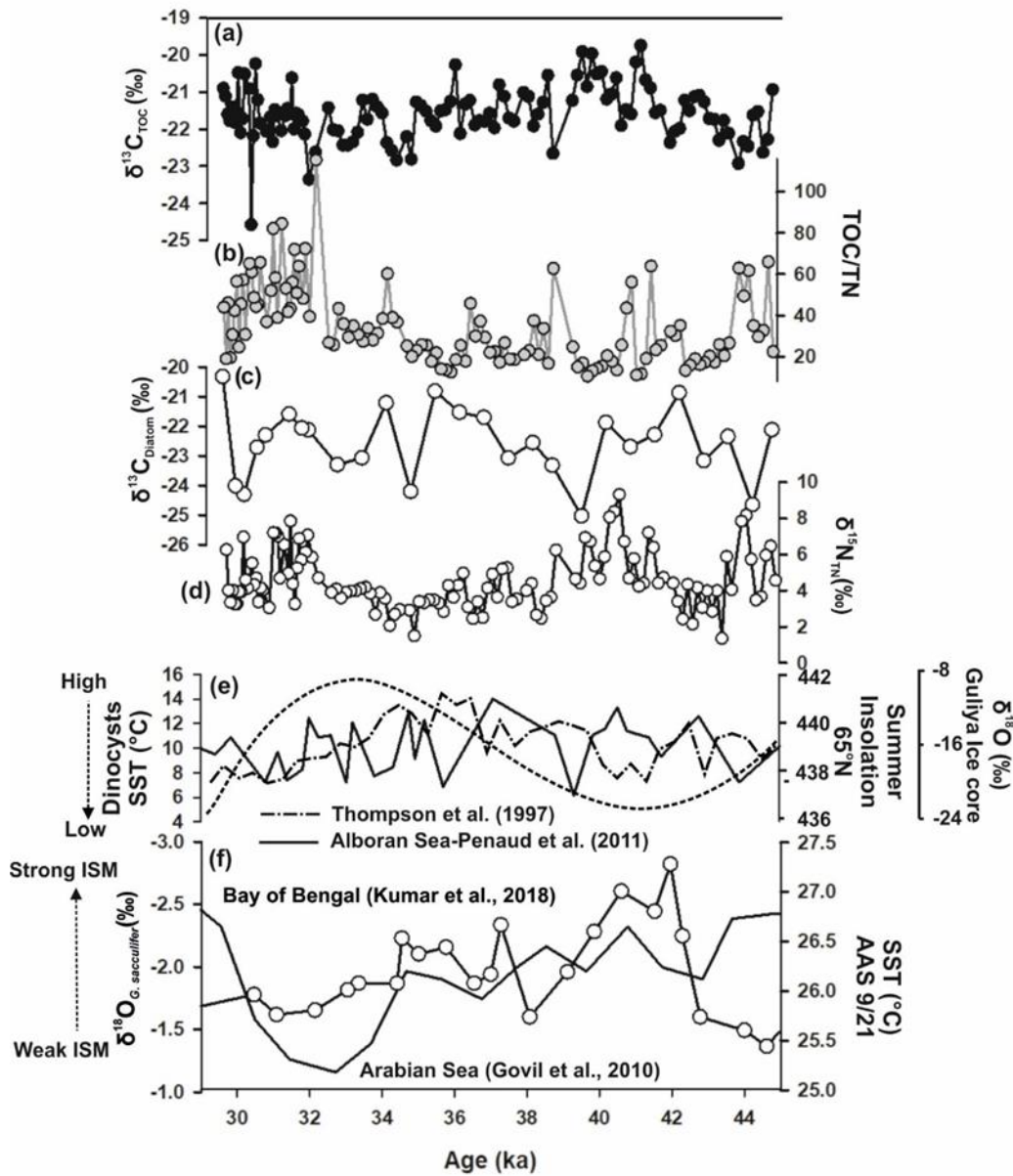
Figure 3.5 Results of the present study in comparison with various other regional and global studies (a) $\delta^{13}C$, (b) TOC/TN ratios, (c) $\delta^{13}C_{diatom}$, (d) $\delta^{15}N$, (e) Alboran Sea-Dinocyst SST (°C) - black line; Guliya ice core $\delta^{18}O$ - dashed-dotted line; Northern Hemisphere summer insolation (65°N) - dotted line, and (f) the Bay of Bengal marine core- $\delta^{18}O_{G.sacculifer}$ - dotted black line; Arabian Sea AAS 9/21-SST (°C)- solid line.

3.5   Discussion

The temporal variations in $\delta^{13}C_{Diatom}$, $\delta^{13}C$, $\delta^{15}N$, and TOC/TN ratios of the Pipalkoti paleolake sequence suggested the existence of both wet and dry periods in the central Himalaya during the span of the study period (45–29 ka). Negative excursions in $\delta^{13}C_{Diatom}$ accompanied by relatively higher $\delta^{13}C$ and $\delta^{15}N$ with lower TOC/TN ratios at around ~ 45, ~ 40, ~ 35, and ~ 30 ka (Fig. 3.5), suggested intermittent drier periods in the central Himalayan region. Barring the one at 35 ka, these drier phases in the Himalaya coincided with the globally reported Ice rafted debris or Heinrich events (H4, H3, and H2; Heinrich, 1988; Rabassa and Ponce, 2016). However, the limitation in the resolution of our chronology restricted us from attributing these events as manifestations of the Heinrich events in the Himalayas.

The $\delta^{13}C_{Diatom}$ is a robust proxy to decipher the original lake C dynamics and hence provides an understanding about the overall C biogeochemistry of the region in which the lake is located. This is mainly because the organic matter occluded within diatom frustules is formed within the lake itself and utilizes the DIC available in the lake. Of the different species of DIC, diatoms use both CO_2 and HCO_3^- as C sources for photosynthesis. Studies have shown that during CO_2 limiting conditions, diatoms incorporate HCO_3^- as a C source (Tortell et al., 1997). The $\delta^{13}C$ of DIC in a lake is largely controlled by productivity and respiration in the lake.

During wet and humid conditions, $\delta^{13}C$ of DIC in the epilimnion of a lake increases with the enhancement in aquatic productivity due to preferential uptake of ^{12}C by the phytoplankton (Singer and Shemesh, 1995; Leng et al., 2005). Also, during the wet period, when stratification of the lake water column is likely, $\delta^{13}C$ of DIC in the hypolimnion is relatively lower than that in the epilimnion due to microbial decomposition of organic matter in the hypolimnion (Cohen, 2003). In addition, the weathering of carbonate minerals in the watershed during wet and humid conditions also contributes significantly to enrichment (in ^{13}C) of the DIC pool (mainly HCO_3^-) of the lake with increased $\delta^{13}C$ of DIC (Kendall and Doctor, 2003). The catchment of the studied paleolake was dominated by the Cambrian carbonate rocks and hence likely to

contribute DIC in the form of HCO_3^- leading to an increase in $\delta^{13}C$ of DIC (Fig. 3.6). Therefore, it appeared that during the wet and humid period, the DIC pool in the epilimnion of the lake was dominated by HCO_3^- with relatively higher $\delta^{13}C$ of DIC (Fig. 3.6). Utilization of this ^{13}C enriched DIC by diatoms led to relatively higher $\delta^{13}C_{Diatom}$ during the wet condition. In other words, higher $\delta^{13}C_{Diatom}$ suggested a wet environment with higher rainfall and productivity.

On the other hand, during dry periods, due to a lesser supply of external nutrients such as N and phosphorus because of reduced runoff, there would be a reduction in lake productivity leading to a decrease in $\delta^{13}C$ of DIC relative to wet condition. Also, the availability of ^{13}C depleted CO_2 from the hypolimnion to epilimnion due to erosion in stratification of the water column, combined with lesser transport of HCO_3^- due to reduced weathering, would result in higher availability of CO_2 in the lake during dry conditions (Fig. 3.6). This might have shifted the lake DIC regime from HCO_3^- to CO_2 dominated with relatively lower $\delta^{13}C$ of DIC. Low $\delta^{13}C$ of DIC during winter compared to summer has been reported elsewhere (Bade et al., 2004). Hence, the organic matter formed using this ^{13}C depleted DIC is likely to show relatively lower $\delta^{13}C$ (i.e., $\delta^{13}C_{Diatom}$). Therefore, the observed negative excursions of $\delta^{13}C_{Diatom}$ during this study, i.e., lower $\delta^{13}C_{Diatom}$ observed at ~ 45, ~ 40, ~ 35, and ~ 30 ka (Fig. 3.5), are indicative of lesser rainfall / drier conditions.

The total organic C in lake sediments is a mixture of both in-lake production and terrestrial organic C. In this study, fluctuating TOC/TN ratios with values > 20 for most samples suggested variable but dominant contribution of organic matter from terrestrial sources brought in from the watershed (Fig. 3.5). The $\delta^{13}C$ also reflected largely terrestrial sources, which is likely the mixture of C3 and C4 plants. In modern times, vegetation in the studied region is dominated by C3 plants, such as Banj-oak (*Quercus leucotrichophora A. Campus*), Tilonj-oak (*Quercus floribunda Lindl. ex Rehder*), Kharsu-oak (*Quercus semecarpifolia*), and Chir-pine (*Pinus roxburghii Sarg*) (Kharkwal and Rawat, 2010). The $\delta^{13}C$ of C3 plants ranges from -35 to $-22‰$ with an average of $-27‰$, whereas for C4 plants, it ranges from -10 to $-18‰$ with an average of $-12.5‰$ (Cerling et al., 1997). The $\delta^{13}C < -20‰$ was observed for all

samples during this study (Fig. 3.5), which suggested the dominance of C3 plants in the catchment during 45–29 ka, with a possible mixture of C4 plants. The C4 plants, formed in low pCO_2 conditions, are tolerant to drier conditions (Cerling et al., 1997; Sage et al., 1999). Therefore, increase in $\delta^{13}C$ might indicate some contribution from C4 plants due to its expansion in the catchment. Relatively higher $\delta^{13}C$ with lower TOC/TN ratios during the periods of negative excursions in $\delta^{13}C_{Diatom}$ suggested lower contribution of land derived organic matter to the lake due to drier conditions, possibly due to relatively less rainfall during ~ 45, ~ 40, ~ 35, and ~ 30 ka, when C4 plants might have expanded. However, past expansion of vegetation types in the region warrants another detailed study.

Barring 35 ka, elevated $\delta^{15}N$ during negative $\delta^{13}C_{Diatom}$ excursions also suggested lower inputs of terrestrially derived organic matter to the lake during those periods. In a lake, $\delta^{15}N$ depends on the relative contributions of soil/terrestrially derived organic matter and *in-situ* primary productivity. The terrestrially derived organic matter usually have low $\delta^{15}N$ ($\delta^{15}N_{plants}$ ~ − 5 to + 2‰; $\delta^{15}N_{soil}$ ~ − 10 to + 5‰; Fry, 2006), whereas *in-situ* productivity shows relatively higher values, which depends upon the nutrient availability (Peters et al., 1978; Meyers and Ishiwatari, 1993; Meyers, 2003). However, the N_2-fixers, one of the dominant phytoplankton during warmer environment, have $\delta^{15}N$ ~ 0‰ (Montoya et al., 2002; Lehmann et al., 2004). Therefore, low $\delta^{15}N$ during the wet condition (Fig. 3.5) is indicative of high nutrient loading and a higher supply of terrestrial organic matter to the lake, which is possible due to increased runoff.

During the wet condition, high productivity, as well as terrestrial C loading, lead to high heterotrophic degradation, which results in anoxic or low oxygen conditions in a lake (Lehmann et al., 2002; Talbot, 2005; Hadas et al., 2009). This enhances denitrification in the hypolimnion of the lake, thereby enriching the NO_3^- pool in ^{15}N (Hadas et al., 2009). This isotopically enriched NO_3^-, which could not come up to the surface due to stratification during the wet condition, might end up on the surface during dry (and cold) conditions due to mixing. Also, due to mixing, the lake water column would be oxygenated, and hypolimnion NH_4^+ might get converted to NO_3^- by nitrifying

bacteria resulting in the enrichment of the remaining NH_4^+ pool in ^{15}N (Strauss and Lamberti, 2000; Hadas et al., 2009). Under no external refractory C loading, higher nitrification in lakes by chemoautotrophic ammonium oxidizers has also been reported (Strauss and Lamberti, 2000). The uptake of the ^{15}N enriched NO_3^- and NH_4^+ pool through the mechanisms mentioned above might have resulted in higher $\delta^{15}N$ during drier conditions. In other words, elevated $\delta^{15}N$ during ~ 45, ~ 40, and ~ 30 ka, combined with negative excursions of $\delta^{13}C_{Diatom}$ (Fig. 3.5), indicated drier and possibly colder conditions. On the other hand, generally lower $\delta^{15}N$ during 40–32 ka (Fig. 3.5) indicated productive lake with high nutrients and terrestrial organic matter supply due to high rainfall suggesting wet and humid conditions.
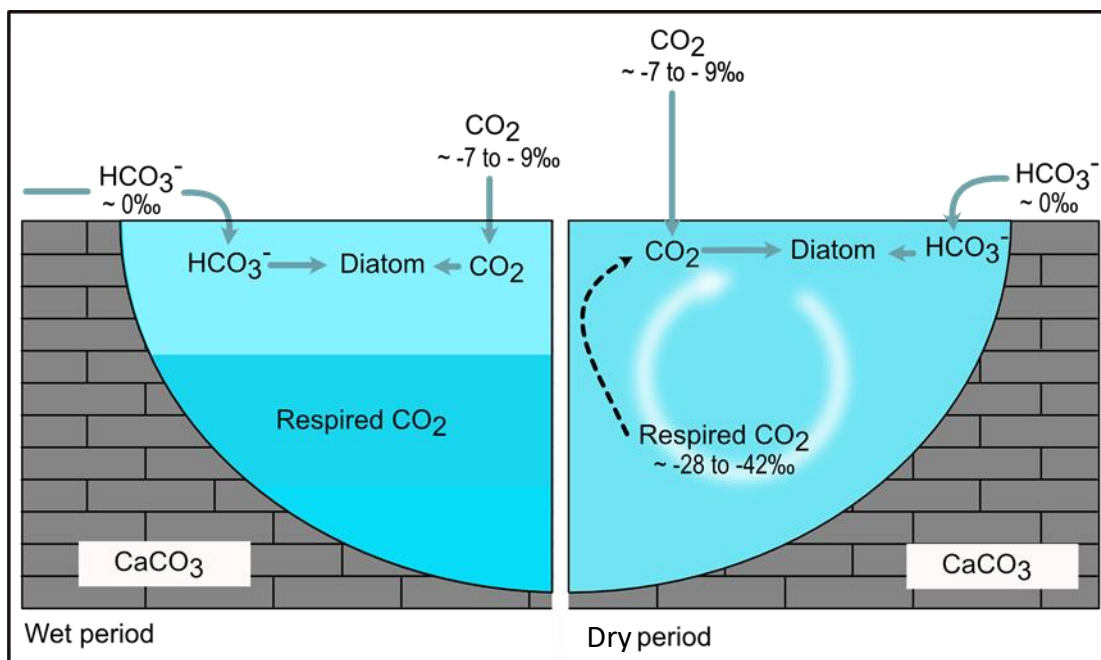
Figure 3.6 Schematic diagram showing possible mechanism of C assimilation by diatoms during the wet and dry conditions. The solid and dashed lines show relatively higher and lower contributions of C species to the lake and assimilation by diatoms during different climatic conditions.

As mentioned earlier, the warm and wet phase in climate during late MIS 3 (40–30 ka) reported from northwest China, Tibetan Plateau, and northwestern India appears to be in contrast with colder signatures from polar $\delta^{18}O$ records (Tandon et al., 1997; Andrews et al., 1998; Shi et al., 2001; Yang et al., 2004). High lake levels in western

China also indicated warm and wet conditions during 40–30 ka (Keqin, 1991; Pachur et al., 1995; Hucai and Wünnemann, 1997; Meng and Liu, 2018; Zhang and Liu, 2020). The Guliya ice core δ^{18}O records also indicated a warmer period during late MIS 3 (Fig. 3.5). This warm and wet period during 40–30 ka in the northwest China and Tibetan Plateau has been reported as a result of the advancement of the northern ice sheet that created a temperature and pressure gradient between the low and high latitudes leading to strong westerlies (Yang et al., 2004, 2006, 2010; Wunnemann and Hartmann, 2007). Barring the intermittent drier phases described earlier, the isotopic compositions ($\delta^{13}C_{Diatom}$, $\delta^{13}C$, and $\delta^{15}N$) and elemental ratios (TOC/TN) of the present sequence also indicated wet and humid conditions during 40–32 ka in the central Himalaya (Fig. 3.5).

The studied lacustrine sequence at the Pipalkoti was located at one of the terraces of the Alaknanda basin (Fig. 3.3), which is an indicator of the fluvial condition (Juyal et al., 2010). Studies from the northern and western regions of India using sedimentary proxies reported wet condition during the studied period due to strong Indian summer monsoon (Tandon et al., 1997; Andrews et al., 1998; Singh et al., 1999; Juyal et al., 2010; Chahal et al., 2019), whereas marine core δ^{18}O records from the Arabian Sea and Bay of Bengal reported a weak Indian summer monsoon during late MIS 3 (Govil and Naidu, 2010; Kumar et al., 2018). Another study based on δ^{13}C of soil organic matter from the eastern Himalaya also showed weak Indian summer monsoon during 46–31 ka (Ghosh et al., 2015). The present study location (central Himalaya) experienced the interplay of the Indian summer monsoon and westerlies (Benn et al., 1998; Kotlia et al., 2015). Decrease in sea surface temperature in the Alboran Sea (Mediterranean Sea) due to gyre induced upwelling (Penaud et al., 2011) and increase in the Northern Hemisphere insolation (~ 65 °N; Berger and Loutre, 1991) during late MIS 3 have been reported (Fig. 3.5). This could provide a strong temperature and pressure gradient between the Himalaya/ Tibetan Plateau and the Mediterranean Sea, leading to strong westerlies, which might have extended up to the central Himalaya during 40–32 ka. Overall, in accordance with the reports from China and northwestern India, the period between 40 and 32 ka in the central Himalaya was wet and humid with sporadic dry events. These dry events were likely the part of globally reported Heinrich events. An extensive multi-proxy high-resolution study is needed in the central

Himalayan region to understand different facets of the past climate variabilities, including the moisture source for the wet and humid conditions during 40–32 ka.

3.6   Conclusion

Stable isotopic compositions and elemental ratios based study showed a sign of largely wet and humid condition during 40–32 ka in the central Himalaya. A similar wet and warm period was previously reported from the northwest China, Tibetan Plateau, and northwestern India. The moisture source for this wet period is under debate. Based on the previous data from the Mediterranean Sea (Alboran) and Northern Hemisphere summer insolation, this study has surmised that the observed wetness in the central Himalayan region might be westerlies induced. This study also found the evidence for intermittent drier phases at around ~ 45, ~ 40, and ~ 30 ka during the larger wet period in late MIS 3. These drier phases coincided with the globally reported extreme cold Heinrich events. However, a study with a better chronological record is needed to establish the same in the central Himalaya. The transition of climate from wet to dry phase influenced lake C biogeochemistry. It appeared that the lake shifted from HCO_3^- to CO_2 dominated regime during wet to dry transition. The lake appeared to be well mixed during dry phases, when productivity was largely sustained through recycled nutrients. During the wetter period, however, lake seemed to receive external nutrient inputs as reflected through N isotopic composition of sediment samples.

Chapter 4
Paleoenvironment of the Kashmir Himalaya

4.1   Introduction

The climate of the western Himalaya, particularly the Kashmir Himalaya, is largely influenced by the westerlies (Zaz et al., 2019). The westerlies, controlled by the temperature and pressure gradient between the Atlantic Ocean and the northwestern Himalaya/ Tibetan Plateau, transport moisture from the Mediterranean Sea, Caspian Sea, and the Black Sea to the western Himalayan region and Tibetan Plateau (Benn and Owen, 1998; Wu et al., 2007). Therefore, the climate of the Kashmir Himalaya is predominantly influenced by the westerlies-induced precipitation in the form of snow and rain. Due to heterogeneous orography and geography, the Himalaya shows diverse climatic conditions along its ~ 2400 km long stretch (Valdiya, 1998). The effect of heterogeneous climate in the Himalayan region is abundantly seen in the distribution and structure of many ecosystems, including aquatic ecosystems (Rashid et al., 2015). As the Kashmir Himalaya shows great internal variation in the relief and continuity of mountain fronts, there are a huge number of lakes in the region. These lakes have a high rate of sedimentation due to the surrounding high mountains. As a result, they can provide very high-resolution climate proxy data; yet, paleoclimate investigations in the Kashmir Himalaya are limited. Apart from limited studies using lake sediments, other archives in the region have also been used to decipher paleoclimate of the region. One such study has used trace element geochemistry of terrestrial loess-paleosol sequence to unravel climate variations in the Kashmir Himalaya from 65.8 ± 7.2 ka to 14.7 ± 5.4 ka (Shah et al., 2021). Another study by Ali and Achyuthan (2020) showed the variation in geochemical characteristics of loess-paleosol sequence, which provided information about the fluctuation in climate condition of the region during MIS 3. So far, there is no study in the Kashmir Himalaya using lake sediments that could provide the paleoclimate and paleoenvironmental information during the pre-Holocene period, such as LGM (MIS 2), MIS 3, Heinrich events, etc. However, there are some studies that have focussed on the Holocene climate of the Kashmir Valley using geochemical

proxies in sediments collected from trenches and cores from in and around the live and paleo-lakes in the region. Shah et al. (2020) studied the early and mid-Holocene paleoenvironmental condition using trace element geochemistry of sediments collected from a trench at the bank of Wular Lake, whereas studies from the Manasbal and Anchar Lakes showed variation in paleoclimatic conditions using the same proxies during the late Holocene (Babeesh et al., 2019; Lone et al., 2020). Another study by Shah et al. (2021) showed the eutrophic evolution of the Wular Lake during the last 500 years. In addition, the Manasbal Lake paleo-productivity has been explored using diatom assemblages (Babeesh et al., 2019).

Taken together, it appears that a comprehensive understanding of the paleoenvironmental condition of the Kashmir Himalaya is limited. Even during the Holocene, there are some studies that are largely based on trace elements or diatom assemblages. Use of robust proxies, which could provide information about the biogeochemical evolution of the Himalayan lakes, such as C and N isotopes, are non-existent. This has limited us to develop a proper understanding of the climate and environmental history of the region, particularly from the point of view of the flow and distribution of the bio-available elements. In this study, an attempt has been made to decipher the past environmental conditions during the past 33 ka using stable isotopes in lake sediments collected from different parts of the Kashmir Himalaya.

4.2   Study area

As mentioned in the methodology section, to achieve the stated goals in the Kashmir Himalaya, two lake sediment cores, one each from the Wular and the Manasbal Lakes in the Kashmir Valley, were extracted (Fig. 4.1a). Also, trench sediment samples were extracted from a paleolake sequence in the Forest Block region of the Kashmir Valley (Fig. 4.1).

The Kashmir Himalaya (Valley) is in the northwestern part of the Himalayan mountain range. Wadia (1931) referred to the Kashmir Valley as the thrust-bounded basin and named it 'Kashmir Nappe Zone,' which consists of Palaeozoic–Mesozoic marine deposits with Precambrian basement thrusted along a regional tectonic plane,

namely the Panjal Thrust, over the younger autochthones belt. The 'Kashmir Nappe' forms two major orogenic upheaval axes that run along the Pir-Panjal and Great Himalayan Ranges. The Kashmir Nappe structural configuration and geographic location are the product of the Great Himalayan Orogeny. In addition, it has been suggested that the Kashmir Valley possesses almost complete stratigraphic records of Archean rocks to recent sediments (Bhatt 1975, 1976; Wadia 1975; Shah, 2019). This valley is filled with up to 1300 m thick Plio -Pleistocene fluvial-glaciolacustrine deposits known as the "Karewa" or "Karewa Group (Fig. 4.1b).

The hydrology of the Kashmir Valley is controlled by the westerlies-induced precipitation and glacial meltwater, largely through the Jhelum River. There are three major tributaries (Veshav, Rambiara, and Romushi) of the Jhelum River, which emerge from the high altitude lakes and snow-covered mountains of the Pir Panjal Range in the southwest. The Jhelum River in the valley supplies water to the Wular Lake, one of Asia's largest freshwater lakes. The westerly influenced moisture brings copious precipitation to the Kashmir Valley that can amount to ~ 105 mm/month during winter-spring, whereas the autumn season remains relatively dry; 33 mm/month (Ganai et al., 2010). The average temperature varies from – 2 ℃ during winter to 32 ℃ during summer (Data source: https://en.climate-data.org/asia/india/jammu-and-kashmir/srinagar-3424/).
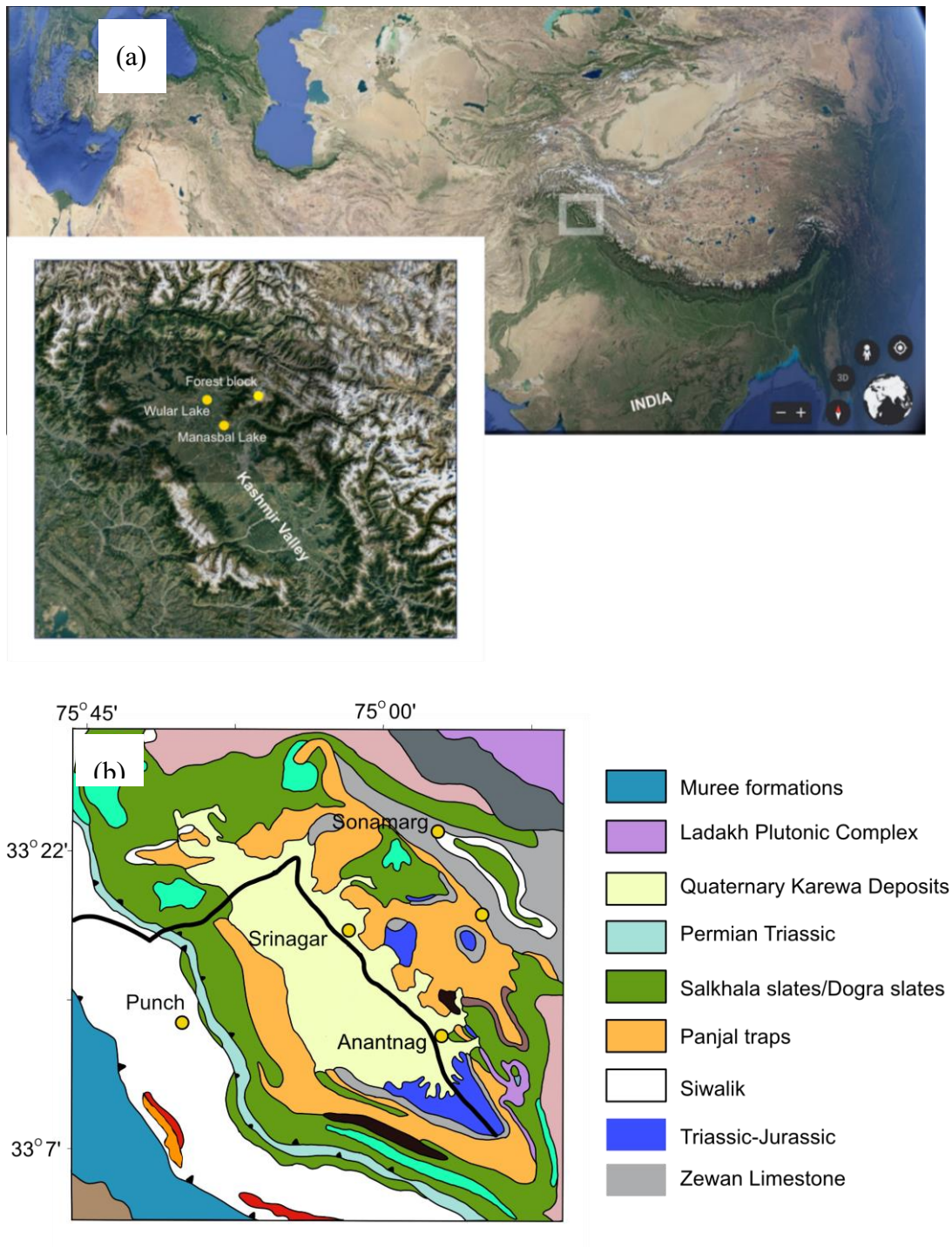
Figure 4.1 (a) Map of the study locations (Wular Lake, Manasbal Lake, and Forest Block paleolake) in the Kashmir Valley and (b) geological map showing major lithological units of the Kashmir Himalaya (after Thakur, 1998).

4.3   Paleoenvironment during last ~ 33 ka: Forest Block paleolake sequence

The Forest Block paleolake sequence is situated at an altitude of ~ 3300 m above mean sea level. Such high mountain lakes are severe ecosystems susceptible to harsh climate conditions. Only alpine plants or sparse vegetation can thrive above the tree line at such a high altitude due to the extreme winter temperatures (Hinder et al., 1999). These lakes are covered with snow and ice for most of the year, preventing sunlight from entering the underlying water column (Felip et al., 2002), which also appears to be the case for the present study region. Photosynthesis cannot occur in the absence of light and the lakes stay in darkness resulting in heterotrophy until the ice cover melts (Ventelä et al., 1998). When the ice cover melts in the summer, the lake suddenly receives higher solar irradiance with high UV radiation, which is directly related to altitude (Vinebrooke and Leavitt, 1996). It has been shown that altitude-gradient in the atmospheric condition may also influence the thermal structure of such lake, which largely controls the ecology and biogeochemistry of the lake (Livingstone et al., 2005; Ceppi et al., 2012; Pepin et al., 2015; Woolway et al., 2019). Aquatic organisms can finish their life cycle during this brief time of optimum circumstances before the snow returns to cover the lakes. High-mountain lakes are considered "natural laboratories" where global climate changes can be investigated through the advancement in the understanding of temporal biogeochemical evolution of the lake. In this section of the thesis, an attempt has been made to comprehend the temporal biogeochemical evolution of one of the high mountain lakes in the Kashmir Himalaya as well as the accompanying regional and global environmental changes using the $\delta^{13}C$ and $\delta^{15}N$ and their concentrations in the Forest Block paleolake sequence covering 33–0.2 ka

4.3.1   Chronology

For high resolution chronology construction, sediment samples from the Forest Block paleolake sequence have been dated using the radiocarbon dating technique that has been mentioned earlier in the chapter dealing with the methodology. For this, organic matter in eight sediment samples from the Forest Block sediment sequence were dated using AMS, which are shown in Table 4.1 with depths and corresponding calibrated

ages. Overall, the ages obtained showed that the sampled Forest Block paleolake sequence covered the time span ranging from 33 to 0.2 ka in the Quaternary history of the Kashmir Himalaya. The photograph of the sampled trench with the litholog and age-depth model plot is shown in Fig. 4.2.
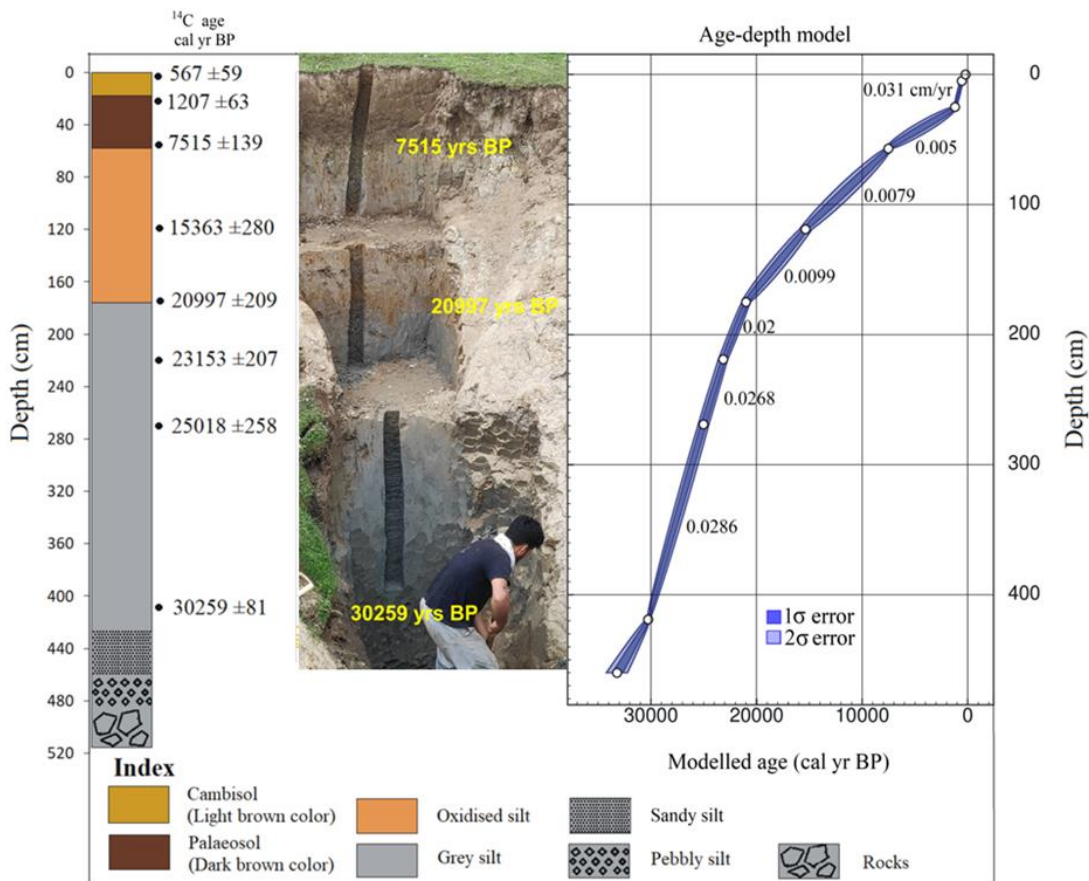
Figure 4.2 Lithology of the Forest Block paleolake sedimentary sequence with section photograph and age depth model. The black dot near the lithology section showed the depths of radiocarbon dated samples.

Table 4.1 Calibrated AMS ^{14}C ages (2σ error bar) of the Forest Block paleolake sequence.

Sample ID	Depth (cm)	Age (Cal ka BP)
Top	0	0.21 ± 0.17
PRL3536	5	0.57 ± 0.06
PRL3537	25	1.21 ± 0.06
PRL3538	57	7.51 ± 0.14
PRL3539	119	15.36 ±280
PRL3540	175	21.00 ± 0.21
PRL3541	219	23.15 ± 0.21
PRL3542	269	25.02 ± 0.26
PRL3545	419	30.26 ± 0.08
Bottom	460	33.21 ± 0.50

4.3.2 Forest Block paleolake: C and N contents and isotopic compositions

The temporal variation in δ^{13}C and δ^{15}N of the sampled sediments is shown in Fig. 4.3. No significant temporal change in TOC and TN contents, except for surface samples representing the last 7 ka was noticed. Overall, δ^{13}C varied from − 25.5 to – 23.0 ‰ (maximum difference ~ 2.5‰), and TOC ranged from 0.05 to 5.36 %. The δ^{15}N showed a large variation, ranging from 3.6 to 11.0 ‰ with a maximum difference of 7.3‰. TN also showed a significant variation and ranged from 0.02 to 1.36% (Fig. 4.3).

The δ^{13}C and TOC showed a significant positive correlation ($r^2 = 0.31$ and $p < 0.001$), whereas no significant relationship was noticed between δ^{15}N and TN. The TOC and TN showed a strong correlation ($r^2 = 0.80$ and $p < 0.001$), but no relationship was observed between δ^{13}C and δ^{15}N.

A gradual increase in δ^{13}C from − 24.7 to − 23.0‰ was noticed during 31 to 28 ka (Fig. 4.3a). Further, a consistent decline in δ^{13}C was seen between 28 and 15 ka, with significantly higher values during 28–24 ka, which corresponded to the beginning of the LGM (Fig. 4.3a). A significant positive δ^{13}C excursions were noticed during 11-12 ka, which were not seen later, possibly due to smaller number of data points. Contrary to δ^{13}C, δ^{15}N showed sharp increase from 30 to 28 ka. Afterward, it declined

consistently until 19 ka to jump suddenly within a short span. The $\delta^{15}N$ remained between 7–10 ‰ from 18 to 0.2 ka and showed two peaks at around 18–15 ka and later at around 11 ka.

4.3.3 Paleo-biogeochemistry of the Forest Block paleolake

The TOC/TN ratio (< 10) of the sediment samples from the Forest Block paleolake sequence suggested that, from ~ 33 ka to early Holocene (~ 7 ka), the source of organic matter in the lake was dominantly in-lake primary production. For the same time period, the effect of the terrestrially derived organic matter on the lake biogeochemistry appeared to be almost negligible due to the location of the lake, which was on the top of a mountain. The paleosol at the top of the sequence exhibited comparatively higher TOC/TN (> 10) after 7 ka, implying the presence of soil organic matter that could have been possible due to the vanishment of the lake around that time (Fig. 4.3 and 4.4). It seems possible that due to significant precipitation during Holocene Thermal Maximum, lake level could have risen leading to weakened lake boundary and outflow of the lake water. This could have possibly emptied the lake at around 7 ka exposing the lake bottom to the atmosphere to allow grass and other terrestrial plants to grow, which was marked through relatively higher TOC/TN ratio after 7 ka.

Overall, $\delta^{13}C$ and $\delta^{15}N$ signatures of the Forest Block paleolake sequence during 30–7 ka represented the change in lake biology and associated biogeochemical processes (Fig. 4.4 and 4.5) through time. These elevated signatures in isotopic compositions of lake C and N indicated existence of relatively colder climate during that time period. The present altitude of the paleolake sequence is ~ 3300 m and modern climate shows that it is situated in a low-temperature (annual average − 10 °C) region. Assuming similar altitudinal effect on the lake, it is highly likely that the surface of the lake was frozen sometime during its existence. The complete or partial freezing of the lake surface might have cut off the CO_2 exchange between air and water as well as stopped the inputs of nutrients from the catchment to the lake (Gammons et al., 2014). In the present study, the higher $\delta^{13}C$ and $\delta^{15}N$ values at ~ 29–28 ka showed limiting surface CO_2 and nutrient condition in the lake due to the ice cover. The ice cover might have also resulted in winter stratification that would not allow hypolimnion nutrients

and recycled CO_2 enriched water to upwell to the surface (Gammons et al., 2014). Therefore, in the absence of supply of nutrients from the catchment and atmospheric CO_2 exchange along with limited upwelled DIC (and recycled nutrients) from the hypolimnion, phytoplankton was possibly using the available DIC in the surface. The uptake of this limited surficial nutrients and DIC pools might have led to its isotopic enrichment leading to higher $\delta^{13}C$ and $\delta^{15}N$. In addition, during the cold period, low C isotopic fractionation associated with the growth of primary producers has been reported previously (Watanabe et al., 2004), which could be an additional reason for enrichment in ^{13}C of the organic matter of the Forest Block paleolake.

A gradual decrease in $\delta^{13}C$ and $\delta^{15}N$ between 29 and 19 ka (29–24 and 24–19 ka) indicated an enhancement in air-water CO_2 exchange and nutrient supply to the lake, which might be due to rising temperature and progressive melting of ice cover. A sudden shift in $\delta^{15}N$ during 18–16 ka associated with no significant change in $\delta^{13}C$ might have resulted due to the upwelling of hypolimnion nutrients and CO_2 to the lake surface as a result of overturning of the lake (Hadas et al., 2009). In a lake, the bottom water is enriched in NH_4^+ due to decomposition of organic matter and consumption of dissolved oxygen in the water column (Hadas et al., 2009; Gammons et al., 2014). When there is no terrestrial organic matter supply to a lake, nitrification is supposedly the dominant process that transforms NH_4^+ into NO_3^- by the preferential consumption of ^{14}N (Strauss and Lamberti, 2000). The resulting NH_4^+ would be enriched in ^{15}N, which once upwelled to the surface during lake mixing (wind-induced or break in stratification), would be taken up by the primary producers leading to increased $\delta^{15}N$ (Fig. 4.4 and Fig. 4.5). Unlike NH_4^+ availability, which strongly depended on the upwelled water, CO_2 majorly depended on the exchange between the lake surface and atmosphere (Fig. 4.5). The respired CO_2 might also play a significant role in photosynthesis as $\delta^{13}C$ of the organic matter during this study showed a mixed signature of both respired and atmospheric CO_2. The declining signature of $\delta^{13}C$ after 29 ka indicated a possible mixed source of C to the primary producers in the lake, i.e., atmospheric and respired CO_2, which was indicative of progressively warming climate. As the uptake of surficial DIC by phytoplankton led to enrichment of the remaining

pool in ^{13}C, the supply of the respired CO_2 with depleted ^{13}C signature (δ^{13}C ~ $-$ 42‰; McCallister and Del Giorgio, 2008), due to the break in the winter stratification of the lake, might have resulted in the observed δ^{13}C of the lake organic matter after 29 ka.

An increase in δ^{13}C and δ^{15}N at around 12–11 ka suggested possibility of relatively cooler or dry climate in the region again, possibly due to increase in frozen lake surface area, leading to limited exchange of CO_2 and nutrients, as explained earlier. Taken together, sediment samples from the high altitude lake suggested colder period in the Forest Block region at ~ 29 and ~ 11 ka. The observed gradual decrease in δ^{13}C and δ^{15}N between 29 and 19 ka suggested the weakening of westerlies, which were interlinked with a time of maximum ice sheet extension during the LGM.

4.3.4 Interconnection with the global climate

It is well known that the Kashmir Himalayan climate is dominantly controlled by the westerlies (Zaz et al., 2019). Between 33 and 0.2 ka of the Kashmir Himalayan paleoclimate history, evidences for two extreme colder periods at ~ 29 and ~ 11 ka were noticed in this study, which coincided with the globally reported Heinrich (H3) and YD (12.7–11.5 cal. ka BP; Lohne et al., 2013, 2014) events, respectively. The Heinrich and YD events resulted from the ocean surface cooling as indicated by δ^{18}O records of planktonic foraminifera of the North Atlantic Ocean (Keigwin and Lehman, 1994; Bagniewski et al., 2017). The sediment cores from the North Atlantic Ocean demonstrated that the ocean surface cooling during H3 was due to freshwater inputs resulting from the polar ice sheets melting (Gwiazda et al., 1996; Barker et al., 2015). On the other hand, the YD event was due to an abrupt rerouting of Lake Agassiz overflow through the Great Lakes and St. Lawrence Valley. As a result, the deepwater formation in the subpolar North Atlantic and the strength of the Atlantic Meridional Overturning Circulation weakened (Broecker et al., 1989). Another study showed that the meltwater discharge from the Arctic, rather than the St. Lawrence Valley, was more likely to have triggered the YD cooling (Condron and Winsor, 2012). The melting of ice sheets and cooling of the North Atlantic surface ocean played a significant role in the southward shifting of westerlies (Peterson et al., 2000; An et al., 2012). The grain size-based study from the Lake Qinghai's loess-like sediments indicated cold/dry

conditions during both H3 and YD events, suggesting strong instabilities in the westerlies-dominated climate regions, i.e., central Asia and central loess plateau (China) region during glacial times (An et al., 2012; Cheng et al., 2020).
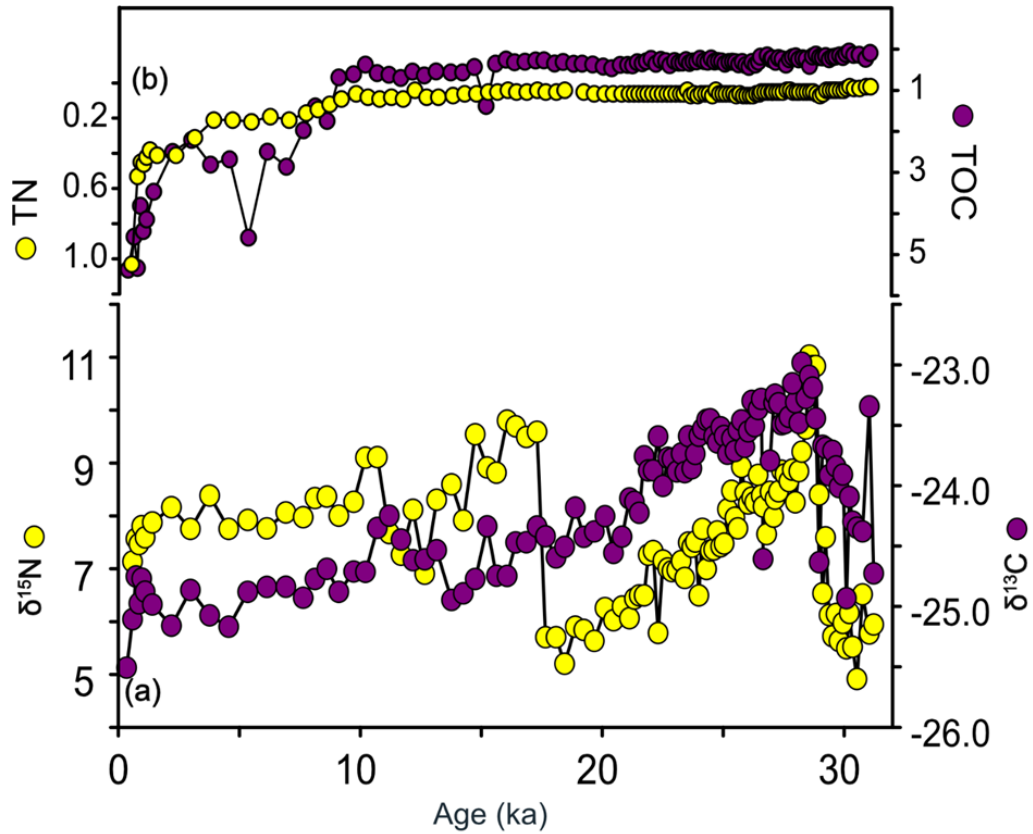
Figure 4.3 (a) $\delta^{13}C$ and $\delta^{15}N$ and (b) TOC and TN content of the Forest Block paleolake sequence. Violet dot and yellow dot are representing the C and N content and isotopic composition in (a) and (b), respectively.

Therefore, it appeared that biogeochemical changes in the Forest Block high altitude paleolake during this study were also, directly and indirectly, influenced by westerlies, which were impacted by cooling during the globally reported H3 and YD events.
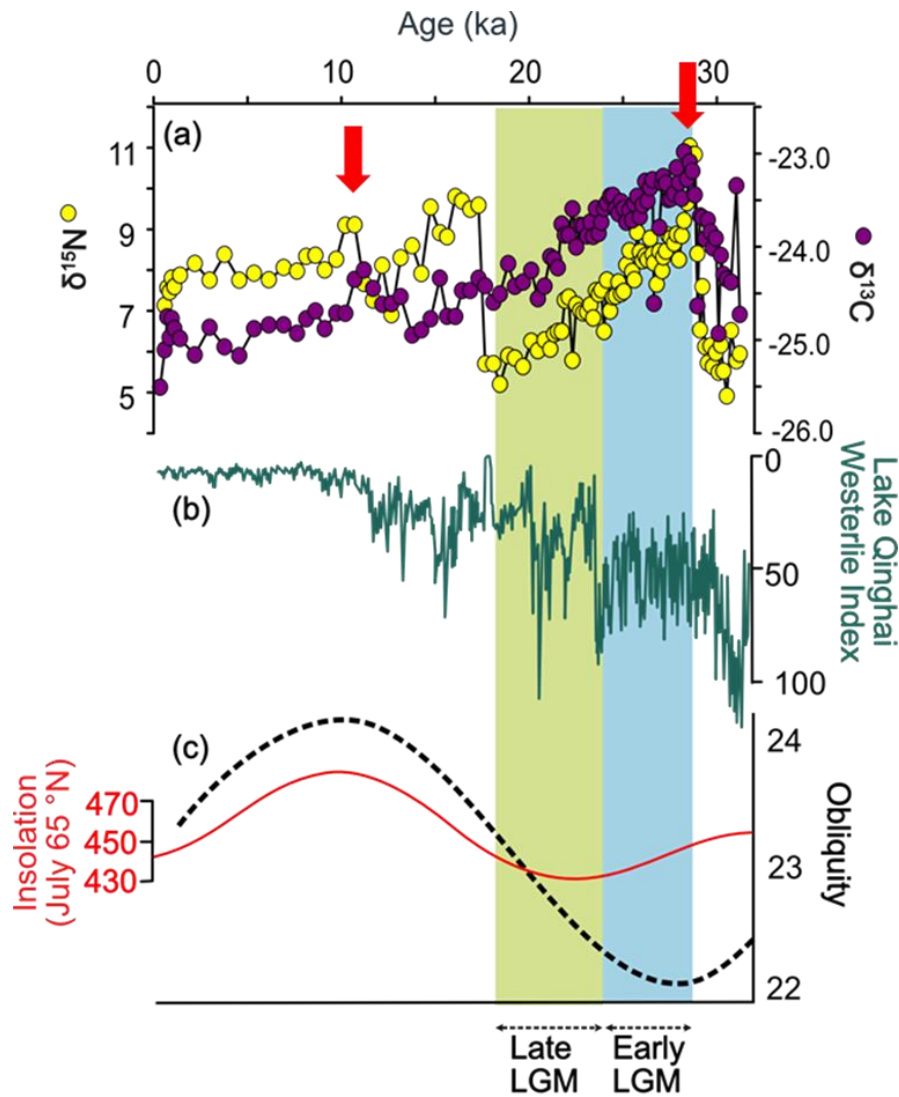
Figure 4.4 Comparison of our results with previously reported studies that showed the variation of westerlies during the LGM (a) $\delta^{13}C$ (violet dot) and $\delta^{15}N$ (yellow dot) of the Forest Block paleolake sequence, (b) westerlies Index (>25 μm grain size) from Lake Qinghai (An et al., 2012), and (d) Obliquity (represented by dotted line) and July Insolation (65°N) (represented by the red line) (Berger & Loutre, 1991). The red arrows are representing the extreme cooling period in the study are which coincided with globally reported H3 and YD event.
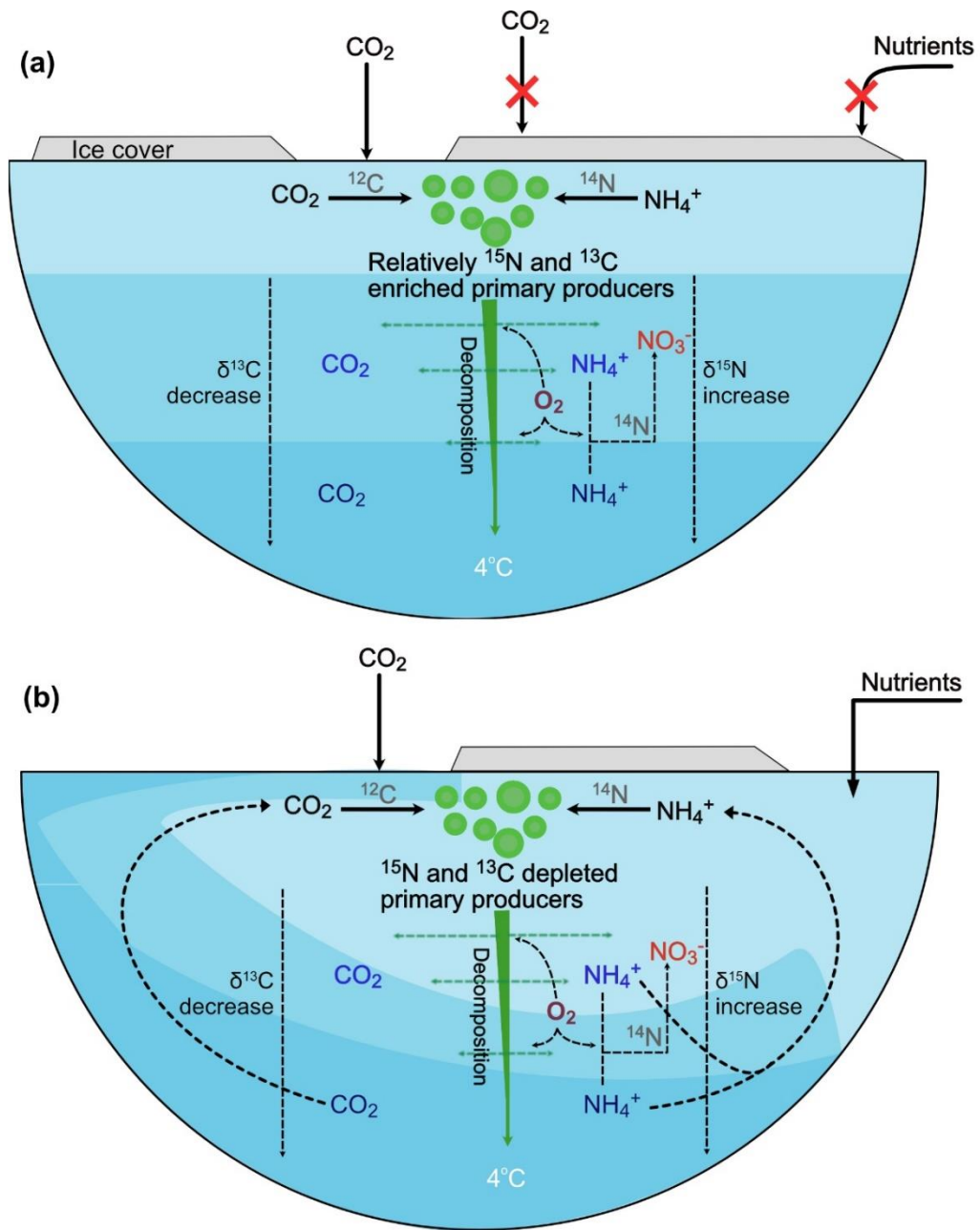
Figure 4.5 Schematic diagram of possible biogeochemical cycling in the Forest Block paleolake during (a) drier (colder) and (b) wetter (warmer) conditions.

As discussed earlier, the LGM has been defined as the period of maximum ice cover on the Earth. Clarke et al. (2009) suggested that the development of ice sheets was at their maximum between 33.0 and 26.5 ka due to the response of climate forcing from decreases in northern summer insolation, tropical Pacific sea surface temperatures, and

atmospheric CO_2. All ice sheets were at their LGM position during 26.5–20.0 ka. Another study by Ivy-Osch et al. (2008) from Alps Mountain has shown extensive glaciation between 30 and 18 ka, which was synchronous with the global ice volume maximum of MIS 2. In this study, a gradual decrease was observed in $\delta^{13}C$ and $\delta^{15}N$ from 28 to 19 ka, which included the LGM. Within this 28-19 ka time period, slight shift in both $\delta^{13}C$ and $\delta^{15}N$ was observed around ~ 24 ka. Based on this observation, this period (28-19 ka) could be divided into two phases of LGM, i.e., early LGM (28–24 ka) and late LGM (24–19 ka). Similar to this, two phases of the LGM have been reported earlier by Cheng et al. (2020) based on dust accumulation in loess deposits from the central Asia and the central loess plateau. However, the early LGM in Cheng et al (2020) has been classified as a time span between 26.5–23 ka and characterized by low dust accumulation compared to late LGM, which covered the period from 23 to 19 ka. Findings from other studies such as higher biogenic silica contents in the Lake Baikal of Siberia, higher Amphibole-epidote ratio from the central Asia, and the lower mean grain size for Jingyuan loess on the western central loess plateau during the early LGM (26.5–23 ka) compared to the late LGM (23–19 ka) suggested that the Siberian High was weaker during the early LGM than the late LGM (Prokopenko et al., 2006; Cheng et al., 2020, 2021). Additionally, increased dust collection in the Greenland ice during the early LGM compared to the late LGM suggested strong westerlies (Svensson et al., 2000). The stable isotope proxies used in this study revealed a steady increase in lake productivity, which could be attributed to a rise in temperature due to the weakening of westerlies during 28–19 ka. For the same time period, the weakening of westerlies has been previously reported in the central Asia (An et al., 2020; Cheng et al., 2020). Another study has shown that the westerlies strength was dominantly controlled by the variation in obliquity in the geological past (Jackson and Broccoli, 2003). It has also been reported that obliquity strongly affects the meridional insolation gradient between northern mid and high latitudes, especially in summer (Masson-Delmotte et al., 2006). The low obliquity allowed more radiation in mid-latitudes than the pole resulting in a steeper meridional insolation gradient (Loutre et al., 2004; Cruz et al., 2006). The lower obliquity supported a strong meridional insolation gradient, enhancing the strength of westerlies during the early LGM compared to late LGM (Fig.

4.4). Therefore, it seems more likely that strong westerlies during the early LGM (28–24 ka) lowered the temperature across the Kashmir Valley, resulting in ice-cover over the lake, which later melted with time owing to the weakening of westerlies. In summary, it appears likely that the strength of westerlies decreased due to an increase in obliquity from early to late LGM and influenced the high altitude Forest Block paleolake lake C and N biogeochemistry (Fig. 4.4 and Fig 4.5). In this regard, a detailed study to understand the interaction among strength of westerlies, Northern Hemisphere insolation, and western Himalayan environment is warranted.

4.4 Late Holocene environment (last 3.7 ka)

The Forest Block paleolake sequence has covered ~ 33 to 0.2 ka of the climate and environmental history of the Kashmir Himalaya. However, due to sparse resolution in the upper part of the Forest Block paleolake sequence, it was not possible to extract detailed information about the mid and late Holocene. In addition, the available paleoclimate studies from the Kashmir Himalaya also showed gaps in the environmental and climate information for the last 5 ka. As discussed earlier, other studies from the region were based on geochemical proxies and diatom assemblages and have not covered the stable isotope approach to unravel the past lake ecology and biogeochemical evolution during the Holocene. Therefore, by considering these aspects, two sediment cores, one each from the Wular and the Manasbal Lakes, were extracted to understand the environmental condition during the Holocene, particularly the late Holocene, of the Kashmir region.

4.4.1 Wular Lake

The Wular Lake, situated in the Bandipora district (34°16'-34°20'N and 74°33'-74°44'E), is one of the largest freshwater lakes in Asia with an average surface area of 189 km^2 (Shah et al., 2017). The lake is surrounded by the great Himalayan mountain range towards the northeastern side and the Pir-Panjal range towards the southwestern side. The Wular Lake receives most of its water from the Jhelum River draining through south and central Kashmir along with two small rivers (Madhumati and Erin) (Mushtaq and Pandey, 2014).

Presently, the surface water temperature of the lake varies from 6 ℃ during January to 27 ℃ during July (Ganai et al., 2010). The pH of the lake ranges from 8.8 during January to 7.0 during July (Rashid et al., 2013). Similarly, dissolve O_2 varies from the lowest 4.4 mg/l during July to the highest 12.0 mg/l during January (Ganai et al., 2010). The CO_2 and HCO_3^- vary from 4 to 16 mg/l (January to July) and 86 to 190 mg/l (July to January), respectively (Ganai et al., 2010).

The Wular Lake shows lotic and lentic nature consisting various types of phytoplankton, zooplankton, and macrophytes. The *Bacillariophyceae* (diatom) is one

of the most abundant phytoplankton in the lake, including *Chlorophyceae* (green algae)*,* *Cyanophyceae* (blue-green algae), and *Euglenophyceae* (Ganai et al., 2010; Ganai and Parveen, 2014). Shah and Pandit (2013) reported *cladoceran* (23 species) as one of the dominant zooplankton in the lake. On the other hand, *Ceratophyllum demersum* and *Potamogeton crispus* are dominant macrophytes in the lake.

Chronology

To establish the chronology, organic matter in five sediment samples were dated using AMS, which are shown in Table 4.2 with depths and corresponding calibrated ages. The obtained ages showed that Wular Lake sediment samples covered from 3.7 to 0.3 ka of the Holocene. The age-depth model plot for the same is shown in Fig. 4.6. In Wular Lake sediment samples, no reservoir correction has been performed as it was previously observed by Shah et al. (2020).

Table 4.2 Calibrated AMS ^{14}C ages (2σ error bar) of the Wular Lake sediment samples.

Sample ID	Depth (cm)	Cal Ages (ka BP)
	0	0.3
PRL 3651	48	0.9 ± 0.1
PRL 3579	90	1.9 ± 0.1
PRL 3655	144	2.4 ± 0.1
PRL 3656	186	2.5 ± 0.1
PRL 3657	216	3.3 ± 0.1
	Bottom	3.7
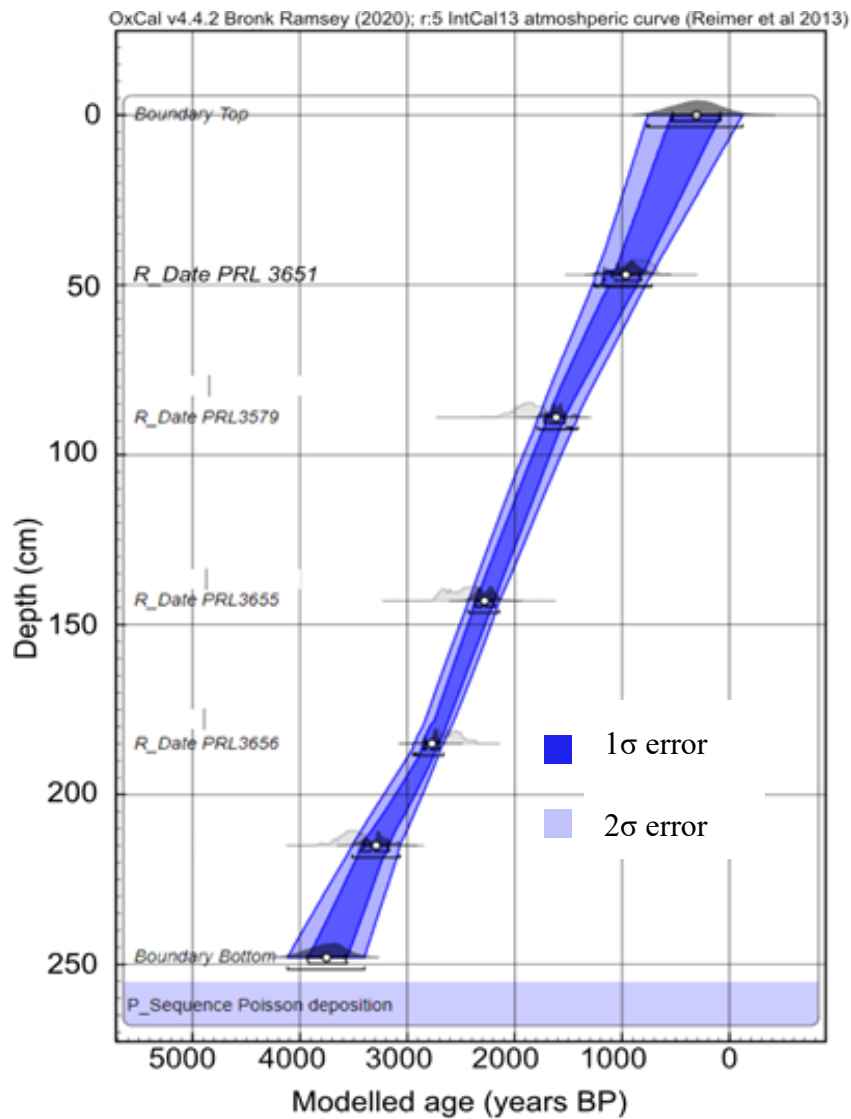
Figure 4.6 Age-depth model for the Wular Lake sediment core.

C and N isotopic compositions and their contents

As stated earlier, based on five radiocarbon ages, it has been found that the Wular Lake core covered between 3.7 ka to 0.3 ka of the Kashmir Himalayan climate history (Table 4.2). Between this time period, the down-core profiles of δ^{13}C, TOC, δ^{15}N, and TN data showed two distinct environmental phases, i.e., from 3.7 to 1.5 ka and 1.5 to 0.3 ka, that can be seen in Fig. 4.7 a-d.

The first phase, between 3.7 and 1.5 ka, showed relatively higher δ^{13}C (average: $-23.63 \pm 0.83‰$) and δ^{15}N (average: $5.32 \pm 0.70‰$) than the second phase and were

associated with lower TOC (average: 2.04 ± 0.70%) and TN (average: 0.22 ± 0.05%) contents. Within this phase, a sub-phase of higher $\delta^{13}C$ and $\delta^{15}N$ from 2.8 to 2.2 ka with $\delta^{13}C$ peak at 2.5 ka was also noticed.

The second phase, observed between ~ 1.5 and 0.3 ka, was characterized by relatively lower average $\delta^{13}C$ and $\delta^{15}N$ and higher TOC and TN contents than the first phase, i.e., − 26.27 ± 0.46‰, 4.17 ± 0.65‰, 3.83 ± 1.12%, and 0.38 ± 0.09%, respectively. The increasing trends in TOC and TN contents were noticed from ~ 1.5 to 1.0 ka. Between 1.0 and 0.3 ka, the TOC and TN contents showed an irregular pattern, while $\delta^{15}N$ (~ 5‰) showed a positive excursion at ~ 0.5 ka.

A positive correlation ($r^2 = 0.49$, $p < 0.001$) was observed between $\delta^{13}C$ and $\delta^{15}N$ (Fig. 4.8a), whereas $\delta^{13}C$ and TOC were negatively correlated ($r^2 = 0.68$, $p < 0.001$) (Fig. 4.8b). Similarly, $\delta^{15}N$ showed a strong negative correlation with TOC ($r^2 = 0.45$, $p < 0.001$; Fig. 4.8b) and TN contents ($r^2 = 0.61$, $p < 0.001$; Fig. 4.8c). Like $\delta^{13}C$ and $\delta^{15}N$, the TOC and TN contents were also positively correlated ($r^2 = 0.44$, $p < 0.001$; Fig. 4.8d).

Wular Lake paleobiogeochemistry and associated environmental changes

The temporal variation in $\delta^{13}C$, $\delta^{15}N$, TOC, and TN contents of the sediment samples from the Wular Lake showed a distinct pattern that suggested a change in the environmental condition of the Kashmir Valley during the last 3.7 ka (Fig. 4.7 and Fig. 4.9). In this study, C and N contents and their stable isotopic compositions revealed two distinct environmental phases. The first phase was observed from 3.7 to 1.5 ka and was characterized by a drier/colder climate as revealed by relatively higher $\delta^{13}C$ and $\delta^{15}N$ along with lower TOC and TN contents. This drier phase transitioned into a relatively humid/wet condition from 1.5 to 0.3 ka, which was registered as relatively low $\delta^{13}C$ and $\delta^{15}N$ with higher TOC and TN contents. A relatively drier period from 2.8 to 2.2 ka was noticed within the dry phase (3.7 to 1.5 ka), with an extreme dry event at ~2.5 ka. In addition, a drier event was also observed at ~ 0.6 ka within the warmer phase (1.5–0.3 ka), which was documented as high $\delta^{15}N$ with low TOC and TN contents. This drier event coincided with the "LIA" recorded in the Northern

Hemisphere (Grove, 2012). The temporal evolution of the C and N biogeochemistry of the Wular Lake, along with the global climate interconnection during these dry and wet phases, have been discussed below.
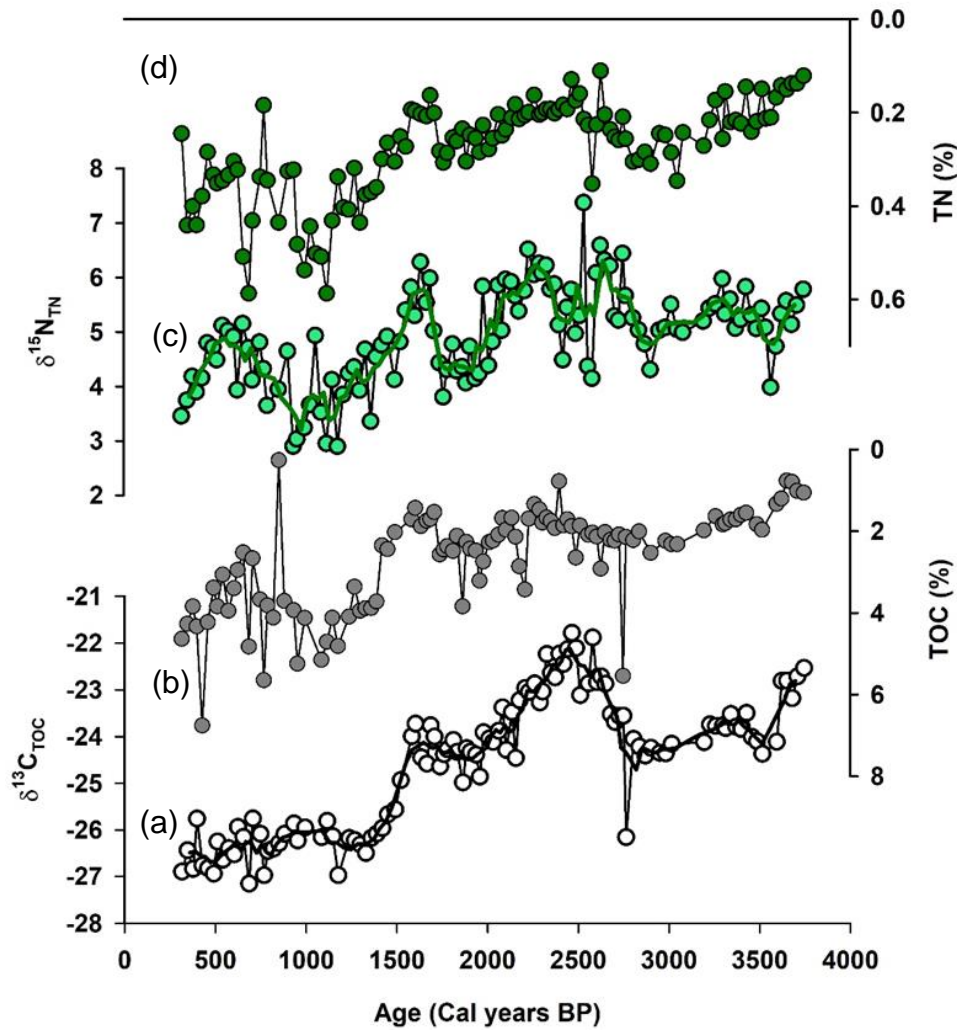
Figure 4.7 Temporal variation of (a) $\delta^{13}C$ and (b) TOC of organic carbon, and (c) $\delta^{15}N$ and (d) TN contents of bulk sediment in the Wular Lake samples.
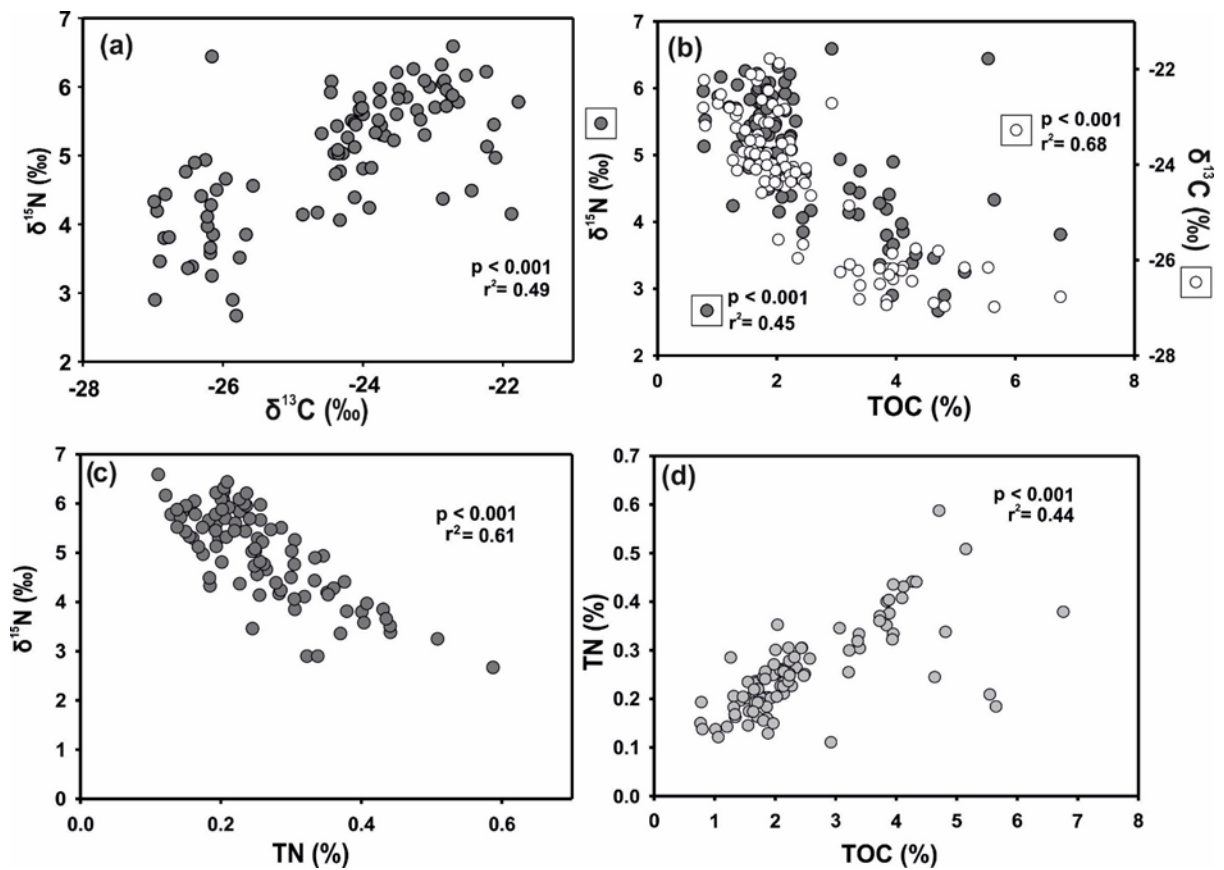
Figure 4.8 Scatter plots between (a) $\delta^{15}N$ and $\delta^{13}C$, (b) $\delta^{15}N$ ($\delta^{13}C$) and TOC (%) represented by grey (white) dots, (c) $\delta^{15}N$ and TN (%), and (d) TOC (%) and TN (%).

Carbon dynamics of the Wular Lake

Higher $\delta^{13}C$ and lower TOC content of organic matter could result from lower productivity and high HCO_3^- (and low CO_2) in the lake. It has been reported that the $\delta^{13}C$ of HCO_3^- is almost ~ 10‰ enriched than CO_2 (Paneth and O'Leary, 1985). A previous study showed that the HCO_3^- (CO_2) concentration was high (low) during the winter and low (high) during summer in the Wular lake (Ganai and Parveen, 2014). This was possibly due to lower runoff of glacial meltwater and consequent respired CO_2 through the Jhelum River into the lake. Evaporation is also found to be responsible for higher $\delta^{13}C$ of DIC in lakes during dry conditions (Talbot and Kelts, 1990). The geochemical, biochemical, and genetic-based studies have provided evidences of active uptake of HCO_3^- as a C source by the phytoplankton (diatom) during photosynthesis (Tortell et al., 1997; Hopkinson et al., 2011). *Bacillariophyceae* (diatom), being one of

the most abundant phytoplankton species in the Wular Lake (Ganai et al., 2010; Ganai and Parveen, 2014) can fractionate ~ -20.4‰ during photosynthesis (Hopkinson et al., 2011). The continuous primary productivity with ^{12}C preferential uptake of DIC can lead to enrichment in ^{13}C of the remaining DIC pool (Singer and Shemesh, 1995; Leng et al., 2005). It is likely that the new growth of phytoplankton in ^{13}C dominated DIC pool would result in higher $\delta^{13}C$ of organic matter. Therefore, the availability of higher HCO_3^- with high $\delta^{13}C$ in the lake due to low runoff and higher evaporation, slow metabolism, and presence of diatom could be controlling factors for the observed higher $\delta^{13}C$ of the organic matter. Taken together, all these evidences point towards the existence of a drier/colder phase between 3.7 and 1.5 ka.

Relatively lower $\delta^{13}C$ and higher TOC contents observed in the sediment samples during 1.5 to 0.3 ka suggested higher productivity in the lake, possibly due to larger inputs of bioavailable nutrients (N and P) transported through the Jhelum River (and glacial meltwater) and precipitated water. As mentioned above, CO_2 was relatively higher during summer, probably due to glacial meltwater passing through the catchment of Jhelum, which could be a possible source of soil respired CO_2. There could also be increased input of terrestrial organic matter to the Wular Lake leading to relatively lower $\delta^{13}C$. All these above evidences point to the fact that relatively lower $\delta^{13}C$ and higher TOC contents could be a result of wetter/warmer environment during 1.5 to 0.3 ka.

Nitrogen dynamics in the Wular Lake

Due to low productivity and nutrient limiting condition during drier/colder period, C loading to the lake was relatively low that enhanced the activity of nitrifying bacteria in the lake (Strauss and Lamberti, 2000; Hadas et al., 2009). The inverse relationship between $\delta^{15}N$ and TOC contents suggested the effect of C loading on the $\delta^{15}N$ of organic matter (Fig. 4.8b). In a lake, during the colder condition, when runoff is low with no or low terrestrial C input, the nitrifying bacteria converts the available NH_4^+ into NO_3^- by preferentially incorporating $^{14}NH_4$ into the process. This results in the enrichment of $^{15}NH_4$ in the remaining nutrient pool (Hadas et al., 2009). During the

warm condition, when productivity and influx of terrestrial C increases, the heterotrophic microbial degradation dominates over the nitrification resulting in low oxygen condition (Strauss and Lamberti, 2000; Lehmann et al., 2002). The low oxygen condition in a lake has the potential to enhance denitrification, converting NO_3^- to N_2. This results in the enrichment of NO_3^- pool in ^{15}N (Hadas et al., 2009). This isotopically enriched NO_3^- trapped in the hypolimnion during summer due to stratification could come up to the surface during winter mixing. Uptake of these ^{15}N enriched NO_3^- and NH_4^+ through photosynthesis can lead to relatively enhanced $\delta^{15}N$ of the organic matter, which appears to be the case during the drier period of the present study. Within the drier condition, $\delta^{15}N$ showed three positive excursions (~ 2.6, 2.3, and 1.6 ka) which could be due to the relatively higher nitrification of the limited nutrient pool, suggesting extreme drier/colder conditions.

The lower $\delta^{15}N$ and higher TN contents observed during 1.5 to 0.3 ka (Fig. 4.7 and 4.8c) suggested high productivity [including nitrogen fixers; 0‰ (Montoya et al., 2002)] in the lake with a large input of nutrients (lower $\delta^{15}N$) due to high runoff through the Jhelum river suggesting warmer/humid condition in the Kashmir Himalaya during that period. Increased supply of terrestrial organic matter due to wet climate and increase runoff might have also contributed to the lowering of $\delta^{15}N$. Based on $\delta^{15}N$ and TN data, it appeared that the Kashmir Himalayan climate was relatively wetter from 2.0 to 1.7 ka and 1.5 to 0.3 ka. Within the warmer period of the last 1.5 ka, an excursion of high $\delta^{15}N$ was observed at ~ 0.5 ka, which suggested a drier condition. In addition, it could be seen that $\delta^{15}N$ varied differently than $\delta^{13}C$. The $\delta^{15}N$ and TN values during the last 1.5 ka showed an irregular pattern suggesting disturbed N dynamics in the lake, possibly due to agricultural activities known to exist in the region since the last 1.5 ka.
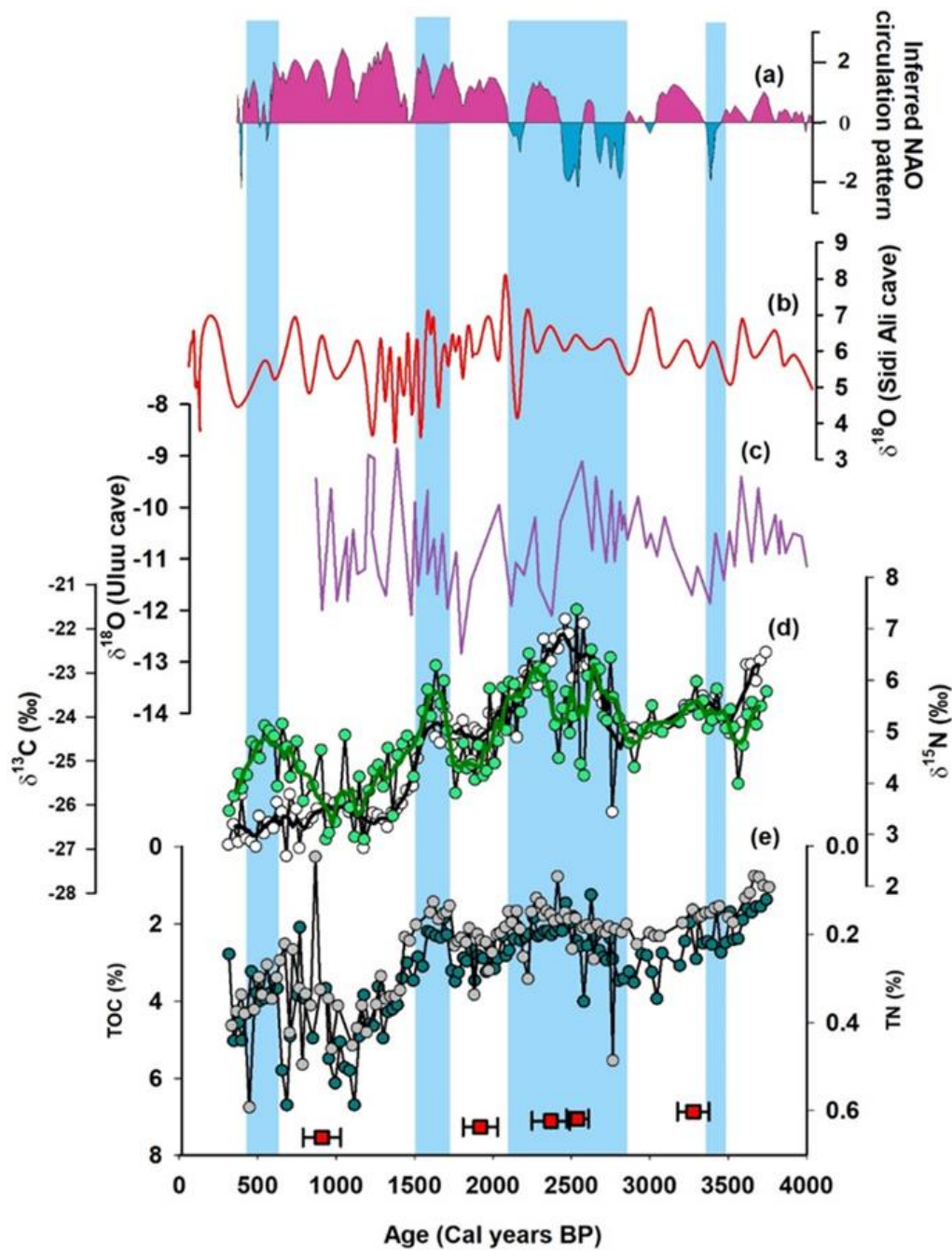
Figure 4.9 Comparison of variation in (a) NAO circulation pattern, (b) δ^{18}O-Sidi Ali Lake, (c) δ^{18}O-Uluu Too cave with the data from the present study including (d) δ^{13}C of organic carbon (white dots) and δ^{15}N of bulk sediments (green dots), and (e) TOC and TN percentage represented by grey and dark green dots, respectively. Red square boxes (with bar) are representing the Cal year (std. error).

Paleoclimate interpretation and possible mechanisms

The reconstruction of the past environment based on the Wular Lake sediment core data of $\delta^{13}C$, $\delta^{15}N$, TOC, and TN suggested that the Kashmir Himalaya was characterized by a larger dry phase before 1.5 ka, which was interspersed by extreme drier episodes between 2.8 and 2.2 ka with its maximum at ~ 2.5 ka (Fig. 4.6). The dry phase transitioned to the wet phase after 1.5 ka until 0.3 ka. This wet phase was interrupted by another dry event at ~ 0.6 ka. Overall, the present study results appeared to be largely in agreement with the previous studies based on different proxies and archives from the region (Babeesh et al., 2019; Lone et al., 2020; Ali et al., 2021). For example, Lone et al. (2020), through differences in geochemistry, mineral magnetism, grain size, and C/N ratio in Anchar Lake sediments, revealed moderate precipitation during 3.9–2.5 ka and 2.5–1.6 ka with catchment stability and cold/dry condition in the Kashmir Valley. They also reported weak westerlies-induced precipitation during ~ 0.6 ka. Babeesh et al. (2019) also observed a drier period from ~ 3.3 to 3.1 ka and 2.5 to 1.8 ka based on changes in grain size, major and trace elements, TOC, organic matter contents, C/N ratios, and diatom assemblage in the Manasbal Lake.

The reconstructed climate from the westerlies-dominated central Asian region also seemed to be in agreement with the present results, demonstrating similar changes in climate and environment during the late Holocene (Fig. 4.9). The results of this study appeared to be comparable with the $\delta^{18}O$ record of the Uluu-Too cave from *Kyrgyzstan*, which showed a drier climate between 3.0 and 2.5 ka and a wetter climate after 1.7 ka (Wolff et al., 2017). In contrast to the present results, Uluu-Too $\delta^{18}O$ record showed a warmer condition at 2.5 ka. Climate records from the Bosten lake in China showed similar changes during the late Holocene, such as drier climate at 3.9–3.6, 3.4–3.2, 2.6–2.5, 1.9–1.1, 0.5–0.3 ka with some intermittent wetter periods (Wünnemann et al., 2006). The $\delta^{18}O$ records from the Sidi Ali Lake in Morocco also showed peaks at 3.3, 2.7, 2.1 ka, and LIA corresponding to the low North Atlantic Oscillation (NAO) stages (Olsen et al., 2012; Zielhofer et al., 2019). Largely, the drier periods observed in the studies mentioned above were temporally in agreement with our results and also interlinked to the negative NAO phases. So far, several studies have shown a strong

connection between NAO and temperature/precipitation in the Northwestern Himalaya (Archer and Fowler, 2004; Bhutiyani et al., 2007; Bookhagen, 2010; Iqbal and Ilyas, 2013; Sharif et al., 2013; Zaz et al., 2019). A recent detailed study by Zaz et al. (2019) has shown a negative (positive) correlation between NAO and average winter temperature (precipitation) in the western Himalaya from 1980 to 2016 AD. The notable excursions of drier climate in our results during ~ 3.3, 2.8 to 2.2, 1.5, and ~ 0.5 ka coincided (within the range of ^{14}C ages error) with the negative mode of NAO. It implied that NAO controlled westerlies were not strong enough to transport moisture to western Himalaya, resulting in a drier climate and low lake productivity. On the other hand, the wetter period from 1.5 to 0.3 ka was controlled by the NAO-originated westerlies-induced precipitation.

4.4.2 Manasbal Lake

Manasbal Lake, one of the deepest (12–14 m) freshwater lakes in India, is located about 30 km north of the Srinagar in the Union Territory of Kashmir (34°14'40″–34º15′20″ N and 74°39'00″–74º41′20″ E) at an altitude of 1584 m above mean sea level (Fig. 4.10). Winter and spring precipitation, as well as groundwater, are the sources of water in the Manasbal Lake. The lake is also seasonally supplied by the irrigational stream Larkul on its eastern side, which is only operative during the summer. The volume of the water in the lake has been estimated as 12.8×10^6 m^3 (Yousuf, 1992). A 1.6 km Nunnyar Nalla near Sumbal village is the outlet of the lake through which the lake water drains into the Jhelum River.
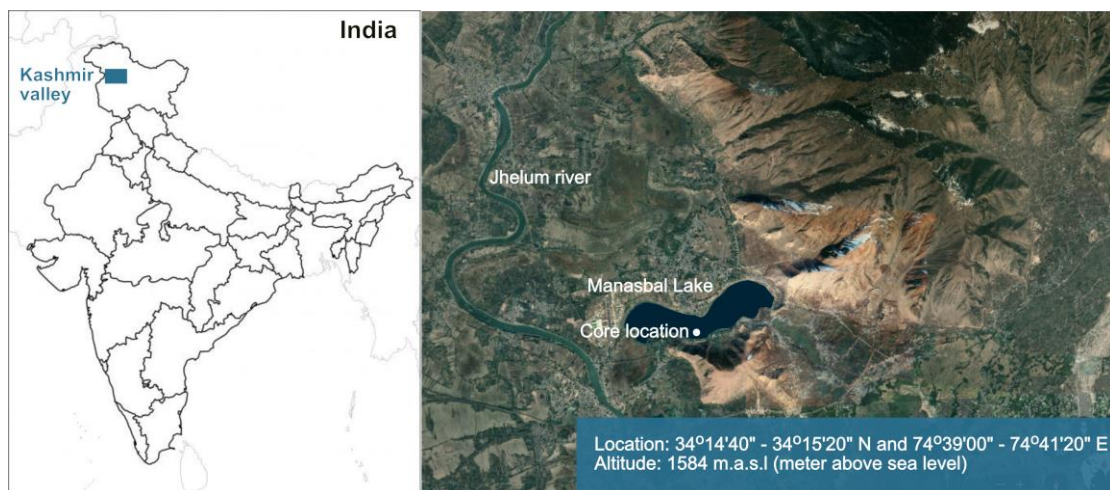
Figure 4.10 Map of India and the Manasbal Lake with its location and altitude. The white dot represents the location of the core in the Manasbal Lake.

Chronology

For the chronology of the Manasbal Lake sediment samples, organic matter in three sediment samples were dated at different depths (Table 4.3) using AMS. Based on previous studies, it has been found that no reservoir effect has been noticed in the lakes of the Kashmir valley (Babeesh et al., 2019; Shah et al., 2020; Lone et al., 2020). Therefore, in this study, no reservoir correction has been performed. The age of the samples, depth, and their corresponded ages are mentioned in Table 4.3 and shown in Fig. 4.11.

Table 4.3 Calibrated AMS ^{14}C ages (2σ error bar) of the Manasbal Lake sediment samples.

PRL ID	Sample depth (cm)	Cal ages (ka Cal BP)
PRL 3583	9	0.6 ± 0.1
PRL 3584	69	1.5 ± 0.2
PRL 3586	177	3.1 ± 0.3
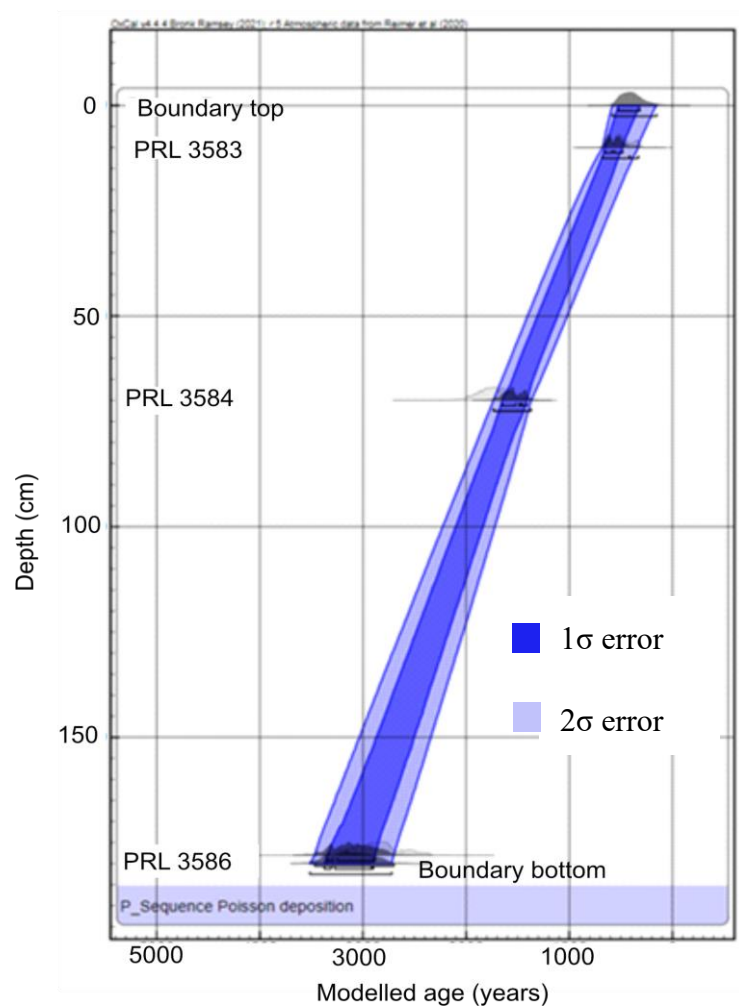
Figure 4.11 Age-depth model of the Manasbal Lake sediment samples.

Temporal variation of stable isotopes in the Manasbal Lake sediment samples

The samples of the Manasbal Lake have been analysed for $\delta^{13}C_{AC}$, $\delta^{18}O_{AC}$ (AC: authigenic carbonate), $\delta^{13}C_{Diatom}$, and $\delta^{15}N$ of bulk sediments for the reconstruction of paleoclimate and paleoenvironment along with the lake biogeochemical evolution between 3.1 and 0.4 ka of time span in the Holocene period. The temporal variations in measured stable isotopic compositions of the Manasbal Lake samples are shown in Fig. 4.12 (a-d). The $\delta^{13}C_{AC}$ and $\delta^{13}C_{Diatom}$ varied between − 2.8 and ∼ − 0.1‰ (average: − 1.7 ± 0.7‰) and − 26.8 and − 19.5‰ (average: − 24.2 ± 1.7‰), respectively (Fig. 4.12a and b). The $\delta^{15}N$ showed a significant variation, i.e., from 0.3 to 3.9‰ with an average of 2.2 ± 0.9‰ (Fig 4.12c). The $\delta^{18}O_{AC}$ in the Manasbal Lake sediment samples ranged from − 9.2 to − 6.5‰ (average: − 7.7 ± 1.6‰) (Fig. 4.12d).

The $\delta^{13}C_{AC}$ showed lower values (average − 2.2 ± 0.5‰) during 3.1–2.8 ka (Fig 4.12a) to increase sharply (− 0.9‰) after that and continued with relatively higher values (average: − 0.8 ± 0.4‰) up to 1.8 ka (Fig 4.12a). Subsequently, $\delta^{13}C_{AC}$ showed a sudden decrease (average − 1.8 ± 0.3‰) and remained so until ∼ 0.4 ka. (Fig 4.12a). On the other hand, the $\delta^{18}O_{AC}$ showed lower values during 3.1–2.8 ka (− 9.3 to − 8.2‰). Afterward, a sudden increase in $\delta^{18}O_{AC}$ was noticed at ∼ 2.8 ka (− 7.4‰) that continued with relatively higher values up to ∼ 1.8 ka (− 6.7‰) (Fig 4.12d). A sudden decline at ∼ 1.8 ka in $\delta^{18}O_{AC}$ (− 6.7 to ∼ − 8‰) was observed to follow an increasing trend up to 0.4 ka (Fig. 4.12d).

The Manasbal Lake sediment samples showed $\delta^{15}N$ values close to 0‰ (average 0.8 ± 0.4‰; excluding 3.7‰ at 174 cm depth) from 3.1 to 2.8 ka (Fig 4.12c). An increase in $\delta^{15}N$ (2.2‰) was noticed at 2.8 ka, which continued up to ∼ 1.8 ka (2.6‰) with slight fluctuations and overall average of 1.7 ± 0.6‰ (Fig 4.12c). Further, $\delta^{15}N$ showed an increase at 1.8 ka (3.8‰) to decrease gradually up to 0.4 ka with an average of 2.9 ± 0.5‰ (Fig 4.12c).

The $\delta^{13}C_{Diatom}$ showed a sharp increase from − 24.8‰ at 3.1 ka to around − 21‰ at 2.8 ka, which continued up to 2.4 ka with an average of − 21.3 ± 0.9‰ (Fig 4.12b). It decreased again to − 25‰ at 2.2 ka. Unlike $\delta^{13}C_{AC}$, $\delta^{18}O_{AC}$, and $\delta^{15}N$, $\delta^{13}C_{Diatom}$ did

not show change at around ~ 1.8 ka, rather it showed at around ~ 2.2 ka to slight increase again up to − 22‰ at ~1.8 ka. It showed gradual decline from 1.8 to 0.4 ka.

No correlation was observed between $\delta^{13}C_{AC}$ and $\delta^{18}O_{AC}$, whereas $\delta^{13}C$ of authigenic carbonate and occluded organic matter within diatom showed a significant correlation ($r^2 = 0.32$, $p < 0.001$, n = 76).

Oxygen isotopic composition of authigenic carbonate in the Manasbal Lake sediments

The $\delta^{18}O_{AC}$ has been extensively used to infer the changes in surface temperature and oxygen isotopic composition of lake water (Valero-Garcés et al., 1997; Zanchetta et al., 2007; Kalm and Sohar, 2010). The $\delta^{18}O_{AC}$ in the sediment samples from the Manasbal Lake showed fluctuating values with an overall increasing trend from the bottom to top of the core, which corresponded to 3.1 to 0.4 ka, respectively (Fig. 4.12d). The lower $\delta^{18}O_{AC}$ observed between 3.1 and 2.8 ka suggested higher precipitation and glacial meltwater as water influx to the lake, which indicated the wetter and warmer conditions in the Kashmir Himalaya. The glacial meltwater has relatively lower $\delta^{18}O$ compared to precipitated water in the region. Therefore, it might be possible that the Manasbal Lake was open during 3.1–2.8 ka and received water from the glacial melt through the Jhelum River. As Manasbal Lake is not presently directly connected to the Jhelum River, it is being speculated based on the $\delta^{18}O_{AC}$ record that the Jhelum River might have been a source of water to the Manasbal Lake during 3.1–2.8 ka. However, this speculation needs to be verified through multi-proxy data. Overall, it appeared that glacial (or ice) meltwater might have been the controlling factor for lower $\delta^{18}O_{AC}$ during 3.1–2.8 ka as it was a common phenomenon in the Himalayan region. Babeesh et al. (2019) also reported wet condition during 3.3–2.5 ka based on chemical weathering index (CWI) and diatom assemblages in the Manasbal Lake sediment samples. Following this wet climatic condition, a dry phase was noticed during 2.8–1.8 ka as documented by relatively higher $\delta^{18}O_{AC}$ (and high $\delta^{13}C_{AC}$; Fig. 4.12), which indicated high evaporative condition in the region. The average $\delta^{18}O_{AC}$ during this period was relatively higher with a maximum difference of ~ 2.6‰. During this drier condition, low runoff through glacial meltwater and low precipitation along with high evaporation might have existed

in the region, resulting in the enhancement of $\delta^{18}O_{AC}$. Horton et al. (2015) reported covariation in carbonate $\delta^{18}O$ and $\delta^{13}C$ in > 70% of the globally recorded studies, which was observed for 2.8 to 1.8 ka during the present study as well. Additionally, several experimental studies have shown enhancement in heavier C and O isotopes during evaporation in most of the lakes and lacustrine carbonate records (Horton et al., 2015). The drier period between 2.8 and 1.8 ka observed in the present study coincided with the cold and dry conditions observed between 3.4 and 1.5 ka based on the $\delta^{13}C$ of soil organic matter record from the Zanskar Valley, western Himalaya (Ali et al., 2020). Relatively lower $\delta^{18}O_{AC}$ between 1.8 and 0.6 ka suggested comparatively higher precipitation conditions in the region up to 0.6 ka. This warm condition coincided with the time range of Medieval Climate Anomaly (950 and 1250 AD; 1.05 and 0.7 ka; Mann et al., 2009). After 0.6 ka, a drier period was noticed between 0.6 and 0.4 ka, which was documented by relatively higher $^{18}O_{AC}$. This drier condition coincided with the LIA (Mann et al., 2009) and was characterized by low precipitation and high evaporation condition in the region.

Lake Carbon dynamics during the late Holocene

The $\delta^{13}C_{AC}$ and $\delta^{13}C_{Diatom}$ of the Manasbal Lake sediment samples showed a significant positive correlation that suggested a common C source (Fig 4.12 a & b). The lower $\delta^{13}C_{AC}$ and $\delta^{13}C_{Diatom}$ during 3.1–2.8 ka probably indicated that the lake was CO_2 enriched due to high runoff owing to wetter climate conditions in the Kashmir Himalaya. This might have been possible due to the addition of glacial melt/Jhelum water, which probably transported respired/decomposed CO_2 and organic matter to the lake resulting in lower $\delta^{13}C$ of DIC. The rivers or streams that move across vegetated lands are prone to receive highly decomposed leached soil organic matter and are generally supersaturated in CO_2 (Mayorga et al., 2005). When such a stream feeds a lake, biological and abiotic processes lead to CO_2 saturation and net heterotrophy (Duarte and Prairie, 2005; Pierre et al., 2019; Looman et al., 2021). A sharp increase in $\delta^{13}C_{AC}$ and $\delta^{13}C_{Diatom}$ at 2.8 to 2.4 ka probably indicated decreased CO_2 availability in the lake due to low or no glacial melt/Jhelum River water, resulting in the shifting of lake biology from heterotrophy to autotrophy. As autotrophic production started with

low CO_2 availability, the C isotope fractionation increased with productivity. Also, the CO_2 evasion during the evaporation in the lake could reduce the CO_2 concentrations (Horton et al., 2015). It has been reported through observations and culture experiments that diatom prefers both CO_2 [$\delta^{13}C \sim -8$‰ for atmospheric CO_2 and -28 to -32‰ for respired CO_2 (McCallister and Del Giorgio, 2008)] and HCO_3^- ($\delta^{13}C \sim 0$‰) for photosynthesis. Taken together, all the above-mentioned points indicated that during 2.8–2.4 ka, the climate was drier with low runoff of glacial melt and precipitated water to the lake resulting in relatively higher $\delta^{13}C_{AC}$ and $\delta^{13}C_{Diatom}$. Between 2.2 and 1.8 ka, $\delta^{13}C_{AC}$ and $\delta^{13}C_{Diatom}$ showed an inverse relationship. Before 2.2 ka, there were few samples (60 to 65 cm depth) in which carbonate was not found. The $\delta^{13}C_{Diatom}$ showed lower values during 2.4–1.8 ka, which was interpreted as a drier period based on $\delta^{13}C_{AC}$ and $\delta^{18}O_{AC}$. It might be possible that diatom metabolism and carbonate precipitation have different C sources during winter and summer seasons of a dry or wet phase. It was likely that the lake was well mixed during the winter season, leading to the upwelling of respired CO_2. In addition, it is well known that diatom growth is dominant during the colder condition, whereas carbonate precipitates during summer when the lake stratifies. The low $\delta^{13}C_{Diatom}$ along with higher $\delta^{13}C_{AC}$ possibly reflected the intense lake winter mixing during 2.4–1.8 ka resulting in depleted ^{13}C-CO_2 source for the primary productivity in epilimnion during the winter. In the Manasbal Lake, it has been shown that the pH of hypolimnion is lower than the surface water due to the continuous addition of CO_2 through decomposition. It is likely that the diatom metabolism at the surface preferred respired hypolimnion CO_2, whereas higher $\delta^{13}C_{AC}$ indicated carbonate precipitation from high $\delta^{13}C$-DIC during summer. Overall, $\delta^{13}C_{AC}$ and $\delta^{13}C_{Diatom}$ covaried (gradual decreased) along with a gradual increase in $\delta^{18}O_{AC}$ indicating a wetter condition between 1.8 and 0.4 ka. This wetter period coincided with the moderate expansion of broad level, non-boreal pollen, and ferns between ~ 1.2 and 0.6 ka from the Chandra valley, western Himalaya, under climate amelioration (Rawat et al., 2015).

Nitrogen dynamics of the Manasbal Lake during the late Holocene

The $\delta^{15}N$ of the bulk sediments of the Manasbal Lake samples showed the evolution of nitrogenous nutrient dynamics and associated biogeochemical processes in the lake during 3.1–0.4 ka. The lower $\delta^{15}N$ (average 0.8 ± 0.4‰, n = 9, most of the values were less than 1‰) along with $\delta^{18}O_{AC,}$ $\delta^{13}C_{AC,}$ and $\delta^{13}C_{Diatom}$ indicated wetter and warmer climate condition between 3.1 and 2.8 ka with possible dominance of N_2-fixers as primary producers in the Manasbal Lake. Previous work has shown the Manasbal Lake to be monomictic with summer stratification throughout the year, except December to late February (winter season) (Vass, 1973). The higher productivity during the summer in a lake creates a limited nutrient condition resulting in the shift of biology from reactive N dependent species to N_2 fixers (~ 0‰). A slight increase in $\delta^{15}N$ during the drier period between 2.8 and 1.8 ka might have resulted from the input of nutrients (NH_4^+ and NO_3^-) due to vertical mixing in the lake (Wurtsbaugh et al., 1985; Hadas et al., 2009). A previous study has shown that the anoxic hypolimnion water has high NH_4^+ concentration in the Manasbal Lake (Yaseen and Yousuf, 2013). Low or no oxygen availability in the lake has been identified as a possible cause of low/no nitrification resulting in the low $\delta^{15}N$ of NH_4^+ pool (Hadas et al., 2009). During the drier/colder period when vertical mixing was dominant, the NH_4^+ entrained to the surface might have been consumed by the phytoplankton leading to slight shift/increase in the $\delta^{15}N$. Within this dry period, higher $\delta^{15}N$ was noticed at ~ 2.3 ka along with a sudden decrease of $\delta^{13}C_{Diatom}$ suggesting a potential shift in the climate from drier to wetter for a short period. Afterward, the higher $\delta^{15}N$ between ~ 1.8 and ~ 0.4 ka showed high productivity and high consumption of the transported soil nutrients to the lake through runoff due to wet climate conditions. It has also been reported that the civilization in the Kashmir Valley started around ~ 2.0 ka resulting in an increase in agricultural, deforestation, and fire activities in the region that might have additionally affected the N dynamics of the lake between ~ 1.8 and ~ 0.4 ka.
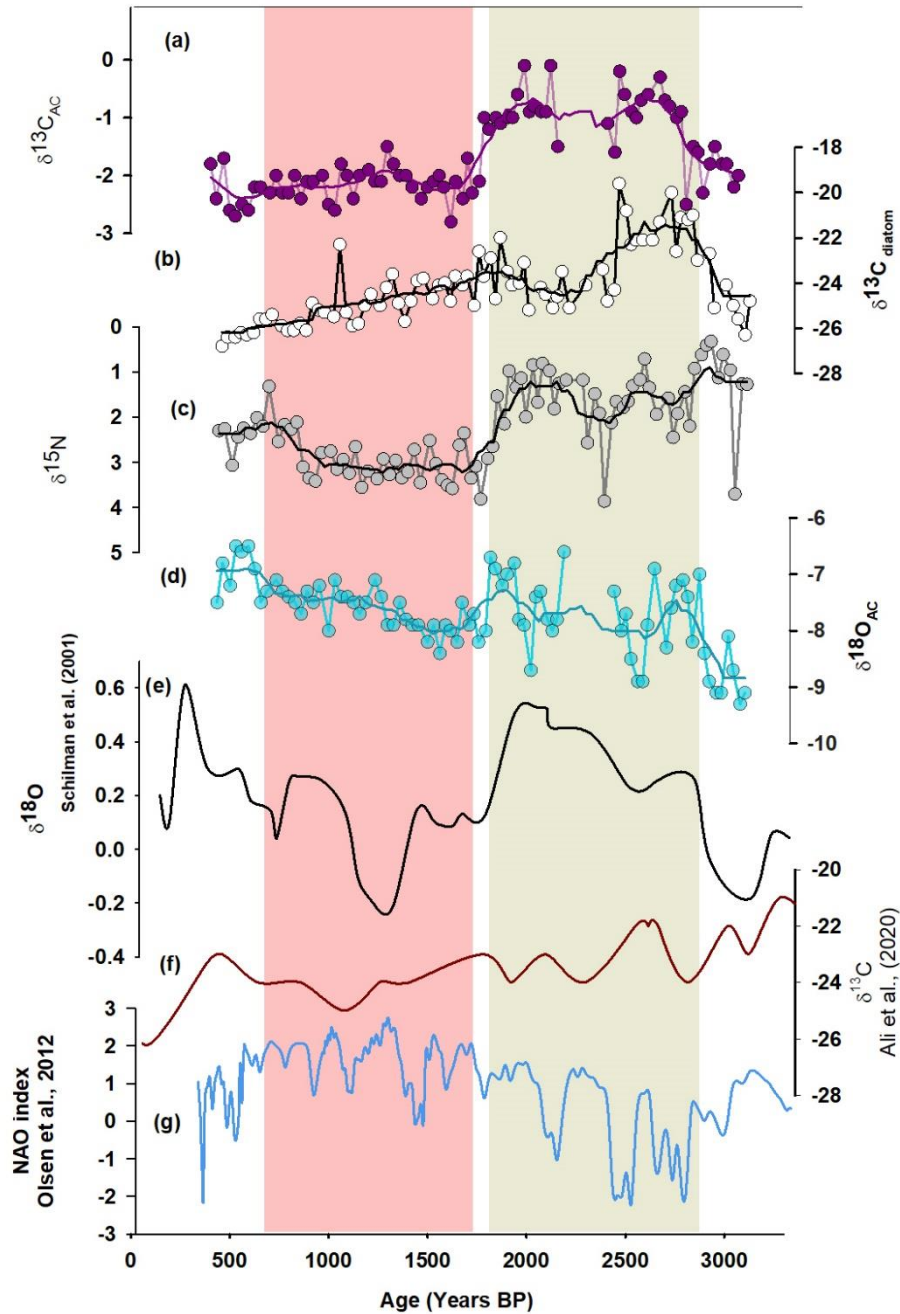
Figure 4.12 Comparison of temporal variation in (a) $\delta^{13}C_{AC}$, (b) $\delta^{13}C_{Diatom}$, (c) $\delta^{15}N$, (d) $\delta^{18}O_{AC}$ with (e) $\delta^{18}O$ of foraminifera from eastern Mediterranean Sea (Schilman et al., 2001), (f) $\delta^{13}C$ of soil organic matter (Ali et al., 2020), and (g) NAO index (Olsen et al., 2012). The light golden and pink color bars represent dry and wet periods, respectively recorded in the Manasbal Lake sediment samples.

Paleoclimate interpretation and possible mechanism

The fluctuations in reconstructed environmental conditions in the present study, i.e., wet and dry episodes, display coherency with other Northern Hemisphere climate records. There are similarities between shift in climate/environment phases witnessed in the Kashmir Himalaya during this study with that of observed through $\delta^{18}O$ of sediment core records from the eastern Mediterranean Sea and the strengthening of NAO (Fig. 4.12). Middle-latitude westerlies dominantly controlled the climate of the western Himalaya as primary moisture source during winter and spring (Dimri et al., 2015), which was largely transported from the North Atlantic, Mediterranean, Black, and Caspian Seas. A recent study from the Kashmir Valley has shown a positive correlation between NAO and precipitation in the region and a negative correlation between NAO and temperature (Zaz et al., 2019). Also, a more complex interplay between the Eurasia and Pacific circulation system based on modelling data and generally high delivery of moisture into central Asia during episodes of strengthened westerlies has been proposed (positive NAO phase; Syed et al., 2010). A wet climate condition observed during 3.1–2.8 ka from the sediment core of the Manasbal Lake during this study coincided with the $\delta^{18}O$ based precipitation in the eastern Mediterranean Sea during 3.5–3.0 ka (Schilman et al., 2001) and $\delta^{15}N$ based precipitation reconstruction at Son Kol during ~ 3.5–2.9 ka (Lauterbach et al., 2014). This wet phase was mainly caused by the westerlies-induced winter precipitation due to the positive NAO phase. The dry/cool period between 2.8 and 1.8 ka observed in this study coincided with lower precipitation in the Zanskar valley (Ali et al., 2020) and more arid condition in the southeastern Mediterranean Sea (i.e., between 3.0 and 1.7 ka) due to weak westerlies (negative NAO) (Schilman et al., 2001). This colder period also coincided with the Dark Age Cold Period (Martín-Chivelet et al., 2011). Followed by this drier period, similar to our results, the paleoclimate records from the Mediterranean, Son Kol, and other parts of the western Himalaya also showed a relatively humid/wet phase between 1.8 and 0.6 ka coinciding with the Medieval Climate Anomaly and positive NAO phase. The $\delta^{15}N$ and $\delta^{18}O_{AC}$ in this study showed a colder period between 0.6 and 0.4 ka, which coincided with the LIA, a period of negative NAO phase. In summary, the western Mediterranean $\delta^{18}O$ record, the Zanskar

valley $\delta^{13}C$ record, δD based moisture record from the Karakuli and Son Kol, along with this study showed the western Himalayan region and central Asian climate to be dominantly controlled by the different phases of NAO during the late Holocene.

4.5 Conclusion

In this chapter, an attempt has been made to understand the paleoenvironment of the western Himalaya during 33–0.2 ka by using stable isotopic compositions of different components of the lake sediments from three different live and paleo-lakes in the Kashmir Himalaya. The significant findings are as follows.

The western Himalayan region experienced strong cold westerlies during the early LGM, resulting in freezing of the high altitude Forest Block paleolake, which registered elevated stable isotopic compositions. The lake appeared to have limited contact with the atmosphere due to frozen surface with little or no nutrient influx. From early to late LGM, the weakening of westerlies enhanced the melting of ice cover resulting in increased exchange of atmosphere-water CO_2 and nutrient supply in the lake. Two prominent colder periods were observed during the last 30 ka from the Forest Block paleolake stable isotope study, which coincided with the Heinrich (H3) and YD event.

The late Holocene records from the Wular Lake showed two distinct climate/environmental phases, i.e., the period from 3.7 to 1.5 ka, which showed signatures of drier climate with extreme dryness at 2.5 ka. This dry phase transitioned into wet/humid phase from 1.5 to 0.3 ka. A dry event was noticed at 0.6 ka within the wetter period, which coincided with the LIA. The Jhelum River runoff/meltwater played a significant role in the Wular Lake C and N biogeochemistry during the late Holocene. This study suggested that the lake transitioned into net heterotrophy from autotrophy due to riverine input transporting terrestrial organic C.

The Manasbal Lake stable isotope data suggested a wet period from 3.1 to 2.8 ka, which transitioned into a drier climate from 2.8–1.8 ka as suggested by signatures of high evaporation. This drier climate transitioned into a wetter climate after 1.8 ka, which continued up to ~ 0.6 ka. The dry and wet climate observed in the Kashmir Valley from the present results along with previous studies showed an agreement with weak

and strong NAO phases, respectively. During drier climate, based on stable isotopes records, it has been indicated that the lake was well mixed and the hypolimnion nutrients and CO_2 largely controlled the C and N biogeochemistry. During the wetter period, however, the C and N biogeochemistry of the Manasbal Lake was primarily controlled by transported nutrients and CO_2 through the stream or river in the region. Taken together, signatures from both Wular and Manasbal Lakes using different stable isotopic data suggested largely similar environmental/ climate patterns, i.e., largely drier climate prior to ~ 1.8–1.5 ka and wetter after that.

Chapter 5
Recent environmental record from a central Himalayan Lake

5.1   Introduction

The Himalayan lakes, a major source of freshwater for drinking and irrigation purposes, are predominantly fed by glacial melt and precipitated water (Sharma et al., 1982; Chakrapani, 2002). Characterised by small surface area, low organic productivity, low temperature, and clear water, they are also important venues for recreational activities. Due to remoteness and inaccessibility, high altitude lakes in general, and some of the Himalayan lakes in particular, are free from direct human interventions and therefore assumed to be an indicator of ecological and climatic changes (Choudhary et al., 2009a, b; Choudhary et al., 2013; Catalan et al., 2013; Chen et al., 2018). These lakes respond quickly to changes in temperature and precipitation, mainly from the surrounding catchment or directly to the lake surface, as they are sensitive to nutrient inputs and climate change (Vreca & Muri, 2006; Adrian et al., 2009; Vincent, 2009).

The increase in population and resulting human activities with environmental pollution during the last few decades have affected water quality of the lakes and soil characteristics of the Himalayan region (Chakrapani, 2002; Das, 2005). Previous studies have shown a dramatic change in lake water quality, algal productivity, and an increase in heavy metal contents of the Himalayan lakes (Sharma, 1982; Chakrapani, 2002). Deforestation and forest fires are also common in the region, which are recorded in historical archives (Dobriyal and Bijalwan, 2017). The effect of urbanization on trophic states of different Himalayan lakes has also been chronicled in the isotopic and geochemical characteristics of the lake sediments (Choudhary et al., 2009a & b; Choudhary et al., 2013). It has been suggested that a high-resolution study on hundred-year time scales using lake sediment can help to improve our understanding of the past climate change as well as the impact of human activities on the environment, which can be used for environmental governance in the future (Yuan et al., 2013).

In general, the composition of the lake sediments has the potential to unravel the details about the environmental conditions in and around the lake that existed at the time of their accumulation. The organic matter in lake sediment plays a vital role in understanding the past environment during the sediment deposition because of its association with biota, nutrients cycle, and biogeochemical processes (Fan et al., 2017; Rahman et al., 2020). As stated earlier in the thesis, the biogeochemical processes involved in the C and N cycles in a lake are also dominantly controlled by autochthonous and allochthonous organic matter sources, which can be differentiated by their $\delta^{13}C$ and $\delta^{15}N$ along with TOC, TN, and their ratios (TOC/TN) (Meyers, 1990; Meyers and Lallier-Vergès, 1999; Fan et al., 2017; Rahman et al., 2020). The relative input of organic matter to the lake through autochthonous and allochthonous sources determines the relative dominance of primary production and respiration along with associated processes, such as nitrification, denitrification, and methanogenesis (Jansson et al., 2000; Strauss & Lamberti, 2000; Duarte & Prairie, 2005; Tranvik et al., 2009; Hadas et al., 2009). The urban and agricultural waste-water, sewage, and modification in the trophic web structure are some of the most common organic matter sources to a lake with specific elemental and isotopic signatures (Harrington et al., 1998; Wolfe et al., 2001, 2003; Anderson and Cabana, 2009; Rawcliffe et al., 2010). Due to the impact of the human-driven activities, eutrophication has been noticed in many lakes worldwide that are recorded as variations in $\delta^{13}C$ and $\delta^{15}N$ along with their concentrations (Jinglu et al., 2007; Zan et al., 2012; Shah et al., 2021). The effect of continuous increase in atmospheric CO_2 and depletion in ^{13}C isotopic signature (known as the Suess effect) due to fossil fuel burning has also been well recorded in the $\delta^{13}C$ of the lacustrine organic matter (Reavie et al., 2021; Xia et al., 2021). Therefore, temporal variations in concentrations and isotopic compositions of C and N of organic matter in lake sediments of smaller high-altitude lakes have the potential to provide the evidences of past changes in environmental and climatic conditions of the region around the lake.

The impact of human activities has also increased the forest fire events in the last few decades, affecting the neighbouring environment (Hemp, 2005; Krishna and Reddy, 2012; Bar et al., 2021). The wildfire has an impact on forest plant diversity by

the preference for more flammable trees such as broader leaf oak trees (Gallagher et al., 2021; McDaniel et al., 2021). To study the impact of fire on the lake or track the fire events in the past, investigation of black carbon in the lake sediments has been a potential practice. The black carbon, formed by incomplete combustion (anthropogenic and natural) of biomass, is chemically inert and resistant to decay (Kuhlbusch and Crutzen, 1995; Wang et al., 2013). Forest fires have been one of the dominant sources of black carbon to the environment in the past (Kuhlbusch and Crutzen, 1995). However, in the modern environment, significant sources of black carbon are biomass burning and liquid fossil fuel/coal consumption (Winiger et al., 2015; Li et al., 2016). Various studies have been conducted in the Tibetan Plateau region to understand black C evolution in the last few decades using the concentration and C isotopic composition of black carbon ($\delta^{13}C_{BC}$) (Cong et al., 2013; Li et al., 2016; Neupane et al., 2019). However, studies related to the use of concentrations and $\delta^{13}C_{BC}$ to understand the effect of anthropogenic activities in the recent past, especially in the decadal and centennial-scale, are limited in the Himalayan region (e.g., Cong et al., 2013; Nair et al., 2013; Neupane et al., 2019).

Previous studies from the Himalaya, particularly in the Kumaon region (in the Uttarakhand), have shown the impact of urbanization on the major lakes, such as Nainital, Bhimtal, and Sattal Lakes, which were closer to the city limits, were found to undergo higher environmental pressure following an estimated pattern as Nainital > Bhimtal > Sattal (Fig. 5.1; Choudhary et al., 2013). In contrast, relatively smaller lakes in the region, such as the Garud Lake, are still unexplored. It remains to be seen if the smaller lakes with small catchments also have the potential to record the regional events as efficiently as the larger ones. In this study, using C and N isotopic compositions and concentrations in different components of the sediments of the Garud Lake, an attempt has been made to track the impact of natural and human-induced changes in the surrounding of the lake during the last seven decades. In addition, this study has also attempted to follow the fire events in the region (natural and human-made) and their possible impact and record in the lake. During this study, it was hypothesized that the

lake sediment might have recorded the natural to the anthropogenic transition of its organic and inorganic components in the region.
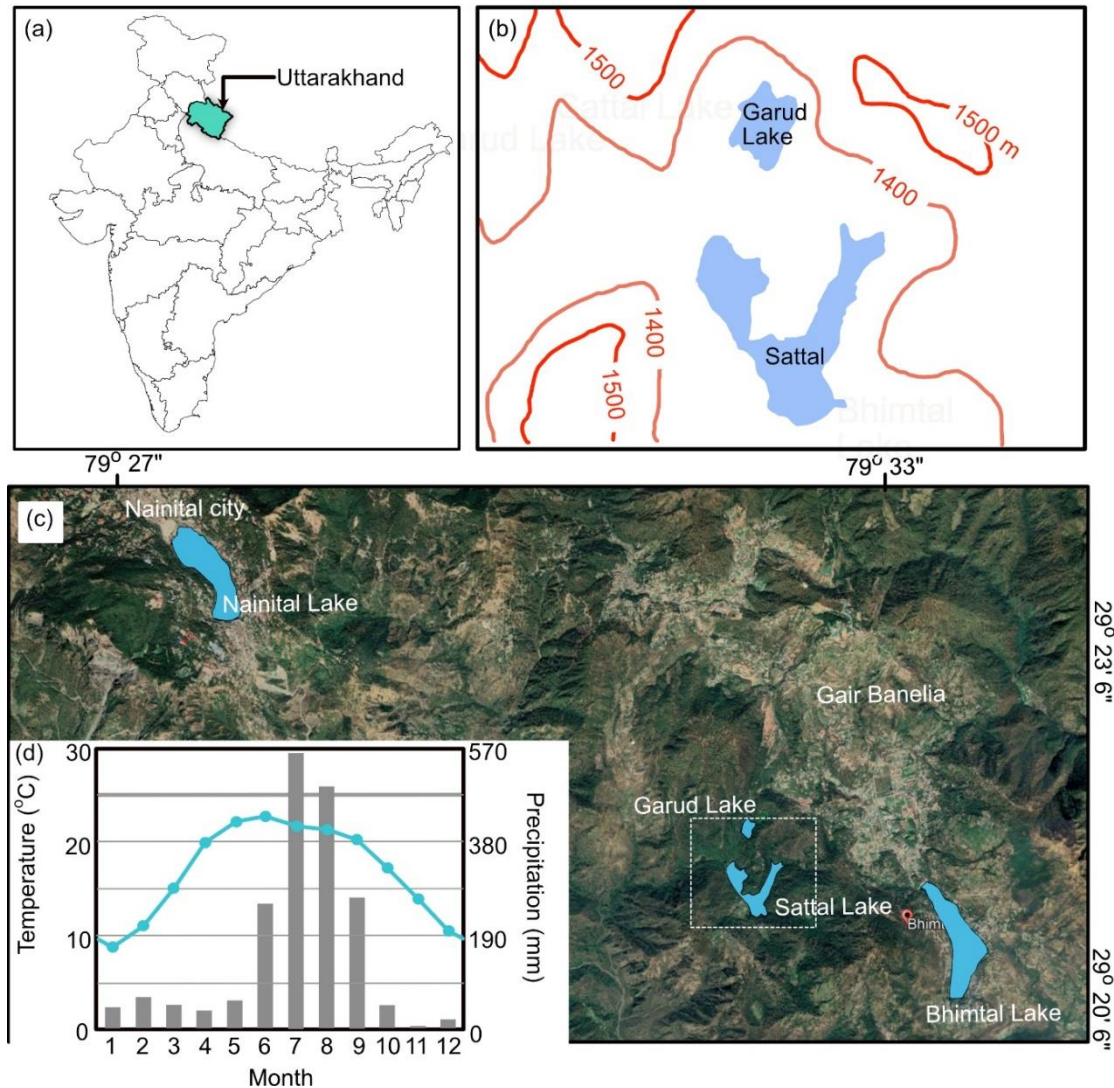
Figure 5.1 Location of the study area (Garud Lake). (a) Map of India (green color shade shows the Uttarakhand state), (b) location of Garud Lake and Sattal lake (the red and orange color contours show the altitude of the region), (c) google earth image of the different lakes in the study region that has been used for comparison in the present study, and (d) the monthly average temperature and precipitation.

5.2   Study area

As indicated in the chapter dealing with methodology, samples for this study were collected from the Garud Lake, situated at a distance of 23 km from the town of Nainital in the Kumaon region of the Himalaya in the Uttarakhand state, India (Fig. 5.1). The samples were retrieved using UWITEC gravity corer with 9 cm diameter during a field campaign in May 2018 from the deepest part (~ 24 m) of the lake. The Garud Lake, located in the Lesser Himalaya range, is one of the seven lakes of the *Sattal* (Seven Lakes), formed as a result of tectonic activities and upliftment of sediments between the Tibetan Plateau and Indo-Gangetic plain during the Holocene (Valdiya, 1981; 2002; Das, 2005). Largely, the rainfall during southwest monsoon feeds the lake during July-September with mean annual precipitation of ~ 2050 mm in the region (Rawat et al., 2013). The summer temperature of the region ranges from 10.6 to 26.7 ºC, whereas winter temperature varies from 2.8 to 15.6 ºC (Jain et al., 2010).

5.3   Sediment chronology

The vertical distributions of $^{210}Pb_{ex}$ and ^{137}Cs activities in the sediment core are shown in Fig. 5.2a. The $^{210}Pb_{ex}$ profile showed non-exponential variation with higher values in the top layers. For establishing the chronology, constant rate of supply (CRS) model was used as no exponential decline in $^{210}Pb_{xs}$ was observed in the collected core (Fig. 5.2). The CRS model works on the assumption of constant supply of unsupported ^{210}Pb to the lake (or bottom sediment), where the sediment supply fluctuates (Krishnaswamy et al., 1971). Earlier studies have used the CRS model as it provides a fairly accurate chronology and has been widely tested at various sites (Appleby and Oldfield, 1983), including the Himalaya (Das and Vasudevan, 2021). Therefore, the model can be used to calculate interannual variations in sedimentation rates. A brief overview of the principle behind the model is as follows.

The cumulative residual excess ^{210}Pb (A_d) beneath sediments of age t varies as:

$$A_d = A_0^{-\lambda t} \qquad (1)$$

where, A_d is the unsupported ^{210}Pb in the core below depth 'd' and 'A_0' is the entire unsupported ^{210}Pb below the mud/water interface.

For the CRS model,

$$a = h/t$$

$$t = h/a \tag{2}$$

where, a = sedimentation rate, h = depth below the surface, and t = time in years

The sediment chronology at depth 'x (h)' is then given by:

$$t_x = (1/\lambda) \times \ln(A_0/A_x)$$

$$(x/a) \times \lambda = \ln A_0 - \ln A_x$$

$$\ln A_x = \ln A_0 - (x/a) \times \lambda$$

which is a equation of straight line with co-ordinates of depth (x) and A_0 (y). The slope (m) of this straight line would be m = λ/a, therefore, a = λ/m. So, from equation 2

$$t_x = (x \times m)/\lambda.$$

As the CRS model assumes a constant ^{210}Pb flux but allows for variation in sediment supply, this model is applied to most sedimentary basins where sediment can fluctuate in response to climatic or anthropogenic changes.

In this study, using the CRS model, the age-depth relationship was established from $^{210}Pb_{ex}$, which resulted in the sedimentation rate of 0.85 cm/year (Fig. 5.2a and b). The ^{137}Cs peaked at 47 cm with 9.31 dpm/gm, which is linked to nuclear testing and is widely used as a time marker (1963 AD) to calculate sedimentation rate (DeJong et al., 1982). Using both ^{210}Pb and ^{137}Cs techniques, the sedimentation rate during the present study was 0.85 cm/year, and the bottom of the sediment core was found to be around 1949 AD. The derived sedimentation rate from ^{137}Cs was estimated using the equation

$$s = d/(n - x) \tag{3}$$

where, 's' is the sedimentation rate (cm/year) for the sample, 'd' the depth (cm) of the ^{137}Cs the peak for the respective time marker 'x' (1963), and 'n' denotes the year of sampling.
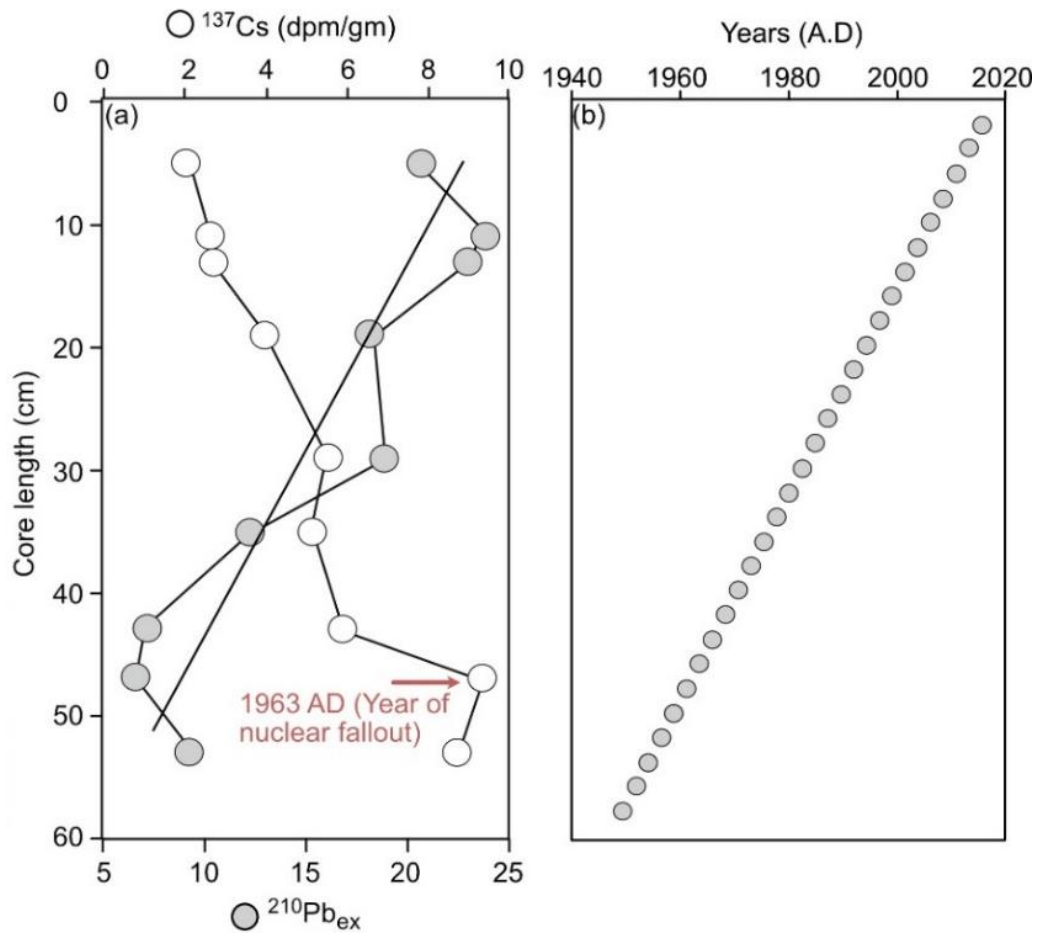
Figure 5.2 (a) Distribution of ^{210}Pb (grey dots) and ^{137}Cs (white dots) activity with depth in the Garud Lake and (b) calculated Age vs. depth (sedimentation rate was calculated using CRS model, i.e., 0.85 cm/year). The calculated sedimentation rate is the same as the ^{137}Cs peak (red arrow showing year of human nuclear impact ~ 1963 AD at 47 cm depth) based on sedimentation rate (0.85 cm/year).

5.4   Results

5.4.1   C and N contents and their isotopic compositions

The $\delta^{13}C$ showed a narrow range from -29.0 to $-27.0‰$ with two clear positive excursions at 6 and 38 cm, which corresponded to 1973 and 2010 AD (Fig. 5.3a). Since 1949 AD, $\delta^{13}C$ showed an increasing trend with a maximum value around 1973 AD, followed by a decreasing trend until 2005 AD, characterized by a secondary enriched peak around 2010 AD. The TOC and TN ranged from 6.24 to 18.74% and 0.43 to 1.05%, respectively (Fig. 5.3b). The TOC (%) showed a similar increasing trend as $\delta^{13}C$ from 1949 to 1973 AD. However, afterward, until 2005 AD, it showed a rising trend, in contrast to $\delta^{13}C$. Further, during the later stage, TOC and $\delta^{13}C$ show a similar trend (Fig. 5.3). The TOC/TN ratios showed a significant variation from 7 to 27 with an average of 12 and coincided with peaks of $\delta^{13}C$ (Fig. 5.3c). The $\delta^{15}N$ varied from 2.2 to 4.6‰ with prominent negative excursions around 1973, 1985, and 2010 AD (Fig. 5.3d). The four distinct positive peaks were also observed at periods corresponding to 1958, 1977, 1991, and 2003 AD. Relatively lower TN at the periods of negative $\delta^{15}N$ excursions were also observed (Fig. 5.3 b and d).

The $\delta^{13}C$ of organic matter depended on the historical isotopic signatures of DIC when organic C was produced photosynthetically (Schelske and Hodell, 1995). However, $\delta^{13}C$ of organic matter is likely to be influenced in recent past due to increased anthropogenic inputs of CO_2 in the atmosphere and its interaction with the lakes. Decrease in $\delta^{13}C$ of atmospheric CO_2 due to fossil fuel combustion have been noticed through measurements of fossil air trapped in ice cores (Friedli et al., 1986; Keeling et al., 1989). According to Schelske and Hodell (1995), a decrease of $\sim -1.4‰$ in $\delta^{13}C$ of atmospheric CO_2 has occurred since 1840 AD. To correct for any potential influence on $\delta^{13}C$ of organic matter due to decreasing $\delta^{13}C$ of atmospheric CO_2 during the present study, following equation (Schelske and Hodell, 1995) was used.

$$\delta^{13}C \ (depletion) = -4{,}577.8 + 7.3430 \times t - 3.9213 \times 10^{-3} \times t^2 + 6.9821 \times 10^{-7} \times t^3$$

Where t is the year of samples. The calculated time-dependent depletion in $\delta^{13}C$ was subtracted from the measured $\delta^{13}C$ of organic matter for each dated sediment section.
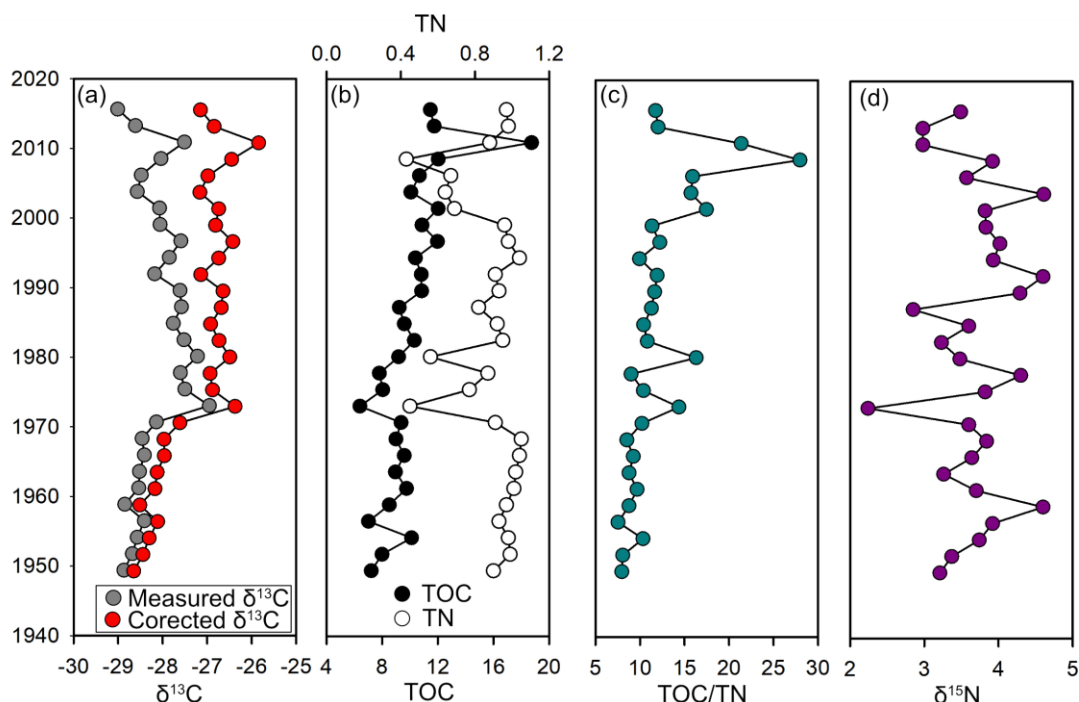
Figure 5.3 Temporal variations in (a) measured $\delta^{13}C$ (grey dots) and corrected $\delta^{13}C$ (red dots), (b) TOC (black dots) and TN (white dots) percentage, (c) TOC/TN ratios, and (d) $\delta^{15}N$ in the Garud Lake.

5.4.2 Black carbon concentration and isotope composition

Due to the loss of samples from the top layers during the analytical procedure, the black carbon concentrations in the sediment core could only be calculated up to 2002 AD (Fig. 5.4). The black carbon concentrations showed an extensive range and varied from 9.40 to 80.0 mg g^{-1} with an average concentration of 37.42 ± 18.25 mg g^{-1} (Fig. 5.4). The $\delta^{13}C_{BC}$ ranged from − 30.1 to − 27.6‰ (average = − 28.6 ± 0.7‰) and showed a gradually increasing trend from − 30.1 to − 29‰ during 1949 to 1971 AD with a sharp peak at ~1972 AD (− 27.84‰) (Fig. 5.4).
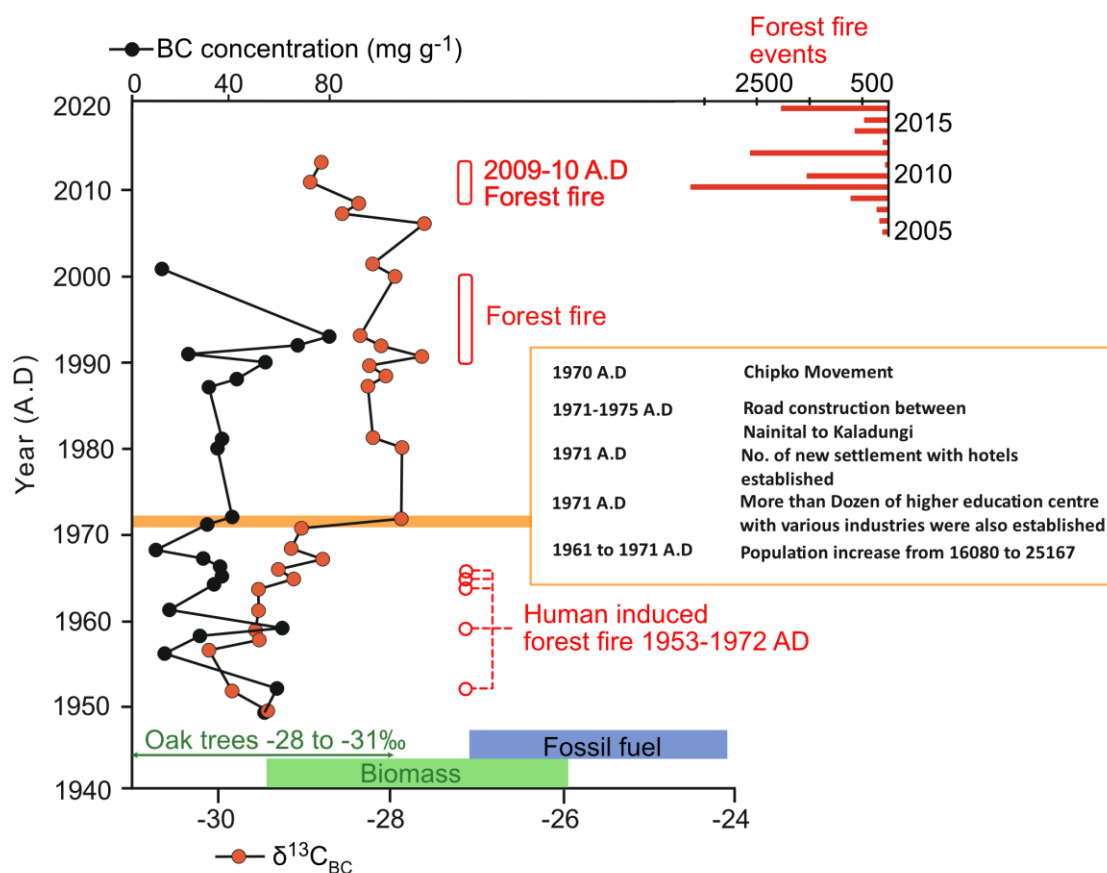
Figure 5.4 Variation in black carbon concentration (black dots) and $\delta^{13}C_{BC}$ (orange dots) in the sediment core. The green and blue boxes represent the typical range of $\delta^{13}C_{BC}$ produced by biomass burning and fossil fuel consumption, respectively. The green arrow showed the $\delta^{13}C$ range of oak trees (Mostaghimi et al., 2021). The red boxes and circles show the time of forest fires in Uttarakhand (Dobriyal and Bijalwan, 2017). The horizontal red bars on the upper right side show number of forest fire events in Uttarakhand from 2005 to 2016 (Sharma & Pant, 2017).

5.5 Discussion

The variability in isotopic compositions and elemental ratios in the lake sediment indicated temporal changes in the source of organic matter, primary productivity, and nutrient dynamics in the lake during the studied period (1949–2016 AD; Fig. 5.3). In general, the aquatic organisms (e.g., phytoplankton, benthic organisms, and zooplankton) are rich in protein and are characterized by a low TOC/TN ratio (< 10), whereas the lignin-rich terrestrial plants have a higher TOC/TN ratio (≥ 20) (Bordovskiy, 1965; Meyers and Eadie, 1993; Anoop et al., 2013; Rahman et al., 2020).

The temporal fluctuations in TOC/TN ratios of the sediment suggested a transition in the source of organic matter from *in situ* production (TOC/TN ≤ 10) to increased contribution from the catchment (TOC/TN > 20; Meyers & Eadie, 1993; Fan et al., 2017). It appeared that the organic matter in the lake was largely sustained through in-lake production between 1949 and 1970 AD (TOC/TN ≤ 10) when a gradual increase in TOC contents and $\delta^{13}C$ of organic matter was noticed, possibly indicating increased in-lake productivity during that period (Fig. 5.3). Little difference in the measured and Suess effect corrected $\delta^{13}C$ was noticed between 1949 and 1970 AD, which suggested the minimal impact of historic depletion of ^{13}C in the atmospheric CO_2 on $\delta^{13}C$ of organic matter (Fig. 5.3a). In turn, it indicated potentially limited fossil fuel impact on regional atmospheric CO_2 suggesting minimal human activities or urbanization during that period (1949–1970 AD). An increase in $\delta^{15}N$ at ~ 1958 AD and a slight decrease in TOC content with no change in TOC/TN ratio might be an indication of nitrification in the water column (Hadas et al., 2009). In a previous study, it has been shown that low TOC/TN ratio enhances nitrification, consuming ^{14}N from available NH_4^+, which is further utilized by phytoplankton leading to enhanced $\delta^{15}N$ of deposited organic matter (Strauss and Lamberti, 2000; Hadas et al., 2009).

A sharp increase in the measured and corrected $\delta^{13}C$ and TOC/TN (~ 14) ratio along with simultaneous decrease in $\delta^{15}N$ was noticed in the early 1970s (Fig. 5.3). These sudden fluctuations in the biogeochemical parameters coincided with the initiation of urbanization in the region around the lake (Choudhary et al., 2013). Based on the historical records, the study region witnessed a significant increase in human activities during that time (Bungla, 2009; Choudhary et al., 2013). An increase and a decrease in C and N isotopic compositions, respectively, along with an increase in TOC/TN ratio in the lake sediment, suggested increased loading of soil organic matter to the lake, possibly due to disturbance in the catchment. The $\delta^{13}C$ of soil organic matter in the study region is around ~ − 22 ‰ (Khan et al., 2018); whereas terrestrially derived organic matter usually have low $\delta^{15}N$ ($\delta^{15}N_{plants}$ ~ − 5 to + 2 ‰; $\delta^{15}N_{soil}$ ~ − 10 to + 5 ‰; Fry, 2006). Therefore, the above-mentioned fluctuations might have been due to the supply of organic matter from the catchment. However, we do not have definitive

proof of whether this supply was due to anthropogenic disturbance in the catchment or increased precipitation.

After 1972 AD, a slight but gradual increase in TOC/TN ratios (~ 10) and TOC contents along with a simultaneously decreasing trend in $\delta^{13}C$ was notice d until 2000 AD, which suggested utilization of CO_2 with increased primary productivity in the lake (Fig. 5.3). The Suess effect corrected $\delta^{13}C$ after 1970 AD showed relatively higher values compared to measured $\delta^{13}C$ of organic matter for the period 1970–2016 AD, clearly indicating utilization of atmospheric CO_2 by phytoplankton in the lake (Fig. 5.3a). Also, a consistent increase in the difference between measured and corrected $\delta^{13}C$ of organic matter was observed for the same time period (i.e., the early 1970s-2016 AD). This suggested the effect of increased fossil fuel-induced CO_2 (with depleted ^{13}C) in the regional atmosphere on the lake biota, clearly showing the role of urbanization on the aquatic ecosystems of the region.

Around 2000 AD, TOC/TN ratios (> 10) started increasing to reach a peak at around 2010 AD (> 20), which coincided with increased $\delta^{13}C$ and TOC contents along with decreased $\delta^{15}N$ (Fig. 5.3). It has been reported that rainfall in the region was significantly higher during 2010 and 2011 AD (1817 and 1741 mm annually, respectively) compared to previous years (Sharma, 2012). Flash floods and landslides were also reported from the region during the same period (Sharma, 2012). Therefore, it appeared that the studied lake received significantly high soil organic matter input (TOC/TN >20) from the catchment during this period.

Previous studies from the region using lake sediment have also reported the influence of urbanization and atmospheric CO_2 (fossil fuel) on the primary productivity of lakes (Choudhary et al., 2009a, b), which we showed through the Suess effect correction during this study. Similar to the present study, relatively larger lakes, such as Bhimtal and Sattal, from the region, showed decreasing temporal trend in $\delta^{13}C$ of organic matter in lakes sediment (Fig. 5.5a; Choudhary et al., 2009a; Choudhary et al., 2013), which was not seen in another larger lake (Nainital) (Fig. 5.5a; Choudhary et al., 2009b). The spatial location of the lakes suggested that Nainital Lake endured a

relatively higher effect of urbanization and received higher sewage and agricultural waste, which kept its δ^{13}C of organic matter elevated. It has been argued earlier that the distance of the lake from the city also controlled the environmental condition of the lake (Choudhary et al., 2013).
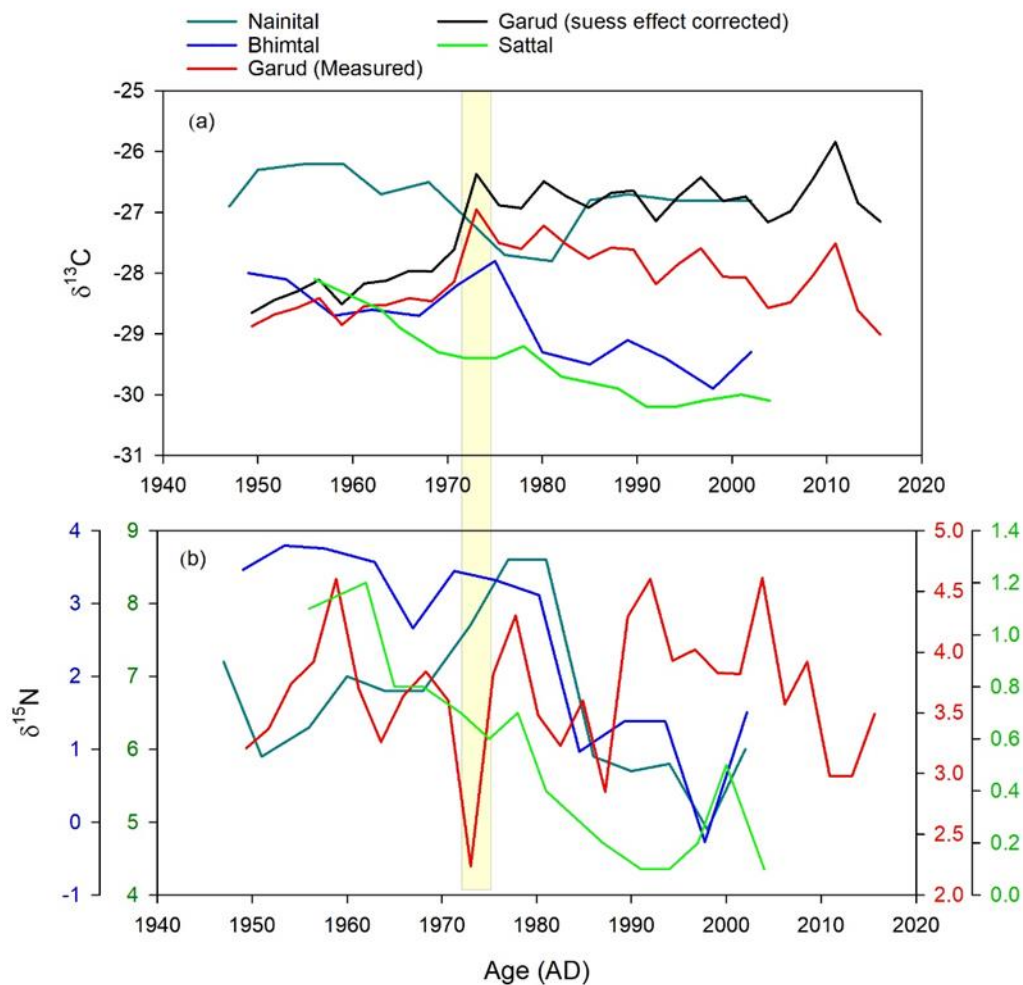
Figure 5.5 Comparison of (a) δ^{13}C of the organic matter and (b) δ^{15}N of bulk sediments from different lakes in the study region, including the present study (Garud Lake).

During the last four decades (1975–2015 AD), rapid urbanization and various other anthropogenic activities, such as the construction of roads, parking areas, hotels, schools, and development of recreational sites, have increased the region's susceptibility to landslides, rock falls, creeping, and subsidence (Tiwari and Joshi,

2014; Tiwari et al., 2018). The comparison of the temporal evolution of $\delta^{15}N$ of lake sediments in the region revealed a decreasing trend in $\delta^{15}N$ of Nainital, Bhimtal, and Sattal Lakes after 1970 AD, which was not seen in the presently studied Garud Lake (Fig. 5.5b). The decreasing trend in $\delta^{15}N$ of relatively larger lakes in the region has been attributed to urbanization-mediated eutrophication (Choudhary et al., 2013). The Garud Lake, on the other hand, surrounded by ~ 1500 m hillocks and sparse settlements with no decreasing trend in $\delta^{15}N$, appeared to have suffered relatively lesser direct human-induced changes than other lakes in the region.

The black carbon concentrations in the Garud Lake sediment were significantly higher compared to lakes in the Tibetan Plateau. However, it was comparable to Gosainkunda Lake in Nepal (Table 5.1 and reference therein). Generally, the high altitude lakes are relatively less affected by human activities compared to low altitude lakes resulting in a lower concentration of black carbon. However, due to higher natural and anthropogenic activities in the region, the black carbon concentrations in the Garud Lake sediment are high. The Garud Lake is located in an area that is one of India's major tourist destinations, where a huge crowd gathers, particularly during the summer, leading to increased anthropogenic activities such as vehicle emission and biomass burning.

In general, the black carbon concentration in the lake core remained around 40 mg g^{-1} from 1949 to 1990 AD (Fig. 5.4). However, the upper portion (1988–1994 AD) showed a relatively higher concentration than the middle (1972–1988 AD) and the lower portion (1949–1972 AD) (Fig. 5.4). The higher concentration of black carbon in the lower part of the sediment core is possibly related to human-induced fire events in the Uttarakhand state, which occurred during the years 1953, 1954, 1957, 1958, 1959, 1961, 1964, 1966, 1968, 1970, and 1972 AD (Dobriyal and Bijalwan, 2017). Several forest fire events were also reported during 1990–2000 AD (Ashutosh and Satendra, 2014) in the state, which could be attributed to the higher concentration of black carbon in the upper portion of the core. Previous studies related to atmospheric black carbon emission suggested that the Himalaya receives a significant amount of black carbon from various local, regional, and global sources (Xu et al., 2009; Agnihotri et al., 2011;

Cong et al., 2013; Li et al., 2016; Negi et al., 2019; Neupane et al., 2019). Agricultural biomass burning in the neighboring states like Punjab and Haryana has been suggested to be one of the dominant black carbon sources in the Himalaya, which gets transported eastward through westerlies (Negi et al., 2019).

The $\delta^{13}C_{BC}$ provides an insight into black carbon sources and helps us to delineate whether black carbon originates from biomass burning, liquid fossil fuel, or coal burning. Typically, $\delta^{13}C$ of modern atmospheric black carbon varies from -26.3 ± 1.4 to $-28.4 \pm 0.8‰$ (Winiger et al., 2019). However, $\delta^{13}C_{BC}$ originated from different sources show distinct signatures, such as $-23.4 \pm 1.3‰$ from coal burning, $-25.5 \pm 1.3‰$ through liquid fossil fuel, $-26.7 \pm 1.8‰$ from biomass (C3 plants) burning, and -36 to $-40‰$ from gas flaring (Winiger et al., 2015). The $\delta^{13}C_{BC}$ in the Garud Lake sediment varied from -27.62 to $-30.11‰$ (average $-28.75 \pm 0.70‰$; Fig. 5.4). The low $\delta^{13}C_{BC}$ in the lower portion (1949–1972 AD) of the core suggested that black carbon contribution in the lake was dominantly through biomass burning due to human-induced forest fires (Dobriyal and Bijalwan, 2017). It has been reported that banj oak (*Q. leucotrichophora*) in the Himalayan forests are susceptible to fire (Dobriyal and Bijalwan, 2017). Through an experimental study, it has been confirmed that flammability is higher for oak trees compared to non-oak trees, and flammability decreases linearly with increasing non-oak leaf litter contribution to the fuel bed (McDaniel et al., 2021). The $\delta^{13}C$ of black carbon produced by oak trees is not known; however, $\delta^{13}C$ of oak trees (*Q. libani, Q. infectoria, and Q. brantii)* have been reported to be around -28.7 to $-31.0‰$ (Mostaghimi et al., 2021). Assuming that these values encompass Oak trees in the Himalaya and given the mean C isotopic fractionation for black carbon produced by the burning of C3 plants to be $\sim -0.3‰$ (Wang et al., 2013), it is likely that black carbon produced before the early 1970s in the region was through human-induced burning of oak trees.

The sudden positive shift in $\delta^{13}C_{BC}$ around 1972 AD, which remained almost consistent until 2000 AD, coincided with the initiation of urbanization in the region and the famous forest conservation "Chipko movement" during 1973 AD to protect the

forests (Ashutosh and Satendra, 2014). Also, fewer forest fires were noticed after 1972 AD until 1995 AD (Dobriyal and Bijalwan, 2017). The tourism industry in the region, however, boomed after the Indo-Pak war of 1971 AD and new settlements, including a dozen higher education centers, opened up along with a steady rise in population (Bungla, 2009). The construction of a new road between Nainital and Kaladhungi also started after 1970 AD. Overall, this signified that although the concentration of black carbon in the region did not change significantly, the source shifted from biomass to fossil fuel burning, which can be seen very clearly in the $\delta^{13}C_{BC}$ of the sediment core (Fig. 5.4). The black carbon does not exist after 2000 AD; however, a significant drop in $\delta^{13}C_{BC}$ around 2010 AD (Fig. 5.4) coincided with a massive forest fire in the region (Sharma and Pant, 2017). Taken together, the black carbon concentration and its isotopic composition in the Garud Lake sediment clearly showed the natural and anthropogenic influences in the studied region with time.

Overall, concurring with the hypothesis of the study, C and N isotopic compositions in different components of the lake sediment and its comparison with other lakes in the region suggested that similar to larger lakes, Garud Lake also recorded fluctuations in the regional environment quite well. However, the degree and route of impact on the lake due to regional environmental change appeared to be dependent on the location of the lake and the size of its catchment. The C and N dynamics of the larger lakes in the region were affected through both atmospheric and terrestrial routes, whereas Garud Lake appeared to be largely impacted via the atmospheric route.

Table 5.1 Concentrations of black carbon (mg g−1) during the present and some other studies around the world.

Lake	Description	Above Sea Level (m)	Age span (AD)	Concentration (mean)	References
Garud	Nainital, India	2050	1949–2000	9.40–80.00 (37.42 ± 18.26)	This study
Gokyo	Nepal	4750	1853–2005	0.04–0.30 (0.16 ± 0.07)	Neupane et al. (2019)
Gosainkunda	Nepal	4390	1895–2010	9.45–64.5 (42.45 ± 16.70)	Neupane et al. (2019)
Ranwu	Tibetan Plateau	3800	1883–2015	1.15–2.05 (1.53 ± 0.21)	Neupane et al. (2019)
Qiangyong Co	Tibetan Plateau	4866	1922–2011	1.53–2.58 (2.03 ± 0.30)	Neupane et al. (2019)
Tanglha	Tibetan Plateau	5152	1890–2011	0.81–1.27 (0.97 ± 0.12)	Neupane et al. (2019)
Lingee Co	Tibetan Plateau	5051	1869–2011	0.14–0.3 (0.27 ± 0.14)	Neupane et al. (2019)
Nam Co	Tibetan Plateau	4722	1857–2009	0.49–1.09(0.74)	Cong et al. (2013)
Daihai	North China	1221	1800–2001	0.52–4.90 (2.26)	Han et al. (2010)
Taihu	East China	4	1825–2003	0.43–1.95 (1.01)	Han et al. (2010)
West Pine Pond	New York State	484	1835–2005	0.6–8	Husain et al. (2008)
Ledvica	Alps Slovenia	1830	1815–1998	3.6–9.2	Muri et al. (2002)
Engstlen	Alps, Switzerland	1850	1963–2008	1.5–3.3	Bogdal et al. (2011)

5.6   Conclusion

Using stable isotopic compositions of different constituents of lake sediment, this study has focused on the evolution of lake biogeochemistry under natural to anthropogenic transition along with the fire history of the region. The results revealed that from 1949 to 2016 AD, the organic matter in the lake was largely of lacustrine origin. However, there was a noticeable increase in the contribution of fossil fuel-induced atmospheric CO_2 as a C source to the lake biota in the early 1970s, which kept increasing with time, as deciphered by a consistent increase in the measured and Suess effect corrected $\delta^{13}C$ of organic matter. A considerable change in almost all measured biogeochemical signatures in the early 1970s and 2010 AD suggested an increased contribution of soil organic matter to the lake, possibly due to disturbances in the catchment or heavy precipitation in the region. A sudden shift in the C isotopic composition of black carbon in the lake sediment in the early 1970s advocated the increased contribution of fossil fuel-induced black carbon in the region due to the initiation of urbanization. Before the 1970s, the black carbon contribution was largely through human-induced biomass burning of broader leaf oak trees. Although the degree and pathways of anthropogenic stress suffered by lakes in the region appeared to be dependent on the location and size of the catchment, the studied lake, despite being smaller, also recorded the natural to anthropogenic transition in the regional environment quite efficiently.

Chapter 6
Summary and scope for future works

This thesis aimed to understand changes in past environmental conditions, such as hydroclimate, lake primary productivity, CO_2 and nutrients dynamics in lakes, and catchment vegetation, of the Himalayan region during the last ~ 45 ka using stable isotopic compositions of different components (organic matter, diatom, black carbon, and carbonate) of lake sediments. Such studies are necessary to understand regional environmental changes in the past as well as its teleconnection with the global climate events. The fluctuations in the regional environment exert control on the lacustrine ecosystems, which ultimately record these changes in its sediments. After thorough investigation of the studies carried out in the Himalayan region, this thesis has attempted to answer some of the outstanding questions such as the effect of insolation, polar ice melting, and North Atlantic Oscillation on the Himalayan environment through the reconstruction of the evolution of lake biogeochemistry at different temporal and spatial scales, with focus on bioavailable elements, such as C and N, during the last 45 ka.

Specifically, this thesis covered the last 45 ka of the climate and environmental history of the central and western Himalaya and its relationship with the strengthening / weakening of the westerlies. Apart from climate change, the effect of geology, altitude, open and closed basin, and human activities on the lake biogeochemistry were also investigated in detail. The major findings of this thesis are summarized below.

Starting from 45 ka, the Himalayan climate/environment has shown a coherency with the Northern Hemisphere Summer Insolation. From the central Himalayan lacustrine sequence, signatures of wet and humid condition during 40–32 ka was observed, which coincided with the increasing Northern Hemisphere Summer Insolation leading to westerlies induced precipitation. On the other hand, after 30 ka, weakening of the westerlies was noticed in the stable isotopes record of the Forest Block paleolake sequence from the Kashmir Himalaya, which coincided with increase

in obliquity resulting in the decrease in meridional insolation gradient between northern mid and high latitudes during 28–19 ka.

The studied lakes, Pipalkoti paleolake sequence in the central Himalaya and Forest Block paleolake in the Kashmir Himalaya, are situated at altitudes of 1500 and 3300 m, respectively. Due to differences in location and altitude, the Pipalkoti region received precipitation in the form of rainwater, whereas the Forest Block in the form of snow. Therefore, during strong westerlies, the Pipalkoti region might have received a high amount of rainfall leading to wetter condition. The Forest Block region, on the other hand received snow, resulting in colder conditions leading to freezing of lake surface. As the Pipalkoti paleolake existed on the carbonate terrain, during the wetter period, the lake appeared to be HCO_3^- enriched, which was registered in the stable isotopes record during 40–32 ka. On the other hand, the Forest Block paleolake was partially frozen during the strong westerlies, which were gradually weakening due to decrease in meridional insolation gradient between northern mid and high latitudes from 28 to 19 ka. During the time span when the lake was partially frozen, cut-off or limited exchange of atmospheric-lake surface CO_2 with no or low nutrient inputs to the lake along with winter stratification were registered as high $\delta^{13}C$ and $\delta^{15}N$ of organic matter and bulk sediments in the lake, respectively. As the lake surface started to melt, an increase in exchange of atmospheric CO_2 with lake surface and nutrient inputs likely led to documentation of the same as low $\delta^{13}C$ and $\delta^{15}N$.

During the time span of the present study (i.e., 45 to 0.2 ka), evidences for four extreme cold events at 45, 40, 30 (~ 29), and ~ 11 ka were found from the westerlies affected Himalayan region. These cold events coincided with the globally reported polar ice sheet melting events, i.e., Heinrich (H5, H4, H3) and YD events. The stable isotopes record (negative excursion of $\delta^{13}C_{Diatom}$) from the Pipalkoti paleolake sequence indicated existence of three colder events that coincided with H5, H4, and H3 in the central Himalayan region; however, due to lack of better resolution in the chronology, this study could not confidently validate these events. The stable isotopic compositions associated with high-resolution radiocarbon ages of the Forest Block paleolake from the Kashmir Himalaya have indicated two extreme cold climate events at 29 and 11 ka

aligned with H3 and YD events, respectively. The H3 event has been recorded in both the paleolake sequences. During the colder events, the Pipalkoti paleolake was probably CO_2 enriched due to minimal carbonate weathering in the catchment, which was recorded as low $\delta^{13}C_{Diatom}$. At the same time, the lake overturning was also observed, leading to transport of nutrients and respired CO_2 to the surface from hypolimnion, which were registered as high $\delta^{15}N$ and low $\delta^{13}C_{Diatom}$.

Through the stable isotopes results obtained from the Pipalkoti and Forest Block paleolake sequence, it was possible to cover the climate and environmental history of the central and western Himalaya between 45 to ~ 11 ka (pre-Holocene) with great deal of certainty. Although the Forest Block paleolake sequence covered the time span from 33 to 0.2 ka; the upper part of the sequence, which corresponded to the last ~ 7 ka, has sparse data and could not provide significant information. In this thesis, some part of this time span was covered using live lake sediment samples from the Wular and Manasbal Lakes in the Kashmir Himalaya that went up to 3.8 and 3.1 ka (late Holocene), respectively. From the stable isotopic compositions of these sediment samples, it was evident that the environmental changes in the Kashmir Himalaya during the late Holocene largely coincided with the fluctuations in the NAO phases. Overall, on the basis of the stable isotopic records from the Wular and Manasbal Lakes, late Holocene climate/environment of the Kashmir Himalaya appeared to have two significant phases. Evidence for a relatively drier climate was noticed between 3.7 and 1.5 ka (1.8 ka in the case of Manasbal Lake), which coincided with the negative NAO phase. Within the drier phase, an extreme dry episode was noticed at 2.5 ka through the $\delta^{13}C$ and $\delta^{15}N$ records of the Wular Lake sediment samples. During this episode, no carbonate precipitation occurred in the Manasbal Lake, which was quite intriguing. After 1.5 ka (1.8 ka in Manasbal), a relatively wet climate phase was noticed through the stable isotopic compositions of different components of sediment samples from both the lakes, which showed a coherency with positive NAO phase. The slight offset in the ages for the beginnings of the wetter climate in the Wular and Manasbal samples might be due to relatively lower resolution in radiocarbon ages of the Manasbal Lake sediment samples. Within the wetter phase, a relatively drier event around 0.6 ka was

noticed in the results from both the lakes, which coincided with the LIA (negative NAO phase).

During dry and wet climate/environment in the Kashmir Himalaya, both Wular and Manasbal Lakes showed different biogeochemical characteristics in the late Holocene. From the present result, it has been revealed that the Wular Lake biogeochemistry was dominantly controlled by the Jhelum River that regulated the contribution of transported nutrients and respired CO_2 to the lake. The Manasbal Lake, on the other hand, appeared to be controlled by the glacial melt water (possibly through Jhelum River) and the lake overturning, which was common in monomictic deeper lakes. The lake overturning provided nutrients to the primary producers on the lake surface from the hypolimnion during drier climate conditions, which were recorded in $\delta^{13}C_{Diatom}$ and $\delta^{15}N$ of Manasbal Lake sediment samples.

Apart from understanding past natural variabilities in Himalayan environment, a part of this thesis also focussed on anthropogenic stress on the Himalayan lake using recent sediment samples extracted from a central Himalayan lake (Garud Lake). Using stable isotopic compositions of different components (organic matter, bulk sediments and black carbon) of lake sediment, this study studied the evolution of lake biogeochemistry under the influence of human growth along with the fire history of the region. Our results revealed that from 1949 to 2016 AD, the organic matter in the lake was largely of lacustrine origin. However, there was a noticeable increase in the contribution of fossil fuel-induced atmospheric CO_2 as a C source to the lake biota in the early 1970s, which kept increasing with time, as deciphered by a consistent increase in the measured and Suess effect corrected $\delta^{13}C$ of organic matter. A considerable change in almost all measured biogeochemical signatures in the early 1970s and 2010 AD suggested an increased contribution of soil organic matter to the lake, possibly due to disturbances in the catchment or heavy precipitation in the region. A sudden shift in the C isotopic composition of black carbon in the lake sediment in the early 1970s advocated the increased contribution of fossil fuel-induced black carbon in the region due to the initiation of urbanization. Before the 1970s, the black carbon contribution was largely through human-induced biomass burning of broader leaf oak trees.

Although the degree and pathways of anthropogenic stress suffered by lakes in the region appeared to be dependent on the location and size of the catchment, the studied lake, despite being smaller, also recorded the effect of population growth and associated activities in the regional environment quite efficiently.

Scope for future works

In this doctoral thesis, understanding of the regional paleoenvironmental conditions in the Himalayan region has been developed through the biogeochemical evolution of lakes during the last 45 ka. However, given the expanse of the region and outstanding questions, there are need for more such studies, particularly the ones with high-resolution chronology with continuous long-term records. Below are some of the recommendations which need to be pursued in the future.

I.   Most of the paleoclimate studies from the Himalaya are based on geomorphic features and cover few thousand years (Holocene to MIS 4/5) of geological history. To develop a comprehensive understanding of paleoenvironmental conditions in this region, we recommend studies based on a robust dataset (such as stable isotopes and geochemistry) in abiotic and biotic archives.

II. The regions influenced by the westerlies and Indian summer monsoon need to be studied in detail with the high temporal and spatial resolution to develop a better understanding of the Himalayan climate system.

III. This thesis tried to explore environmental conditions at different elevation level. However, given the vastness of elevation in the Himalaya, paleoenvironmental reconstruction at different elevations is needed. This is particularly important in light of some studies suggesting elevation-dependent significant changes in the past regional environment. It would also be interesting to observe elevation-dependent biogeochemical evolution of lakes as well.

IV.   The understanding of climate-vegetation-human-fire interaction is missing from the Himalayan region. It would be interesting to decipher this aspect, particularly in light of the civilizational shift during the Holocene.

V.   Given the hard water effect in radiocarbon dating of some lake sediments, radiocarbon dating of pollen to establish better chronology in lake sediments is recommended.

VI.   The lakes from the central and western Himalaya showed carbonate precipitation. Stable isotopic composition ($\delta^{18}O$) of carbonate is a robust proxy for hydrological reconstruction, including water and moisture source along with precipitation and evaporation condition. However, Himalayan region has scarce paleohydrological dataset, which needs to be rectified. Also, single isotope based studies have limitation as they are unable to provide details about the precipitated water in the region due to evaporation induced kinetic fractionation. Therefore, a new technique, i.e., clumped isotope based study in carbonates may be helpful to identify the moisture source and associated hydrological conditions in the region.

VII. Civilization-wise, the western part of the Himalaya was active and affected by humans in the last 2000 years. It has been well known that there is a strong relationship between humans and fire. The black carbon and charcoal are the proxies which have been used previously to understand paleofire conditions in the past. The black carbon based studies from the Himalayan lakes can provide details about the interaction between humans and environment in the past by tracing fire events and human historical records during last few thousands of years.

Bibliography

Achyuthan, H., Nagasundaram, M., Gourlan, A.T., Eastoe, C., Ahmad, S.M. and Padmakumari, V.M., 2014. Mid-holocene Indian summer monsoon variability off the andaman islands, Bay of Bengal. Quaternary International, 349, pp.232-244.

Affek, H.P., Yakir, D., 2014. 5.7 The Stable Isotopic Composition of Atmospheric CO_2, in: Treatise on Geochemistry. Elsevier, pp. 179–212.

Agnihotri, R., Mandal, T.K., Karapurkar, S.G., Naja, M., Gadi, R., Ahammmed, Y.N., Kumar, A., Saud, T., Saxena, M., 2011. Stable carbon and nitrogen isotopic composition of bulk aerosols over India and northern Indian Ocean. Atmospheric Environment. 45, 2828–2835. https://doi.org/10.1016/j.atmosenv.2011.03.003

Ahmad, K., Davies, C., 2017. Stable isotope (δ^{13}C and δ^{15}N) based interpretation of organic matter source and paleoenvironmental conditions in Al-Azraq basin, Jordan. Applied Geochemistry 78, 49–60. https://doi.org/10.1016/j.apgeochem.2016.12.004

Alex Elliott, J., Thackeray, S.J., Huntingford, C., Jones, R.G., 2005. Combining a regional climate model with a phytoplankton community model to predict future changes in phytoplankton in lakes. Freshwater Biology. 50, 1404–1411.

Ali, A. and Achyuthan, H., 2020. Paleoenvironment shifts during MIS 3: Loess and loess paleosols of Kashmir Valley, India. Journal of Earth System Science, 129(1), pp.1-17.

Ali, S. N., Juyal, N., 2013. Chronology of late quaternary glaciations in Indian Himalaya: A critical review. Journal of Geological Society of India. https://doi.org/10.1007/s12594-013-0201-9

Ali, S.N., Quamar, M.F., Dubey, J., Morthekai, P., Bisht, P., Pandey, P., Shekhar, M. and Ghosh, R., 2020. Surface pollen distribution in alpine zone of the higher Himalaya: a case study from the Kalla glacier valley, India. Botany Letters, *167*(3), pp.340-352.

Ali, S.N., Biswas, R.H., Shukla, A.D., Juyal, N., 2013. Chronology and climatic implications of Late Quaternary glaciations in the Goriganga valley, central Himalaya, India. Quaternary Science Review. 73, 59–76.

Ali, S.N., Dubey, J., Ghosh, R., Quamar, M.F., Sharma, A., Morthekai, P., Dimri, A.P., Shekhar, M., Arif, M., Agrawal, S., 2018. High frequency abrupt shifts in the Indian summer monsoon since Younger Dryas in the Himalaya. Scientific Report. 8, 1–8.

Ali, Sheikh Nawaz, Agrawal, S., Sharma, A., Phartiyal, B., Morthekai, P., Govil, P., Bhushan, R., Farooqui, S., Jena, P., Shivam, A., 2020. Holocene hydroclimatic

variability in the Zanskar Valley, Northwestern Himalaya, India. Quaternary Research. 97, 1–17. https://doi.org/10.1017/qua.2020.22

Altabet, M.A., Murray, D.W. and Prell, W.L., 1999. Climatically linked oscillations in Arabian Sea denitrification over the past 1 my: Implications for the marine N cycle. Paleoceanography, 14(6), pp.732-743.

Amir, M., Paul, D. and Malik, J.N., 2021. Geochemistry of Holocene sediments from Chilika Lagoon, India: inferences on the sources of organic matter and variability of the Indian summer monsoon. Quaternary International, 599, pp.148-157.

An, Z., Colman, S.M., Zhou, W., Li, Xiaoqiang, Brown, E.T., Jull, A.J.T., Cai, Y., Huang, Y., Lu, X., Chang, H., Song, Y., Sun, Y., Xu, H., Liu, W., Jin, Z., Liu, Xiaodong, Cheng, P., Liu, Y., Ai, L., Li, Xiangzhong, Liu, Xiuju, Yan, L., Shi, Z., Wang, X., Wu, F., Qiang, X., Dong, J., Lu, F., Xu, X., 2012. Interplay between the Westerlies and Asian monsoon recorded in Lake Qinghai sediments since 32 ka. Sci. Rep. 2, 1–7. https://doi.org/10.1038/srep00619

Andersen, K.K., Svensson, A., Johnsen, S.J., Rasmussen, S.O., Bigler, M., Röthlisberger, R., Ruth, U., Siggaard-Andersen, M.L., Steffensen, J.P., Dahl-Jensen, D. and Vinther, B.M., 2006. The Greenland ice core chronology 2005, 15–42 ka. Part 1: constructing the time scale. Quaternary Science Reviews, 25(23-24), pp.3246-3257.

Andrews, J.E., Singhvi, A.K., Kailath, A.J., Kuhn, R., Dennis, P.F., Tandon, S.K. and Dhir, R.P., 1998. Do stable isotope data from calcrete record Late Pleistocene monsoonal climate variation in the Thar Desert of India?. Quaternary Research, 50(3), pp.240-251.

Anoop, A., Prasad, S., Plesen, B., Basaviah, N., Gaye, B., Naumann, R., Menzel, P., Weise, S., Brauer, A., 2013. Palaeoenvironmental implications of evaporative gaylussite crystals from Lonar Lake, central India. Journal of Quaternary Science. 28, 349–359. https://doi.org/doi:10.1002/jqs.2625

Appleby, P.G. and Oldfield, F., 1992. Applications of lead-210 to sedimentation studies. In Uranium-series disequilibrium: applications to earth, marine, and environmental sciences. 2. ed.

Archer, D.R., Fowler, H.J., 2004. Spatial and temporal variations in precipitation in the Upper Indus Basin, global teleconnections and hydrological implications. Hydrology and Earth System Science. https://doi.org/10.5194/hess-8-47-2004

Satendra and Kaushik, A.D., 2014. *Forest fire disaster management*. New Delhi: National Institute of Disaster Management, Ministry of Home Affairs, Government of India.

Babeesh, C., Achyuthan, H., Kumar Jaiswal, M., Lone, A., 2017. Late Quaternary loess-like paleosols and pedocomplexes, geochemistry, provenance and source area

weathering, Manasbal, Kashmir Valley, India. https://doi.org/10.1016/j.geomorph.2017.01.004

Babeesh, C., Achyuthan, H., Resmi, M.R., Nautiyal, C.M. and Shah, R.A., 2019. Late Holocene paleoenvironmental changes inferred from Manasbal Lake sediments, Kashmir Valley, India. Quaternary International, 507, pp.156-171.

Bade, D.L., Carpenter, S.R., Cole, J.J., Hanson, P.C. and Hesslein, R.H., 2004. Controls of δ^{13}C-DIC in lakes: Geochemistry, lake metabolism, and morphometry. Limnology and Oceanography, 49(4), pp.1160-1172.

Bagniewski, W., Meissner, K.J. and Menviel, L., 2017. Exploring the oxygen isotope fingerprint of Dansgaard-Oeschger variability and Heinrich events. Quaternary Science Reviews, 159, pp.1-14.

Bahadur, J., 1993. The Himalayas: a third polar region, in: Snow and Glacier Hydrology. Proc. International Symposium, Kathmandu, 1992. IAHS; Publication, 218, pp. 181–190.

Bali, R., Nawaz Ali, S., Agarwal, K.K., Rastogi, S.K., Krishna, K., Srivastava, P., 2013. Chronology of late Quaternary glaciation in the Pindar valley, Alaknanda basin, Central Himalaya (India). Journal of Asian Earth Science. 66, 224–233. https://doi.org/https://doi.org/10.1016/j.jseaes.2013.01.011

Banerji, U.S., Arulbalaji, P., Padmalal, D., 2020. Holocene climate variability and Indian Summer Monsoon: An overview. The Holocene 30, 744–773. https://doi.org/10.1177/0959683619895577

Barker, P.A., Hurrell, E.R., Leng, M.J., Plessen, B., Wolff, C., Conley, D.J., Keppens, E., Milne, I., Cumming, B.F., Laird, K.R., Kendrick, C.P., Wynn, P.M., Verschuren, D., 2013. Carbon cycling within an East African lake revealed by the carbon isotope composition of diatom silica: a 25-ka record from Lake Challa, Mt . Kilimanjaro. Quaternary Science Review. 66, 55–63. https://doi.org/10.1016/j.quascirev.2012.07.016

Barker, S., Chen, J., Gong, X., Jonkers, L., Knorr, G. and Thornalley, D., 2015. Icebergs not the trigger for North Atlantic cold events. Nature, 520(7547), pp.333-336.

Baron, J.S., Hall, E.K., Nolan, B.T., Finlay, J.C., Bernhardt, E.S., Harrison, J.A., Chan, F., Boyer, E.W., 2013. The interactive effects of excess reactive nitrogen and climate change on aquatic ecosystems and water resources of the United States. Biogeochemistry 114, 71–92.

Beaulieu, J.J., DelSontro, T., Downing, J.A., 2019. Eutrophication will increase methane emissions from lakes and impoundments during the 21st century. Nature Communication. 10, 1–5.

Beklioğlu, M., Meerhoff, M., Davidson, T.A., Ger, K.A., Havens, K., Moss, B., 2016. Preface: Shallow lakes in a fast changing world. Hydrobiologia 778, 9–11. https://doi.org/10.1007/s10750-016-2840-5

Benn, D.I. and Owen, L.A., 1998. The role of the Indian summer monsoon and the mid-latitude westerlies in Himalayan glaciation: review and speculative discussion. Journal of the Geological Society, 155(2), pp.353-363.

Berger, A. and Loutre, M.F., 1991. Insolation values for the climate of the last 10 million years. Quaternary Science Reviews, 10(4), pp.297-317.

Berman-Frank, I., Zohary, T., Erez, J., Dubinsky, Z., 1994. CO_2 availability, carbonic anhydrase, and the annual dinoflagellate bloom in Lake Kinneret. Limnology and Oceanography. 39, 1822–1834.

Bhat, M.A., Romshoo, S.A., Beig, G., 2017. Aerosol black carbon at an urban site-Srinagar, Northwestern Himalaya, India: Seasonality, sources, meteorology and radiative forcing. Atmos. Environ. 165, 336–348.

Bhushan, R., Yadava, M.G., Shah, M.S. and Raj, H., 2019. Performance of a new 1MV AMS facility (AURiS) at PRL, Ahmedabad, India. Nuclear Instruments and Methods in Physics Research Section B: Beam Interactions with Materials and Atoms, 439, pp.76-79.

Bhutiyani, M.R., Kale, V.S., Pawar, N.J., 2007. Long-term trends in maximum, minimum and mean annual air temperatures across the Northwestern Himalaya during the twentieth century. Clim. Change. https://doi.org/10.1007/s10584-006-9196-1

Binford, M.W. and Brenner, M., 1986. Dilution of 210Pb by organic sedimentation in lakes of different trophic states, and application to studies of sediment-water interactions 1. Limnology and Oceanography, 31(3), pp.584-595.

Bini, M., Zanchetta, G., Perşoiu, A., Cartier, R., Català, A., Cacho, I., Dean, J.R., Di Rita, F., Drysdale, R.N., Finnè, M., Isola, I., Jalali, B., Lirer, F., Magri, D., Masi, A., Marks, L., Mercuri, A.M., Peyron, O., Sadori, L., Sicre, M.A., Welc, F., Zielhofer, C., Brisset, E., 2019. The 4.2 ka BP Event in the Mediterranean region: An overview. Climate of the Past 15, 555–577. https://doi.org/10.5194/cp-15-555-2019

Bogdal, C., Bucheli, T.D., Agarwal, T., Anselmetti, F.S., Blum, F., Hungerbühler, K., Kohler, M., Schmid, P., Scheringer, M., Sobek, A., 2011. Contrasting temporal trends and relationships of total organic carbon, black carbon, and polycyclic aromatic hydrocarbons in rural low-altitude and remote high-altitude lakes. J. Environ. Monit. https://doi.org/10.1039/c0em00655f

Bohra, A., Kotlia, B.S., Basavaiah, N., 2017. Palaeoclimatic reconstruction by using the varvite sediments of Bharatpur, Upper Lahaul Valley, NW Himalaya, India. Quaternary International. 443, 39–48.

Bond, G., Heinrich, H., Broecker, W., Labeyrie, L., McManus, J., Andrews, J., Huon, S., Jantschik, R., Clasen, S., Simet, C. and Tedesco, K., 1992. Evidence for massive discharges of icebergs into the North Atlantic ocean during the last glacial period. Nature, 360(6401), pp.245-249.

Bookhagen, B., 2010. Appearance of extreme monsoonal rainfall events and their impact on erosion in the Himalaya. Geomatics, Nat. Hazards Risk. https://doi.org/10.1080/19475701003625737

Bordovskiy, O.K., 1965. Sources of organic matter in marine basins. Marine Geology. 3, 5–31. https://doi.org/https://doi.org/10.1016/0025-3227(65)90003-4

Bøtter-Jensen, L., McKeever, S.W. and Wintle, A.G., 2003. Optically stimulated luminescence dosimetry. Elsevier.

Bracegirdle, T.J., Colleoni, F., Abram, N.J., Bertler, N.A.N., Dixon, D.A., England, M., Favier, V., Fogwill, C.J., Fyfe, J.C., Goodwin, I., 2019. Back to the future: Using long-term observational and paleo-proxy reconstructions to improve model projections of Antarctic climate. Geosciences 9, 255.

Broecker, W.S., Kennett, J.P., Flower, B.P., Teller, J.T., Trumbore, S., Bonani, G. and Wolfli, W., 1989. Routing of meltwater from the Laurentide Ice Sheet during the Younger Dryas cold episode. Nature, 341(6240), pp.318-321.

Bungla, K., 2009. Urban Development and Its Environmental Impact and Management in the Lake Region of Kumaun.

Buylaert, J.P., Murray, A.S., Thomsen, K.J. and Jain, M., 2009. Testing the potential of an elevated temperature IRSL signal from K-feldspar. Radiation measurements, *44*(5-6), pp.560-565.

Cangemi, M., Censi, P., Reimer, A., D'Alessandro, W., Hause-Reitner, D., Madonia, P., Oliveri, Y., Pecoraino, G., Reitner, J., 2016. Carbonate precipitation in the alkaline lake Specchio di Venere (Pantelleria Island, Italy) and the possible role of microbial mats. Applied Geochemistry 67, 168–176.

Ceppi, P., Scherrer, S.C., Fischer, A.M. and Appenzeller, C., 2012. Revisiting Swiss temperature trends 1959–2008. International Journal of Climatology, 32(2), pp.203-213.

Cerling, T.E., Harris, J.M., MacFadden, B.J., Leakey, M.G., Quade, J., Eisenmann, V. and Ehleringer, J.R., 1997. Global vegetation change through the Miocene/Pliocene boundary. Nature, 389(6647), pp.153-158.

Chakraborty, S., Bhattacharya, S.K., Ranhotra, P.S., Bhattacharyya, A. and Bhushan, R., 2006. Palaeoclimatic scenario during Holocene around Sangla valley, Kinnaur northwest Himalaya based on multi proxy records. Current Science (00113891), 91(6).

Chauhan, O.S., 2003. Past 20,000-year history of Himalayan aridity: Evidence from oxygen isotope records in the Bay of Bengal. Indian Academy of Sciences.

Chen, Jie, Liu, J., Xie, C., Chen, G., Chen, Jianhui, Zhang, Z., Zhou, A., Rühland, K.M., Smol, J.P., Chen, F., 2018. Biogeochemical responses to climate change and anthropogenic nitrogen deposition from a ~200-year record from Tianchi Lake, Chinese Loess Plateau. Quaternary International. https://doi.org/10.1016/j.quaint.2018.09.004

Chen, X., Yang, L., Xiao, L., Miao, A., Xi, B., 2012. Nitrogen removal by denitrification during cyanobacterial bloom in Lake Taihu. Journal of Freshwater Ecology. 27, 243–258. https://doi.org/10.1080/02705060.2011.644405

Cheng, L., Song, Y., Chang, H., Li, Y., Orozbaev, R., Zeng, M. and Liu, H., 2020. Heavy mineral assemblages and sedimentation rates of eastern Central Asian loess: Paleoenvironmental implications. Palaeogeography, Palaeoclimatology, Palaeoecology, 551, p.109747.

Cheng, L., Song, Y., Wu, Y., Liu, Y., Liu, H., Chang, H., Zong, X., Kang, S., 2021. Drivers for Asynchronous Patterns of Dust Accumulation in Central and Eastern Asia and in Greenland During the Last Glacial Maximum. Geophysical Research Letter. 48. https://doi.org/10.1029/2020GL091194

Choudhary, P., Routh, J. and Chakrapani, G.J., 2009. An environmental record of changes in sedimentary organic matter from Lake Sattal in Kumaun Himalayas, India. Science of the total environment, 407(8), pp.2783-2795.

Choudhary, P., Routh, J., Chakrapani, G., 2012. A 100-year record of changes in organic matter characteristics and productivity in Lake Bhimtal in the Kumaon Himalaya, NW India. Journal of Paleolimnology. 49. https://doi.org/10.1007/s10933-012-9647-9

Choudhary, P., Routh, J., Chakrapani, G.J. and Kumar, B., 2009. Biogeochemical records of paleoenvironmental changes in Nainital Lake, Kumaun Himalayas, India. Journal of Paleolimnology, 42(4), pp.571-586.

Clark, I.D. and Fritz, P., 2013. Environmental isotopes in hydrogeology. CRC press.

Clark, P., Dyke, A., Shakun, J., Carlson, A., Clark, J., Wohlfarth, B., Mitrovica, J., Hostetler, S., McCabe, A., 2009. The Last Glacial Maximum. Science 325, 710–714. https://doi.org/10.1126/science.1172873

Clemens, S., 2006. Extending the historical record by proxy, in: The Asian Monsoon. Springer, pp. 615–630.

Cole, J.J., Caraco, N.F., Kling, G.W., Kratz, T.K., 1994. Carbon dioxide supersaturation in the surface waters of lakes. Science (80-.). 265, 1568–1570.

Condron, A. and Winsor, P., 2012. Meltwater routing and the Younger Dryas. Proceedings of the National Academy of Sciences, 109(49), pp.19928-19933.

Cong, Z., Kang, S., Gao, S., Zhang, Y., Li, Q., Kawamura, K., 2013. Historical trends of atmospheric black carbon on Tibetan Plateau as reconstructed from a 150-year lake sediment record. Environmental Science and Technology. 47, 2579–2586. https://doi.org/10.1021/es3048202

Contreras, S., Werne, J.P., Araneda, A., Urrutia, R. and Conejero, C.A., 2018. Organic matter geochemical signatures (TOC, TN, C/N ratio, δ^{13}C and δ^{15}N) of surface sediment from lakes distributed along a climatological gradient on the western side of the southern Andes. Science of the total environment, 630, pp.878-888.

Couture, R.-M., de Wit, H.A., Tominaga, K., Kiuru, P., Markelov, I., 2015. Oxygen dynamics in a boreal lake responds to long-term changes in climate, ice phenology, and DOC inputs. J. Geophys. Res. Biogeosciences 120, 2441–2456. https://doi.org/doi:10.1002/2015JG003065

Craig, H., Gordon, L.I., Paleotemperatures, C. on S.I. in O.S. and, 1965. Deuterium and oxygen 18 variations in the ocean and the marine atmosphere.

Crosta, X., Shemesh, A., 2002. Reconciling down core anticorrelation of diatom carbon and nitrogen isotopic ratios from the Southern Ocean. Paleoceanography 17, 10-1-10–8. https://doi.org/10.1029/2000pa000565

Currás, A., Zamora, L., Reed, J.M., García-Soto, E., Ferrero, S., Armengol, X., Mezquita-Joanes, F., Marqués, M.À., Riera, S., Julià, R., 2012. Climate change and human impact in central Spain during Roman times: High-resolution multi-proxy analysis of a tufa lake record (Somolinos, 1280 m asl). Catena 89, 31–53.

Cutshall, N.H., Larsen, I.L. and Olsen, C.R., 1983. Direct analysis of 210Pb in sediment samples: self-absorption corrections. Nuclear Instruments and Methods in Physics Research, 206(1-2), pp.309-312.

Das, S. and Vasudevan, S., 2021. A comprehensive study on sedimentation rate and sediment age of Satopanth Tal Garhwal Himalaya, using 210Pb and 137Cs techniques. Journal of Radioanalytical and Nuclear Chemistry, *329*(2), pp.633-646.

Dean, W.E., Gorham, E., 1998. Magnitude and significance of carbon burial in lakes, reservoirs, and peatlands. Geology 26, 535–538.

DeConto, R.M., Pollard, D., Wilson, P.A., Pälike, H., Lear, C.H., Pagani, M., 2008. Thresholds for Cenozoic bipolar glaciation. Nature 455, 652–656.

DeJong. E, H. Villar, and, J.R.B., 1982. Preliminary investigations on the use of 137Cs to estimate erosion in Saskatchewan. Can. J. soil Sci.

Deplazes, G., Lückge, A., Stuut, J.B.W., Pätzold, J., Kuhlmann, H., Husson, D., Fant, M. and Haug, G.H., 2014. Weakening and strengthening of the Indian monsoon during Heinrich events and Dansgaard-Oeschger oscillations. Paleoceanography, 29(2), pp.99-114.

Dhyani, R., Shekhar, M., Joshi, R., Bhattacharyya, A., Ranhotra, P.S., Pal, A.K., Thakur, S. and Nandi, S.K., 2021. Reconstruction of pre-monsoon relative humidity since 1800 CE based on tree-ring data of Pinus roxburghii Sarg.(chir–pine) from Pithoragarh, Western Himalaya. Quaternary International.

Dimri, A.P., Niyogi, D., Barros, A.P., Ridley, J., Mohanty, U.C., Yasunari, T. and Sikka, D.R., 2015. Western disturbances: a review. Reviews of Geophysics, 53(2), pp.225-246.

Dixit, Y., Hodell, D.A., Giesche, A., Tandon, S.K., Gázquez, F., Saini, H.S., Skinner, L.C., Mujtaba, S.A.I., Pawar, V., Singh, R.N., Petrie, C.A., 2018. Intensified summer monsoon and the urbanization of Indus Civilization in northwest India. Sci. Rep. 8. https://doi.org/10.1038/s41598-018-22504-5

Dixit, Y., Tandon, S., 2016. Hydroclimatic variability on the Indian-subcontinent in the past millennium: Review and assessment. Earth-Science Rev. 161. https://doi.org/10.1016/j.earscirev.2016.08.001

Dobriyal, M.J.R., Bijalwan, A., Dobriyal, M.J., 2017. Forest fire in western Himalayas of India: A Review. New York Sci. J. 10. https://doi.org/10.7537/marsnys100617.06

Dortch, J.M., Owen, L.A., Caffee, M.W., 2010. Quaternary glaciation in the Nubra and Shyok valley confluence, northernmost Ladakh, India. Quat. Res. 74, 132–144. https://doi.org/DOI: 10.1016/j.yqres.2010.04.013

Dortch, J.M., Owen, L.A., Caffee, M.W., 2013. Timing and climatic drivers for glaciation across semi-arid western Himalayan–Tibetan orogen. Quat. Sci. Rev. 78, 188–208.

Downing, J.A., Prairie, Y.T., Cole, J.J., Duarte, C.M., Tranvik, L.J., Striegl, R.G., McDowell, W.H., Kortelainen, P., Caraco, N.F., Melack, J.M. and Middelburg, J.J., 2006. The global abundance and size distribution of lakes, ponds, and impoundments. Limnology and Oceanography, 51(5), pp.2388-2397.

Duarte, C.M. and Prairie, Y.T., 2005. Prevalence of heterotrophy and atmospheric CO 2 emissions from aquatic ecosystems. Ecosystems, 8(7), pp.862-870.

Dubois, N., Saulnier-Talbot, É., Mills, K., Gell, P., Battarbee, R., Bennion, H., Chawchai, S., Dong, X., Francus, P., Flower, R., Gomes, D.F., Gregory-Eaves, I., Humane, S., Kattel, G., Jenny, J., Langdon, P., Massaferro, J., McGowan, S., Mikomägi, A., Ngoc, N.T.M., Ratnayake, A.S., Reid, M., Rose, N., Saros, J., Schillereff, D., Tolotti, M., Valero-Garcés, B., 2017. First human impacts and responses of aquatic

systems: A review of palaeolimnological records from around the world. Anthr. Rev. 5, 28–68. https://doi.org/10.1177/2053019617740365

Dumka, U.C., Moorthy, K.K., Kumar, R., Hegde, P., Sagar, R., Pant, P., Singh, N., Babu, S.S., 2010. Characteristics of aerosol black carbon mass concentration over a high altitude location in the Central Himalayas from multi-year measurements. Atmos. Res. 96, 510–521. https://doi.org/10.1016/j.atmosres.2009.12.010

Dutta, S., Mujtaba, S.A.I., Saini, H.S., Chunchekar, R., Kumar, P., 2018. Geomorphic evolution of glacier-fed Baspa Valley, NW Himalaya: record of Late Quaternary climate change, monsoon dynamics and glacial fluctuations. Geol. Soc. London, Spec. Publ. 462, 51–72.

Duval, M., Guilarte, V., Campaña, I., Arnold, L., Miguens, L., Iglesias, J. and González-Sierra, S., 2018. Quantifying hydrofluoric acid etching of quartz and feldspar coarse grains based on weight loss estimates: implication for ESR and luminescence dating studies.

Fan, J., Xiao, J., Wen, R., Zhang, S., Wang, X., Cui, L., Yamagata, H., 2017. Carbon and nitrogen signatures of sedimentary organic matter from Dali Lake in Inner Mongolia: Implications for Holocene hydrological and ecological variations in the East Asian summer monsoon margin. Quaternary International. 452, 65–78. https://doi.org/https://doi.org/10.1016/j.quaint.2016.09.050

Farooqi, I.A. and Desai, R.N., 1974. Stratigraphy of Karewas, Kashmir, India. Journal of Geological Society of India (Online archive from Vol 1 to Vol 78), 15(3), pp.299-305.

Farquhar, G.D., Ehleringer, J.R., Hubick, K.T., 1989. Carbon isotope discrimination and photosynthesis. Annual Review of Plant Biology. 40, 503–537.

Felip, M., Wille, A., Sattler, B. and Psenner, R., 2002. Microbial communities in the winter cover and the water column of an alpine lake: system connectivity and uncoupling. Aquatic Microbial Ecology, 29(2), pp.123-134.

Fernández-Donado, L., González-Rouco, J.F., Raible, C.C., Ammann, C.M., Barriopedro, D., García-Bustamante, E., Jungclaus, J.H., Lorenz, S.J., Luterbacher, J., Phipps, S.J., 2013. Large-scale temperature response to external forcing in simulations and reconstructions of the last millennium. Climate of the Past 9, 393–421.

Fields, S., 2004. Global nitrogen: cycling out of control.

Finkel, R.C., Owen, L.A., Barnard, P.L., Caffee, M.W., 2003. Beryllium-10 dating of Mount Everest moraines indicates a strong monsoon influence and glacial synchroneity throughout the Himalaya. Geology 31, 561–564.

Fontes, J.C., Gasse, F., Gibert, E., 1996. Holocene environmental changes in Lake Bangong basin (Western Tibet). Part 1: Chronology and stable isotopes of carbonates of a

Holocene lacustrine core. Palaeogeography Palaeoclimatology Palaeoecology. 120, 25–47. https://doi.org/10.1016/0031-0182(95)00032-1

Friedli, H., Lötscher, H., Oeschger, H., Siegenthaler, U. and Stauffer, B., 1986. Ice core record of the 13 C/12 C ratio of atmospheric CO 2 in the past two centuries. Nature, 324(6094), pp.237-238.

Froehlich, P.N., 1980. Analysis of organic carbon in marine sediments. Limnology and Oceanography. 25, 564–572.

Fry, B., 2006. Stable isotope ecology (Vol. 521). New York: Springer.

Gammons, C.H., Henne, W., Poulson, S.R., Parker, S.R., Johnston, T.B., Dore, J.E., Boyd, E.S., 2014. Stable isotopes track biogeochemical processes under seasonal ice cover in a shallow, productive lake. Biogeochemistry 120, 359–379. https://doi.org/10.1007/s10533-014-0005-z

Ganai, A. H., & Parveen, S., 2014. Effect of physico-chemical conditions on the structure and composition of the phytoplankton community in Wular Lake at Lankrishipora, Kashmir. International Journal of Biodiversity and Conservation, 6(1), 71-84

Ganai, A.H., Parveen, S., Khan, A.A., 2010. Phytoplankton diversity at Watlab Ghat in Wular Lake, Kashmir. Journal of Ecology and the Natural Environment. 2, 140–146.

Gansser, A., 1981. The geodynamic history of the Himalaya. Zagros Hindu Kush Himalaya Geodynamic Evolution, 3, pp.111-121.

Gardner, W.S., McCarthy, M.J., An, S., Sobolev, D., Sell, K.S., Brock, D., 2006. Nitrogen fixation and dissimilatory nitrate reduction to ammonium (DNRA) support nitrogen dynamics in Texas estuaries. Limnology and Oceanography. 51, 558–568. https://doi.org/https://doi.org/10.4319/lo.2006.51.1_part_2.0558

Gardner, W.S., Nalepa, T.F., Malczyk, J.M., 1987. Nitrogen mineralization and denitrification in Lake Michigan sediments1. Limnology and Oceanography. 32, 1226–1238. https://doi.org/https://doi.org/10.4319/lo.1987.32.6.1226

Ghosh, S., Sanyal, P., Roy, S., Bhushan, R., Sati, S.P., Philippe, A., Juyal, N., 2020. Early Holocene Indian summer monsoon and its impact on vegetation in the Central Himalaya: Insight from δD and δ¹³C values of leaf wax lipid. The Holocene 30, 1063–1074. https://doi.org/10.1177/0959683620908639

Goes, J.I., Tian, H., do Rosario Gomes, H., Anderson, O.R., Al-Hashmi, K., deRada, S., Luo, H., Al-Kharusi, L., Al-Azri, A. and Martinson, D.G., 2020. Ecosystem state change in the Arabian Sea fuelled by the recent loss of snow over the Himalayan-Tibetan Plateau region. Scientific reports, 10(1), pp.1-8.

Goedicke, C., 1985. TL dating: a novel form of differential dating. Nuclear Tracks and Radiation Measurements (1982), 10(4-6), pp.811-816.

Golubić, S., Krumbein, W., Schneider, J., 1979. The carbon cycle, in: Studies in Environmental Science. Elsevier, pp. 29–45.

Grove, J.M., 2012. The little ice age. Routledge.

Gu, B., Schelske, C.L., Hodell, D.A., 2004. Extreme 13C enrichments in a shallow hypereutrophic lake: Implications for carbon cycling. Limnology and Oceanography. https://doi.org/10.4319/lo.2004.49.4.1152

Hadas, O., Altabet, M.A., Agnihotri, R., 2009. Seasonally varying nitrogen isotope biogeochemistry of particulate organic matter in Lake Kinneret, Israel. Limnology and Oceanography. 54, 75–85. https://doi.org/10.4319/lo.2009.54.1.0075

Han, Y., Cao, J., Jin, Z.D., Liu, S., An, Z., 2010. Comparison of char and soot variations in sediments from lakes Daihai and Taihu. Quaternary Science Review. 30, 550–558.

Hays, J.D., Martinson, D., Mix, A.C., 1984. The Orbital Theory of Pleistocene Climate: Support frim a Revised Chronology of the Marine d18O Record The Biological Pump During the Last Glacial Maximum and Early Deglaciation View project.

Hedges, J.I. and Stern, J.H., 1984. Carbon and nitrogen determinations of carbonate-containing solids 1. Limnology and oceanography, 29(3), pp.657-663.

Hedges, J.I., Stern, J.H., 1984. Carbon and nitrogen determinations of carbonate-containing solids. Limnology and Oceanography. 29. 3, 657–663.

Herzschuh, U., 2006. Palaeo-moisture evolution in monsoonal Central Asia during the last 50,000 years. Quaternary Science Reviews, 25(1-2), pp.163-178.

Heiskanen, J., 2015. Lake-atmosphere greenhouse gas exchange in relation to atmospheric forcing and lake biogeochemistry.

Heinrich, H., 1988. Origin and consequences of cyclic ice rafting in the northeast Atlantic Ocean during the past 130,000 years. Quaternary research, 29(2), pp.142-152.

Hinder, B., Gabathuler, M., Steiner, B,. Hanselmann, K., Preisig, H.R. (1999). Seasonal dynamics and phytoplankton diversity in high mountain lakes (Jöri Lakes, Swiss Alps). Journal of Limnology 58(2):152–161

Hohndorf, A., 1969. Determination of half-life of lead-210. zeitschrift fur naturforschung part a-astrophysik physik und physikalische chemie, (4), p.612.

Hopkinson, B.M., Dupont, C.L., Allen, A.E., Morela, F.M.M., 2011. Efficiency of the CO_2-concentrating mechanism of diatoms. Proc. Natl. Acad. Sci. U. S. A. 108, 3830–3837. https://doi.org/10.1073/pnas.1018062108

Horton, T.W., Defliese, W.F., Tripati, A.K., Oze, C., 2016. Evaporation induced 18O and 13C enrichment in lake systems: A global perspective on hydrologic balance effects. Quaternary Science Review. 131, 365–379. https://doi.org/10.1016/j.quascirev.2015.06.030.

Hua, Q., Barbetti, M., Fink, D., Kaiser, K.F., Friedrich, M., Kromer, B., Levchenko, V.A., Zoppi, U., Smith, A.M. and Bertuch, F., 2009. Atmospheric 14C variations derived from tree rings during the early Younger Dryas. Quaternary Science Reviews, 28(25-26), pp.2982-2990.

Hucai, Z. and Wünnemann, B., 1997. Preliminary Study on the Chronology of Lacustrine Deposits and Determination of High Palaeo Lake Level in Tengger Desert Since Late Pleistocene. Journal of Lanzhou University.

Hurrell, E.R., Barker, P.A., Leng, M.J., Vane, C.H., Wynn, P., Kendrick, C.P., Verschuren, D., Perrott, F.A.S., 2011. Developing a methodology for carbon isotope analysis of lacustrine diatoms 1567–1574. https://doi.org/10.1002/rcm.5020

Husain, L., Khan, A.J., Ahmed, T., Swami, K., Bari, A., Webber, J.S., Li, J., 2008. Trends in atmospheric elemental carbon concentrations from 1835 to 2005. Journal of Geophysical Research Atmosphere. https://doi.org/10.1029/2007JD009398

Imbrie, J., Berger, A., Boyle, E., Clemens, S.C., Duffy, A., Howard, W.R., Kukla, G., Kutzbach, J., Martinson, D.G., McIntyre, A. and Mix, A.C., 1993. On the structure and origin of major glaciation cycles 2. The 100,000-year cycle. Paleoceanography, 8(6), pp.699-735.

Imbrie, J., Hays, J.D., Martinson, D.G., McIntyre, A., Mix, A.C., Morley, J.J., Pisias, N.G., Prell, W.L. and Shackleton, N.J., 1984. The orbital theory of Pleistocene climate: support from a revised chronology of the marine $\delta^{18}O$ record.

Ioannidou, A. and Papastefanou, C., 2006. Precipitation scavenging of 7Be and 137Cs radionuclides in air. Journal of Environmental Radioactivity, 85(1), pp.121-136.

Iqbal, M.J., Ilyas, K., 2013. Influence of Icelandic Low pressure on winter precipitation variability over northern part of Indo-Pak Region. Arabian Journal of Geosciences. https://doi.org/10.1007/s12517-011-0355-y

Ivy-Ochs, S., Kerschner, H., Maisch, M., Christl, M., Kubik, P.W., Schlüchter, C. 2009. Latest Pleistocene and Holocene glacier variations in the European Alps. Quaternary Science Reviews 28, 2137-2149.

Jain, C.K., Bandyopadhyay, A., Bhadra, A., 2010. Assessment of ground water quality for drinking purpose, District Nainital, Uttarakhand, India. Environmental Monitoring and Assessment. 166, 663–676. https://doi.org/10.1007/s10661-009-1031-5

Jansen, E., J. Overpeck, K.R. Briffa, J.-C. Duplessy, F. Joos, V. Masson-Delmotte, D. Olago, B. Otto-Bliesner, W.R. Peltier, S. Rahmstorf, R. Ramesh, D. Raynaud, D.

Rind, O. Solomina, R. Villalba, and D. Zhang, 2007: Palaeoclimate. In Climate Change 2007: The Physical Science Basis. Contribution of Working Group I to the Fourth Assessment Report of the Intergovernmental Panel on Climate Change. S. Solomon, D. Qin, M. Manning, Z. Chen, M. Marquis, K.B. Averyt, M. Tignor, and H.L. Miller, Eds. Cambridge University Press, pp. 433-497.

Jha, D.K., Sanyal, P. and Philippe, A., 2020. Multi-proxy evidence of Late Quaternary climate and vegetational history of north-central India: Implication for the Paleolithic to Neolithic phases. Quaternary Science Reviews, 229, p.106121.

Jin, Z., Wu, J., Cao, J., Wang, S., Shen, J., Gao, N., Zou, C., 2004. Holocene chemical weathering and climatic oscillations in north China: Evidence from lacustrine sediments. Boreas 33, 260–266. https://doi.org/10.1080/03009480410001280

Jones, S.E., Zwart, J.A., Kelly, P.T., Solomon, C.T., 2018. Hydrologic setting constrains lake heterotrophy and terrestrial carbon fate. Limnology and Oceanography Letter. 3, 256–264. https://doi.org/https://doi.org/10.1002/lol2.10054

Joshi, P., Phartiyal, B. and Joshi, M., 2021. Hydro-climatic variability during last five thousand years and its impact on human colonization and cultural transition in Ladakh sector, India. Quaternary International, 599, pp.45-54.

Juyal, N., Pant, R.K., Basavaiah, N., Bhushan, R., Jain, M., Saini, N.K., Yadava, M.G., Singhvi, A.K., 2009. Reconstruction of Last Glacial to early Holocene monsoon variability from relict lake sediments of the Higher Central Himalaya, Uttrakhand, India. Journal of Asian Earth Science. 34, 437–449. https://doi.org/10.1016/j.jseaes.2008.07.007

Juyal, N., Sundriyal, Y., Rana, N., Chaudhary, S. and Singhvi, A.K., 2010. Late Quaternary fluvial aggradation and incision in the monsoon-dominated Alaknanda valley, Central Himalaya, Uttrakhand, India. Journal of Quaternary Science, 25(8), pp.1293-1304.

Kalm, V., Sohar, K., 2010. Oxygen isotope fractionation in three freshwater ostracod species from early Holocene lacustrine tufa in northern Estonia. Journal of Paleolimnology. 43, 815–828.

Kangane, J., Nayak, G.N., Tiwari, A.K. and Saalim, S.M., 2021. Changing the paleo-depositional environment in the last 2300 years: a study through sedimentology and geochemistry of a sediment core, western Bay of Bengal. Environmental Earth Sciences, 80(1), pp.1-14.

Kar, A., Singhvi, A.K., Rajaguru, S.N., Juyal, N., Thomas, J. V, Banerjee, D., Dhir, R.P., 2001. Reconstruction of the late Quaternary environment of the lower Luni Plains, Thar Desert, India. Journal of Quaternary Science. 16, 61–68. https://doi.org/https://doi.org/10.1002/1099-1417(200101)16:1<61::AID-JQS562>3.0.CO;2-G

Karami, F., Balci, N., Guven, B., 2019. A modeling approach for calcium carbonate precipitation in a hypersaline environment: A case study from a shallow, alkaline lake. Ecological Complexity. 39, 100774.

Karlsson, J., Jansson, M., Jonsson, A., 2007. Respiration of allochthonous organic carbon in unproductive forest lakes determined by the Keeling plot method. Limnology and Oceanography. 52, 603–608.

Kathayat, G., Cheng, H., Sinha, A., Spötl, C., Edwards, R.L., Zhang, H., Li, X., Yi, L., Ning, Y., Cai, Y. and Lui, W.L., 2016. Indian monsoon variability on millennial-orbital timescales. Scientific reports, 6(1), pp.1-7.

Kathayat, G., Cheng, H., Sinha, A., Yi, L., Li, X., Zhang, H., Li, H., Ning, Y., Edwards, R.L., 2017. The Indian monsoon variability and civilization changes in the Indian subcontinent. Science Advances. 3, 1–9. https://doi.org/10.1126/sciadv.1701296

Keeling, C.D., Bacastow, R.B., Carter, A.F., Piper, S.C., Whorf, T.P., Heimann, M., Mook, W.G. and Roeloffzen, H., 1989. A three-dimensional model of atmospheric CO_2 transport based on observed winds: 1. Analysis of observational data. Aspects of climate variability in the Pacific and the Western Americas, 55, pp.165-236.

Keigwin, L.D. and Lehman, S.J., 1994. Deep circulation change linked to Heinrich event 1 and Younger Dryas in a middepth North Atlantic core. Paleoceanography, 9(2), pp.185-194.

Kendall, C. and Doctor, D.H., 2003. Stable isotope applications in hydrologic studies. Treatise on geochemistry, 5, p.605.

Keqin, L.S.Z.B.J., 1991. Preliminary research on lacustrine deposit and lake evolution on the south slope of the west Kunlun mountains [J]. Scientia Geographica Sinica, 4.

Kershaw, A.P., Bretherton, S.C., van der Kaars, S., 2007. A complete pollen record of the last 230 ka from Lynch's Crater, north-eastern Australia. Palaeogeography Palaeoclimatology Palaeoecology. 251, 23–45.

Kezao, C. and Bowler, J.M., 1986. Late Pleistocene evolution of salt lakes in the Qaidam basin, Qinghai province, China. Palaeogeography, Palaeoclimatology, Palaeoecology, 54(1-4), pp.87-104.

Khan, I., Amir, M., Paul, D., Srivastava, P., 2018. Late Holocene aridification recorded in the stable carbon and nitrogen isotope composition of soils from Nainital, Lesser Himalaya. Quaternary International. 467, 195–203. https://doi.org/10.1016/j.quaint.2018.01.044

Kharkwal, G. and Rawat, Y.S., 2010. Structure and composition of vegetation in subtropical forest of Kumaun Himalaya. African Journal of Plant Science, 4(4), pp.116-121.

Kothyari, G.C., Kandregula, R.S. and Luirei, K., 2018. Response: Discussion of 'Morphotectonic records of neotectonic activity in the vicinity of North Almora Thrust Zone, Central Kumaun Himalaya'by Kothyari et al.(2017), Geomorphology (285), 272–286. Geomorphology, 301, pp.153-166.

Kotlia, B.S., Singh, A.K., Joshi, L.M., Dhaila, B.S., 2015. Precipitation variability in the Indian Central Himalaya during last ca. 4,000 years inferred from a speleothem record: Impact of Indian Summer Monsoon (ISM) and Westerlies. Quaternary International. 371, 244–253.

Krishna, K.S., Ismaiel, M., Srinivas, K., Rao, D.G., Mishra, J. and Saha, D., 2016. Sediment pathways and emergence of Himalayan source material in the Bay of Bengal. Current Science, pp.363-372.

Krishnaswami, S., Trivedi, J.R., Sarin, M.M., Ramesh, R. and Sharma, K.K., 1992. Strontium isotopes and rubidium in the Ganga-Brahmaputra river system: Weathering in the Himalaya, fluxes to the Bay of Bengal and contributions to the evolution of oceanic87Sr/86Sr. Earth and Planetary Science Letters, 109(1-2), pp.243-253.

Kudrass, H.R., Hofmann, A., Doose, H., Emeis, K. and Erlenkeuser, H., 2001. Modulation and amplification of climatic changes in the Northern Hemisphere by the Indian summer monsoon during the past 80 ky. Geology, 29(1), pp.63-66.

Kumar, S., Ramesh, R., Sheshshayee, M.S., Sardessai, S. and Patel, P.P., 2005. Signature of terrestrial influence on nitrogen isotopic composition of suspended particulate. Indian Academy of Sciences.

Kumar, A., Tiwari, S.K., Verma, A., Gupta, A.K., 2018. Tracing isotopic signatures (δD and δ^{18}O) in precipitation and glacier melt over Chorabari Glacier–Hydroclimatic inferences for the Upper Ganga Basin (UGB), Garhwal Himalaya. J. Hydrol. Reg. Stud. 15, 68–89. https://doi.org/https://doi.org/10.1016/j.ejrh.2017.11.009

Kumar, P.K., Band, S.T., Ramesh, R. and Awasthi, N., 2018. Monsoon variability and upper ocean stratification during the last $\sim$ 66 ka over the Andaman Sea: inferences from the δ^{18}O records of planktonic foraminifera. Quaternary International, 479, pp.12-18.

Lamb, A.L., Leng, M.J., Lamb, H.F. and Mohammed, M.U., 2000. A 9000-year oxygen and carbon isotope record of hydrological change in a small Ethiopian crater lake. The Holocene, 10(2), pp.167-177.

Lan, J., Zhang, J., Cheng, P., Ma, X., Ai, L., Chawchai, S., Zhou, en, Wang, T., Yu, K., Sheng, E., Kang, S., Zang, J., Yan, D., Wang, Y., Tan, L., Xu, H., 2020. Late Holocene hydroclimatic variation in central Asia and its response to mid-latitude Westerlies and solar irradiance. https://doi.org/10.1016/j.quascirev.2020.106330

Lathika, N., Rahaman, W., Tarique, M., Gandhi, N., Kumar, A. and Thamban, M., 2021. Deep water circulation in the Arabian Sea during the last glacial cycle: Implications for paleo-redox condition, carbon sink and atmospheric CO_2 variability. Quaternary Science Reviews, 257, p.106853.

Lauterbach, S., Witt, R., Plessen, B., Dulski, P., Prasad, S., Mingram, J., Gleixner, G., Hettler-Riedel, S., Stebich, M., Schnetger, B., Schwalb, A., Schwarz, A., 2014. Climatic imprint of the mid-latitude Westerlies in the Central Tian Shan of Kyrgyzstan and teleconnections to North Atlantic climate variability during the last 6000 years. Holocene. https://doi.org/10.1177/0959683614534741.

Lehmann, M.F., Bernasconi, S.M., Barbieri, A. and McKenzie, J.A., 2002. Preservation of organic matter and alteration of its carbon and nitrogen isotope composition during simulated and in situ early sedimentary diagenesis. Geochimica et Cosmochimica Acta, 66(20), pp.3573-3584.

Lehmann, M.F., Bernasconi, S.M., McKenzie, J.A., Barbieri, A., Simona, M. and Veronesi, M., 2004. Seasonal variation of the $\delta^{13}C$ and $\delta^{15}N$ of particulate and dissolved carbon and nitrogen in Lake Lugano: Constraints on biogeochemical cycling in a eutrophic lake. Limnology and Oceanography, 49(2), pp.415-429.

Leng, M.J., Marshall, J.D., 2004. Palaeoclimate interpretation of stable isotope data from lake sediment archives. Quat. Sci. Rev. 23, 811–831. https://doi.org/10.1016/j.quascirev.2003.06.012

Leng, M.J., Metcalfe, S.E., Davies, S.J., 2005. Investigating Late Holocene climate variability in central Mexico using carbon isotope ratios in organic materials and oxygen isotope ratios from diatom silica within lacustrine sediments. Journal of Paleolimnology. https://doi.org/10.1007/s10933-005-6748-8

Li, C., Bosch, C., Kang, S., Andersson, A., Chen, P., Zhang, Q., Cong, Z., Chen, B., Qin, D., Gustafsson, Ö., 2016. Sources of black carbon to the Himalayan-Tibetan Plateau glaciers. Nature Communication. 7, 1–7. https://doi.org/10.1038/ncomms12574

Li, Y., Wang, N., Li, Z., Zhou, X., Zhang, C., Wang, Y., 2013. Carbonate formation and water level changes in a paleo-lake and its implication for carbon cycle and climate change, arid China. Front. Earth Sci. 7, 487–500. https://doi.org/10.1007/s11707-013-0392-9

Libby, W.F., Anderson, E.C. and Arnold, J.R., 1949. Age determination by radiocarbon content: world-wide assay of natural radiocarbon. Science, 109(2827), pp.227-228.

Lide, T., Tandong, Y., White, J.W.C., Wusheng, Y., Ninglian, W., 2005. Westerly moisture transport to the middle of Himalayas revealed from the high deuterium excess. Chinese Sci. Bull. 50, 1026–1030.

Lim, B. and Cachier, H., 1996. Determination of black carbon by chemical oxidation and thermal treatment in recent marine and lake sediments and Cretaceous-Tertiary clays. Chemical Geology, 131(1-4), pp.143-154.

Limoges, A., Weckström, K., Ribeiro, S., Georgiadis, E., Hansen, K.E., Martinez, P., Seidenkrantz, M., Giraudeau, J., Crosta, X., Massé, G., 2020. Learning from the past: impact of the Arctic Oscillation on sea ice and marine productivity off northwest Greenland over the last 9000 years. Glob. Chang. Biol. https://doi.org/10.1111/gcb.15334

Lisiecki, L.E., Raymo, M.E., 2005. A Pliocene-Pleistocene stack of 57 globally distributed benthic $\delta^{18}O$ records. Paleoceanography 20, 1–17. https://doi.org/10.1029/2004PA001071

Liu, J., Appiah-Sefah, G., Apreku, T.O., 2018. Effects of elevated atmospheric CO_2 and nitrogen fertilization on nitrogen cycling in experimental riparian wetlands. Water Sci. Eng. 11, 39–45.

Liu, J., Qie, W., Algeo, T.J., Yao, L., Huang, J., Luo, G., 2016. Changes in marine nitrogen fixation and denitrification rates during the end-Devonian mass extinction. Palaeogeography Palaeoclimatology Palaeoecology. 448, 195–206. https://doi.org/10.1016/j.palaeo.2015.10.022

Liu, W., Li, X., Zhang, L., An, Z., Xu, L., 2009. Evaluation of oxygen isotopes in carbonate as an indicator of lake evolution in arid areas: the modern Qinghai Lake, Qinghai–Tibet Plateau. Chem. Geol. 268, 126–136.

Liu, Y., Wu, G., Hong, J., Dong, B., Duan, A., Bao, Q., Zhou, L., 2012. Revisiting Asian monsoon formation and change associated with Tibetan Plateau forcing: II. Change. Clim. Dyn. 39, 1183–1195.

Liu, Z., Dreybrodt, W., Wang, H., 2010. A new direction in effective accounting for the atmospheric CO_2 budget: considering the combined action of carbonate dissolution, the global water cycle and photosynthetic uptake of DIC by aquatic organisms. Earth-Science Rev. 99, 162–172.

Livingstone, D.M., Lotter, A.F. and Kettle, H., 2005. Altitude-dependent differences in the primary physical response of mountain lakes to climatic forcing. Limnology and oceanography, 50(4), pp.1313-1325.

Lohne, O. S., Mangerud, J., & Birks, H. H. 2014: IntCal13 calibrated ages of the Vedde and Saksunarvatn ashes and the Younger Dryas boundaries from Kråkenes, western Norway. Journal of Quaternary Science **29**, 506–507

Jackson, C. S., & Broccoli, A. J. (2003). Orbital forcing of Arctic climate: mechanisms of climate response and implications for continental glaciation. Climate Dynamics, 21, 539–557

Lohne, O. S., Mangerud, J., & Birks, H. H., 2013. Precise ^{14}C ages of the Vedde and Saksunarvatn ashes and the Younger Dryas boundaries from western Norway and their comparison with the Greenland Ice Core (GICC05) chronology. Journal of Quaternary Science **28**, 490–500

Lone, A.M., Achyuthan, H., Shah, R.A., Sangode, S.J., Kumar, P., Chopra, S., Sharma, R., 2020. Paleoenvironmental shifts spanning the last ~ 6000 years and recent anthropogenic controls inferred from a high-altitude temperate lake: Anchar Lake, NW Himalaya. Holocene 30, 23–36. https://doi.org/10.1177/0959683619865599

Looman, A., Maher, D.T. and Santos, I.R., 2021. Carbon dioxide hydrodynamics along a wetland-lake-stream-waterfall continuum (Blue Mountains, Australia). Science of The Total Environment, 777, p.146124.

Loutre, M.F., Paillard, D., Vimeux, F. and Cortijo, E., 2004. Does mean annual insolation have the potential to change the climate? Earth and Planetary Science Letters, 221(1-4), pp.1-14.

Mampuku, M., Yamanaka, T., Uchida, M., Fujii, R., Maki, T., Sakai, H., 2008. Changes in C3/C4 vegetation in the continental interior of the Central Himalayas associated with monsoonal paleoclimatic changes during the last 600 kyr. Climate of the Past 4, 1–9.

Mann, M.E., Zhang, Z., Rutherford, S., Bradley, R.S., Hughes, M.K., Shindell, D., Ammann, C., Faluvegi, G., Ni, F., 2009. Global signatures and dynamical origins of the Little Ice Age and Medieval Climate Anomaly. Science (80-.). 326, 1256–1260.

Mann, M.E., Zhang, Z., Rutherford, S., Bradley, R.S., Hughes, M.K., Shindell, D., Ammann, C., Faluvegi, G. and Ni, F., 2009. Global signatures and dynamical origins of the Little Ice Age and Medieval Climate Anomaly. Science, 326(5957), pp.1256-1260.

Marcé, R., Obrador, B., Morguí, J.-A., Riera, J.L., López, P., Armengol, J., 2015. Carbonate weathering as a driver of CO_2 supersaturation in lakes. Nat. Geosci. 8, 107–111.

Marotta, H., Pinho, L., Gudasz, C., Bastviken, D., Tranvik, L.J., Enrich-Prast, A., 2014. Greenhouse gas production in low-latitude lake sediments responds strongly to warming. Nat. Clim. Chang. 4, 467–470.

Marotzke, J., Forster, P.M., 2015. Forcing, feedback and internal variability in global temperature trends. Nature 517, 565–570.

Martín-Chivelet, J., Muñoz-García, M.B., Edwards, R.L., Turrero, M.J. and Ortega, A.I., 2011. Land surface temperature changes in Northern Iberia since 4000 yr BP, based on δ^{13}C of speleothems. Global and Planetary Change, 77(1-2), pp.1-12.

Marty, J., Planas, D., 2008. Comparison of methods to determine algal $\delta^{13}C$ in freshwater. Limnology and Oceanography. methods 6. https://doi.org/10.4319/lom.2008.6.51

Mayorga, E., Aufdenkampe, A.K., Masiello, C.A., Krusche, A.V., Hedges, J.I., Quay, P.D., Richey, J.E. and Brown, T.A., 2005. Young organic matter as a source of carbon dioxide outgassing from Amazonian rivers. Nature, 436(7050), pp.538-541.

McCallister, S.L., Del Giorgio, P.A., 2008. Direct measurement of the d13C signature of carbon respired by bacteria in lakes: Linkages to potential carbon sources, ecosystem baseline metabolism, and CO_2 fluxes. Limnology and Oceanography. 53, 1204–1216.

McDaniel, J.K., Alexander, H.D., Siegert, C.M. and Lashley, M.A., 2021. Shifting tree species composition of upland oak forests alters leaf litter structure, moisture, and flammability. Forest Ecology and Management, 482, p.118860.

Mehraj, G., Khuroo, A.A., Qureshi, S., Muzafar, I., Friedman, C.R., Rashid, I., 2018. Patterns of alien plant diversity in the urban landscapes of global biodiversity hotspots: a case study from the Himalayas. Biodivers. Conserv. 27, 1055–1072.

Meng, Y. and Liu, X., 2018. Millennial-scale climate oscillations inferred from visible spectroscopy of a sediment core in Qarhan Salt Lake of Qaidam Basin between 40 and 10 cal ka BP. Quaternary International, 464, pp.336-342.

Meyers, P., 2003. Application of organic geochemistry to paleolimnological reconstruction: a summary of examples from the Laurention Great Lakes. Org. Geochem. 34, 261–289. https://doi.org/10.1016/S0146-6380(02)00168-7

Meyers, P.A. and Ishiwatari, R., 1993. Lacustrine organic geochemistry—an overview of indicators of organic matter sources and diagenesis in lake sediments. Organic geochemistry, 20(7), pp.867-900.

Meyers, P.A., Eadie, B.J., 1993. Sources, degradation and recycling of organic matter associated with sinking particles in Lake Michigan. Org. Geochem. 20, 47–56. https://doi.org/10.1016/0146-6380(93)90080-U

Meyers, P.A., Lallier-Vergès, E., 1999. Lacustrine sedimentary organic matter records of Late Quaternary paleoclimates. Journal of Paleolimnology. 21, 345–372. https://doi.org/10.1023/A:1008073732192

Montoya, J.P., Carpenter, E.J., Capone, D.G., 2002. Nitrogen fixation and nitrogen isotope abundances in zooplankton of the oligotrophic North Atlantic. Limnology and Oceanography. https://doi.org/10.4319/lo.2002.47.6.1617

Morley, D.W., Leng, M.J., Mackay, A.W., Sloane, H.J., Rioual, P. and Battarbee, R.W., 2004. Cleaning of lake sediment samples for diatom oxygen isotope analysis. Journal of Paleolimnology, 31(3), pp.391-401.

Mörner, N.-A., 1995. The Baltic Ice Lake-Yoldia Sea transition. Quaternary International. 27, 95–98.

Mörner, N.-A., 2013. Sea level changes past records and future expectations. Energy Environ. 24, 509–536.

Mostaghimi, F., Seyedi, N., Shafiei, A.B. and Correia, O., 2021. How do leaf carbon and nitrogen contents of oak hosts affect the heterotrophic level of Loranthus europaeus? Insights from stable isotope ecophysiology assays. Ecological Indicators, 125, p.107583.

Mudelsee, M., Bickert, T., Lear, C.H., Lohmann, G., 2014. Cenozoic climate changes: A review based on time series analysis of marine benthic $\delta^{18}O$ records. Rev. Geophys. 52, 333–374.

Muri, G., Cermelj, B., Faganeli, J., Brancelj, A., 2002. Black carbon in Slovenian alpine lacustrine sediments. Chemosphere. https://doi.org/10.1016/S0045-6535(01)00295-8

Mushtaq, F., Pandey, A.C., 2014. Assessment of land use/land cover dynamics vis-à-vis hydrometeorological variability in Wular Lake environs Kashmir Valley, India using multitemporal satellite data. Arab. J. Geosci. 7, 4707–4715.

Nair, V.S., Babu, S.S., Moorthy, K.K., Sharma, A.K., Marinoni, A., Ajai, 2013. Black carbon aerosols over the Himalayas: Direct and surface albedo forcing. Tellus, Ser. B Chem. Phys. Meteorol. 65. https://doi.org/10.3402/tellusb.v65i0.19738

Nakamoto, A., Harada, M., Mitsuhashi, R., Tsuchiya, K., Kryukov, A.P., Shinohara, A., Suzuki, H., 2021. Influence of Quaternary environmental changes on mole populations inferred from mitochondrial sequences and evolutionary rate estimation. Zool. Lett. 7, 1–11.

Neelavannan, K., Hussain, S.M., Nishath, N.M., Achyuthan, H., Veerasingam, S., Prakasam, M., Kumar, P., Singh, P. and Kurian, P.J., 2021. Paleoproductivity shifts since the last 130 ka off Lakshadweep, Southeastern Arabian Sea. Regional Studies in Marine Science, 44, p.101776.

Negi, P.S., Pandey, C.P., Singh, N., 2019. Black carbon aerosols in the ambient air of Gangotri Glacier valley of north- western Himalaya in India. Atmos. Environ. 214, 116879. https://doi.org/10.1016/j.atmosenv.2019.116879

Neupane, B., Kang, S., Chen, P., Zhang, Y., Ram, K., Rupakheti, D., Tripathee, L., Sharma, C.M., Cong, Z., Li, C., Hou, J., Xu, M., Thapa, P., 2019. Historical Black Carbon Reconstruction from the Lake Sediments of the Himalayan-Tibetan Plateau. Environmental Science and Technology. 53, 5641–5651. https://doi.org/10.1021/acs.est.8b07025

Norris, R.S. and Arkin, W.M., 1996. Known nuclear tests worldwide, 1945-1995. Bulletin of the Atomic Scientists, 52(3), p.61.

Olsen, J., Anderson, N.J., Knudsen, M.F., 2012. Variability of the North Atlantic Oscillation over the past 5,200 years. Nat. Geosci. https://doi.org/10.1038/NGEO1589

Owen, L.A., Dortch, J.M., 2014. Nature and timing of Quaternary glaciation in the Himalayan–Tibetan orogen. Quat. Sci. Rev. 88, 14–54. https://doi.org/https://doi.org/10.1016/j.quascirev.2013.11.016

Owen, L.A., Finkel, R.C., Caffee, M.W., 2002. A note on the extent of glaciation throughout the Himalaya during the global Last Glacial Maximum. Quat. Sci. Rev. 21, 147–157.

Pachur, H.J., Wünnemann, B. and Zhang, H., 1995. Lake evolution in the Tengger Desert, Northwestern China, during the last 40,000 years. Quaternary Research, 44(2), pp.171-180.

Pagani, M., Zachos, J.C., Freeman, K.H., Tipple, B., Bohaty, S., 2005. Marked decline in atmospheric carbon dioxide concentrations during the Paleogene. Science (80-). 309, 600–603.

Paneth, P., O'Leary, M.H., 1985. Carbon isotope effect on dehydration of bicarbonate ion catalyzed by carbonic anhydrase. Biochemistry 24, 5143–5147.

Pang, Y., Zhou, B., Zhou, X., Xu, X.C., Liu, X.Y., Zhan, T., Lu, Y.H., 2021. Abundance and $\delta^{13}C$ of sedimentary black carbon indicate rising wildfire and C4 plants in Northeast China during the early Holocene. Palaeogeography Palaeoclimatology Palaeoecology. 562, 110075. https://doi.org/10.1016/j.palaeo.2020.110075

Pathak, A., Ghosh, S., Kumar, P. and Murtugudde, R., 2017. Role of oceanic and terrestrial atmospheric moisture sources in intraseasonal variability of Indian summer monsoon rainfall. Scientific reports, 7(1), pp.1-11.

Pénaud, A., Eynaud, F., Sánchez-Goñi, M., Malaizé, B., Turon, J.L. and Rossignol, L., 2011. Contrasting sea-surface responses between the western Mediterranean Sea and eastern subtropical latitudes of the North Atlantic during abrupt climatic events of MIS 3. Marine Micropaleontology, 80(1-2), pp.1-17.

Pepin, N., Bradley, R.S., Diaz, H.F., Baraër, M., Caceres, E.B., Forsythe, N., Fowler, H., Greenwood, G., Hashmi, M.Z., Liu, X.D. and Miller, J.R., 2015. Elevation-dependent warming in mountain regions of the world. Nature climate change, 5(5), pp.424-430.

Peters, K.E., Sweeney, R.E. and Kaplan, I.R., 1978. Correlation of carbon and nitrogen stable isotope ratios in sedimentary organic matter 1. Limnology and Oceanography, 23(4), pp.598-604.

Petersen, N.R.-, Rysgaard, S., Nielsen, L.P., Revsbech, N.P., 1994. Diurnal variation of denitrification and nitrification in sediments colonized by benthic microphytes. Limnology and Oceanography. 39, 573–579. https://doi.org/https://doi.org/10.4319/lo.1994.39.3.0573

Petit, J.R., Jouzel, J., Raynaud, D., Barkov, N.I., Barnola, J.M., Basile, I., Bender, M., Chappellaz, J., Davis, M., Delaygue, G. and Delmotte, M., 1999. Climate and atmospheric history of the past 420,000 years from the Vostok ice core, Antarctica. Nature, 399(6735), pp.429-436.

Phadtare, N.R., 2000. Sharp decrease in summer monsoon strength 4000–3500 cal yr BP in the Central Higher Himalaya of India based on pollen evidence from alpine peat. Quat. Res. 53, 122–129.

Phartiyal, B., Singh, R., Nag, D., Sharma, A., Agnihotri, R., Prasad, V., Yao, T., PingYao, Karthick, B., Joshi, P., Gahlaud, S.K.S., Thakur, B., 2021. Reconstructing climate variability during the last four millennia from trans-Himalaya (Ladakh-Karakoram, India) using multiple proxies. Palaeogeography Palaeoclimatology Palaeoecology. 562, 110142. https://doi.org/https://doi.org/10.1016/j.palaeo.2020.110142

Phillips, W.M., Sloan, V.F., Shroder Jr, J.F., Sharma, P., Clarke, M.L., Rendell, H.M., 2000. Asynchronous glaciation at Nanga Parbat, northwestern Himalaya Mountains, Pakistan. Geology 28, 431–434.

Pierre, K.S., Louis, V.S., Lehnherr, I., Schiff, S.L., Muir, D.C.G., Poulain, A.J., Smol, J.P., Talbot, C., Ma, M., Findlay, D.L. and Findlay, W.J., 2019. Contemporary limnology of the rapidly changing glacierized watershed of the world's largest High Arctic Lake. Scientific reports, 9(1), pp.1-15.

Porat, N., Faerstein, G., Medialdea, A. and Murray, A.S., 2015. Re-examination of common extraction and purification methods of quartz and feldspar for luminescence dating. Ancient TL, *33*(1), pp.22-30.

Prell, W. L. (1984), Covariance patterns of foraminiferal δ^{18}O: An evaluation of Pliocene ice volume changes near 3.2 million years ago, Science, 226, 692–694, doi:10.1126/science.226.4675.692

Prokopenko, A. A., Hinnov, L. A., Williams, D. F., & Kuzmin, M. I. (2006). Orbital forcing of continental climate during the Pleistocene: a complete astronomically tuned climatic record from Lake Baikal, SE Siberia. Quaternary Science Reviews, 25, 3431–3457

Rabassa, J. and Ponce, J.F., 2016. The Heinrich and Dansgaard–Oeschger climatic events during marine isotopic stage 3. In Marine Isotope Stage 3 in Southern South America, 60 ka BP-30 ka BP (pp. 7-21). Springer, Cham.

Rahman, A., Sarkar, S., Kumar, S., 2020. Paleoenvironment of the Central Himalaya during late MIS 3 using stable isotopic compositions of lacustrine organic matter occluded in diatoms and sediments. Quaternary International. 558, 1–9. https://doi.org/https://doi.org/10.1016/j.quaint.2020.08.024

Ramesh, R., Managave, S.R., Yadava, M.G., 2013. Paleoclimate of Peninsular India, in: Climate Change and Island and Coastal Vulnerability. Springer Netherlands, pp. 78–98. https://doi.org/10.1007/978-94-007-6016-5_5

Ramsey, C.B., 2017. Methods for summarizing radiocarbon datasets. Radiocarbon, 59(6), pp.1809-1833.

Ranhotra, P.S., Sharma, J., Bhattacharyya, A., Basavaiah, N., Dutta, K., 2018. Late Pleistocene-Holocene vegetation and climate from the palaeolake sediments, Rukti valley, Kinnaur, Himachal Himalaya. Quaternary International. 479, 79–89.

Rashid, H., England, E., Thompson, L. and Polyak, L., 2011. Late glacial to Holocene Indian summer monsoon variability based upon sediment records taken from the Bay of Bengal. TAO: Terrestrial, Atmospheric and Oceanic Sciences, 22(2), p.2.

Rashid, I., Romshoo, S.A., Chaturvedi, R.K., Ravindranath, N.H., Sukumar, R., Jayaraman, M., Lakshmi, T.V. and Sharma, J., 2015. Projected climate change impacts on vegetation distribution over Kashmir Himalayas. Climatic Change, 132(4), pp.601-613.

Rashid, S.A., Masoodi, A. and Khan, F.A., 2013. Sediment-water interaction at higher altitudes: example from the geochemistry of Wular Lake sediments, Kashmir Valley, northern India. Procedia Earth and Planetary Science, 7, pp.786-789.

Rawat, J.S., Biswas, V., Kumar, M., 2013. Changes in land use/cover using geospatial techniques: A case study of Ramnagar town area, district Nainital, Uttarakhand, India. The Egyptian Journal of Remote Sensing and Space Sciences. 16, 111–117. https://doi.org/https://doi.org/10.1016/j.ejrs.2013.04.002

Rawat, S., Gupta, A.K., Sangode, S.J., Srivastava, P., Nainwal, H.C., 2015. Late Pleistocene–Holocene vegetation and Indian summer monsoon record from the Lahaul, northwest Himalaya, India. Quaternary Science Review. 114, 167–181.

Rawat, V., Rawat, S., Srivastava, P., Negi, P.S., Prakasam, M., Kotlia, B.S., 2021. Middle Holocene Indian summer monsoon variability and its impact on cultural changes in the Indian subcontinent. Quaternary Science Review. 255. https://doi.org/10.1016/j.quascirev.2021.106825

Raza, W., Ahmad, S.M., Lone, M.A., Shen, C.C., Sarma, D.S. and Kumar, A., 2017. Indian summer monsoon variability in southern India during the last deglaciation: Evidence from a high resolution stalagmite $\delta^{18}O$ record. Palaeogeography, Palaeoclimatology, Palaeoecology, 485, pp.476-485.

Reed, D.E., Dugan, H.A., Flannery, A.L., Desai, A.R., 2018. Carbon sink and source dynamics of a eutrophic deep lake using multiple flux observations over multiple years. Limnology and Oceanography Letter. 3, 285–292.

Reichart, G.J., den Dulk, M., Visser, H.J., van der Weijden, C.H. and Zachariasse, W.J., 1997. A 225 kyr record of dust supply, paleoproductivity and the oxygen minimum zone from the Murray Ridge (northern Arabian Sea). Palaeogeography, Palaeoclimatology, Palaeoecology, 134(1-4), pp.149-169.

Richards, B.W.M., Benn, D.I., Owen, L.A., Rhodes, E.J., Spencer, J.Q., 2000. Timing of late Quaternary glaciations south of Mount Everest in the Khumbu Himalaya, Nepal. Geological Society of America Bulletin. 112, 1621–1632.

Richards, B.W.M., Rhodes, E.J., Owen, L.A., 2001. Asynchronous glaciation at Nanga Parbat, northwestern Himalaya Mountains, Pakistan: Comment. Geology 29, 287.

Ricketts, R.D., Johnson, T.C., 2019. Early Holocene changes in lake level and productivity in Lake Malawi as interpreted from oxygen and carbon isotopic measurements of authigenic carbonates, in: The Limnology, Climatology and Paleoclimatology of the East African Lakes. Routledge, pp. 475–493.

Ritchie, J.C. and McHenry, J.R., 1990. Application of radioactive fallout cesium-137 for measuring soil erosion and sediment accumulation rates and patterns: A review. Journal of environmental quality, 19(2), pp.215-233.s

Roberts, K., Granum, E., Leegood, R.C., Raven, J.A., 2007. Carbon acquisition by diatoms. Photosynth. Res. 93, 79–88. https://doi.org/10.1007/s11120-007-9172-2

Ronay, E.R., Breitenbach, S.F.M., Oster, J.L., 2019. Sensitivity of speleothem records in the Indian Summer Monsoon region to dry season infiltration. Sci. Rep. 9, 5091. https://doi.org/10.1038/s41598-019-41630-2

Rühland, K.M., Paterson, A.M., Smol, J.P., 2015. Lake diatom responses to warming: reviewing the evidence. Journal of Paleolimnology. 54, 1–35.

Rysgaard, S., Risgaard-Petersen, N., Niels Peter, S., Kim, J., Lars Peter, N., 1994. Oxygen regulation of nitrification and denitrification in sediments. Limnology and Oceanography. 39, 1643–1652. https://doi.org/https://doi.org/10.4319/lo.1994.39.7.1643

Sage, R.F., Wedin, D.A. and Li, M., 1999. The biogeography of C4 photosynthesis: patterns and controlling factors. C4 plant biology, 10, pp.313-376.

Sanwal, J., Rajendran, C.P., Sheshshayee, M.S., 2019. Reconstruction of late Quaternary climate from a Paleo-lacustrine profile in the Central (Kumaun) Himalaya: Viewing the results in a regional context. Frontier in Earth Sciences. 7, 2.

Schelske, C.L. and Hodell, D.A., 1995. Using carbon isotopes of bulk sedimentary organic matter to reconstruct the history of nutrient loading and eutrophication in Lake Erie. Limnology and Oceanography, 40(5), pp.918-929.

Schilman, B., Bar-Matthews, M., Almogi-Labin, A., Luz, B., 2001. Global climate instability re£ected by Eastern Mediterranean marine records during the late Holocene.

Schrag, D.P., Higgins, J.A., Macdonald, F.A., Johnston, D.T., 2013. Authigenic Carbonate and the History of the Global Carbon Cycle.

Schulze, E.D., Ellis, R., Schulze, W., Trimborn, P. and Ziegler, H., 1996. Diversity, metabolic types and $\delta^{13}C$ carbon isotope ratios in the grass flora of Namibia in relation to growth form, precipitation and habitat conditions. Oecologia, 106(3), pp.352-369.

Schwalb, A., 2003. Lacustrine ostracodes as stable isotope recorders of late-glacial and Holocene environmental dynamics and climate. Journal of Paleolimnology. 29, 265–351.

Scott, K.M., Schwedock, J., Schrag, D.P., Cavanaugh, C.M., 2004. Influence of form IA RubisCO and environmental dissolved inorganic carbon on the $\delta^{13}C$ of the clam-chemoautotroph symbiosis Solemya velum. Environ. Microbiol. 6, 1210–1219.

Shah, J.A., Pandit, A.K., 2013. Diversity and Abundance of Cladoceran Zooplankton in Wular Lake, Kashmir Himalaya. Res. J. Environ. Earth Sci. 5, 410–417. https://doi.org/10.19026/rjees.5.5668

Shah, R.A., Achyuthan, H., Lone, A., Kumar, P., Ali, A., Rahman, A., 2020. Palaeoenvironment shifts during last ~500 years and eutrophic evolution of the Wular Lake, Kashmir Valley, India. Limnology. https://doi.org/10.1007/s10201-020-00639-7

Shah, R.A., Achyuthan, H., Lone, A.M., Jaiswal, M.K., Paul, D., 2021. Constraining the timing and deposition pattern of loess-palaeosol sequences in Kashmir Valley, Western Himalaya: Implications to paleoenvironment studies. Aeolian Res. 49, 100660.

Sharif, M., Archer, D.R., Fowler, H.J., Forsythe, N., 2013. Trends in timing and magnitude of flow in the Upper Indus Basin. Hydrology and Earth System Sciences. https://doi.org/10.5194/hess-17-1503-2013

Sharma, S., Chand, P., Bisht, P., Shukla, A.D., Bartarya, S.K., Sundriyal, Y.P., Juyal, N., 2016. Factors responsible for driving the glaciation in the Sarchu Plain, eastern Zanskar Himalaya, during the late Quaternary. Journal of Quaternary Science. 31, 495–511. https://doi.org/https://doi.org/10.1002/jqs.2874

Sharma, S., Pant, H., 2017. Vulnerability of Indian Central Himalayan forests to fire in a warming climate and a participatory preparedness approach based on modern tools. Current Science. 112, 2100–2105. https://doi.org/10.18520/cs/v112/i10/2100-2105

Shatwell, T., Köhler, J., 2019. Decreased nitrogen loading controls summer cyanobacterial blooms without promoting nitrogen-fixing taxa: Long-term response of a shallow lake. Limnology and Oceanography. 64, S166–S178. https://doi.org/https://doi.org/10.1002/lno.11002

Shekhar, M.S., Chand, H., Kumar, S., Srinivasan, K. and Ganju, A., 2010. Climate-change studies in the western Himalaya. Annals of Glaciology, 51(54), pp.105-112.

Shemesh, A., Burckle, L.H., Hays, J.D., 1995. Late Pleistocene oxygen isotope records of biogenic silica from the Atlantic sector of the Southern Ocean. Paleoceanography 10, 179–196. https://doi.org/10.1029/94PA03060

Shukla, A., Garg, P.K., Srivastava, S., 2018. Evolution of glacial and high-altitude lakes in the Sikkim, Eastern Himalaya over the past four decades (1975–2017). Front. Environ. Sci. 6, 81.

Simms, M.J., 2002. The origin of enigmatic, tubular, lake-shore karren: A mechanism for rapid dissolution of limestone in carbonate-saturated waters. Phys. Geogr. 23, 1–20.

Singer, A.J., Shemesh, A., 1995. Climatically linked carbon isotope variation during the past 430,000 years in Southern Ocean sediments. Paleoceanography 10, 171–177.

Singh, I.B., Sharma, S., Sharma, M., Srivastava, P. and Rajagopalan, G., 1999. Evidence of human occupation and humid climate of 30 ka in the alluvium of southern Ganga Plain. Current Science, pp.1022-1026.

Singhvi, A.K., Bluszcz, A., Bateman, M.D. and Rao, M.S., 2001. Luminescence dating of loess–palaeosol sequences and coversands: methodological aspects and palaeoclimatic implications. Earth-Science Reviews, 54(1-3), pp.193-211.

Sinha, A., Cannariato, K.G., Stott, L.D., Cheng, H., Edwards, R.L., Yadava, M.G., Ramesh, R. and Singh, I.B., 2007. A 900-year (600 to 1500 AD) record of the Indian summer monsoon precipitation from the core monsoon zone of India. Geophysical Research Letters, 34(16).

Small, G.E., Bullerjahn, G.S., Sterner, R.W., Beall, B.F.N., Brovold, S., Finlay, J.C., McKay, R.M.L., Mukherjee, M., 2013. Rates and controls of nitrification in a large oligotrophic lake. Limnology and Oceanography. 58, 276–286. https://doi.org/https://doi.org/10.4319/lo.2013.58.1.0276

Somayajulu, B.L.K., Bhushan, R., Sarkar, A., Burr, G.S., Jull, A.J.T., 1999. Sediment deposition rates on the continental margins of the eastern Arabian Sea using 210 Pb, 137 Cs and 14 C, The Science of the Total Environment.

Srivastava, R.N. and Ahmad, A., 1979. Geology and structure of Alaknanda valley, Garhwal Himalaya.

Steffen, W., Persson, Å., Deutsch, L., Zalasiewicz, J., Williams, M., Richardson, K., Crumley, C., Crutzen, P., Folke, C., Gordon, L., Molina, M., Ramanathan, V., Rockström, J., Scheffer, M., Schellnhuber, H.J., Svedin, U., 2011. The Anthropocene: From Global Change to Planetary Stewardship. Ambio 40, 739. https://doi.org/10.1007/s13280-011-0185-x

Steinsberger, T., Wüest, A., Müller, B., 2021. Net ecosystem production of lakes estimated from hypolimnetic organic carbon sinks. Water Resour. Res. e2020WR029473.

Strauss, E.A., Lamberti, G.A., 2000. Regulation of nitrification in aquatic sediments by organic carbon. Limnology and Oceanography. 45, 1854–1859. https://doi.org/10.4319/lo.2000.45.8.1854

Sugimoto, R., Sato, T., Yoshida, T., Tominaga, O., 2014. Using stable nitrogen isotopes to evaluate the relative importance of external and internal nitrogen loadings on phytoplankton production in a shallow eutrophic lake (Lake Mikata, Japan). Limnology and Oceanography. 59, 37–47. https://doi.org/https://doi.org/10.4319/lo.2014.59.1.0037

Sun, Z., Yuan, K., Hou, X., Ji, K., Li, C.-G., Wang, M., Hou, J., 2020. Centennial-scale interplay between the Indian Summer Monsoon and the Westerlies revealed from Ngamring Co, southern Tibetan Plateau. The Holocene 30, 1163–1173. https://doi.org/10.1177/0959683620913930

Svensson, A., Biscaye, P. E., & Grousset, F. E., (2000). Characterization of late glacial continental dust in the Greenland Ice Core Project ice core. Journal of Geophysical Research: Atmosphere, 105(D4), 4637–4656

Syed, F.S., Giorgi, F., Pal, J.S. and Keay, K., 2010. Regional climate model simulation of winter climate over Central–Southwest Asia, with emphasis on NAO and ENSO effects. International Journal of Climatology: A Journal of the Royal Meteorological Society, 30(2), pp.220-235.

Talbot, M.R., 2002. Nitrogen isotopes in palaeolimnology. In Tracking environmental change using lake sediments (pp. 401-439). Springer, Dordrecht.

Talbot, M.R., Kelts, K., 1990. Paleolimnological signatures from carbon and oxygen isotopic ratios in carbonates, from organic carbon-rich lacustrine sediments: chapter 6.

Tandon, S.K., Sareen, B.K., Rao, M.S. and Singhvi, A.K., 1997. Aggradation history and luminescence chronology of Late Quaternary semi-arid sequences of the Sabarmati basin, Gujarat, western India. Palaeogeography, Palaeoclimatology, Palaeoecology, 128(1-4), pp.339-357.

Thakur, V.C., 1998. Structure of the Chamba nappe and position of the Main Central Thrust in Kashmir Himalaya. *Journal of Asian Earth Sciences*, *16*(2-3), pp.269-282.

Thompson, L.G. o, Yao, T., Davis, M.E., Henderson, K.A., Mosley-Thompson, E., Lin, P.-N., Beer, J., Synal, H.-A., Cole-Dai, J., Bolzan, J.F., 1997. Tropical climate instability: The last glacial cycle from a Qinghai-Tibetan ice core. Science (80-.). 276, 1821–1825.

Thornton, P.E., Lamarque, J., Rosenbloom, N.A., Mahowald, N.M., 2007. Influence of carbon-nitrogen cycle coupling on land model response to CO_2 fertilization and climate variability. Global Biogeochem. Cycles 21.

Tiwari, P.C., Tiwari, A. and Joshi, B., 2018. Urban growth in Himalaya: understanding the process and options for sustainable development. J. Urban. Reg. Stud. on Cont. India, 4(2), pp.15-27.

Tortell, P.D., Reinfelder, J.R., Morel, F.M.M., 1997. Active uptake of bicarbonate by diatoms. Nature 390, 243.

Tranvik, L.J., Downing, J.A., Cotner, J.B., Loiselle, S.A., Striegl, R.G., Ballatore, T.J., Dillon, P., Finlay, K., Fortino, K., Knoll, L.B. and Kortelainen, P.L., 2009. Lakes and reservoirs as regulators of carbon cycling and climate. Limnol. and oceangr., 54(6part2), pp.2298-2314.

Valdiya, K.S., 1981. Tectonics of the Central Sector of the Himalaya. Zagros Hindu Kush Himalaya Geodynamics Evolution., Geodynamics Series. https://doi.org/doi:10.1029/GD003p0087

Valdiya, K.S., 1998. Dynamic Himalaya. Universities press.

Valdiya, K.S., 2002. Emergence and evolution of Himalaya: reconstructing history in the light of recent studies. Progress in Physical Geography: Earth and Environment. 26, 360–399. https://doi.org/10.1191/0309133302pp342ra

Valero-Garcés, B.L., Laird, K.R., Fritz, S.C., Kelts, K., Ito, E., Grimm, E.C., 1997. Holocene climate in the Northern Great Plains inferred from sediment stratigraphy, stable isotopes, carbonate geochemistry, diatoms, and pollen at Moon Lake, North Dakota. Quaternary Research. 48, 359–369.

Van Meerbeeck, C.J., Renssen, H. and Roche, D.M., 2009. How did Marine Isotope Stage 3 and Last Glacial Maximum climates differ? perspectives from equilibrium simulations. Climate of the Past, 5(1), pp.33-51.

Vass, K.K. 1973. Studies on hydrobiology and primary productivity of some Kashmir lakes. Ph.D. Thesis, University of Kashmir

Ventelä, A.M., Saarikari, V. and Vuorio, K., 1998. Vertical and seasonal distributions of micro-organisms, zooplankton and phytoplankton in a eutrophic lake. In

Eutrophication in Planktonic Ecosystems: Food Web Dynamics and Elemental Cycling (pp. 229-240). Springer, Dordrecht.

Verpoorter, C., Kutser, T., Seekell, D.A. and Tranvik, L.J., 2014. A global inventory of lakes based on high-resolution satellite imagery. Geophysical Research Letters, 41(18), pp.6396-6402.

Vinebrooke, R.D. and Leavitt, P.R., 1996. Effects of ultraviolet radiation on periphyton in an alpine lake. Limnology and Oceanography, 41(5), pp.1035-1040.

Voβ, M., Struck, U., 1997. Stable nitrogen and carbon isotopes as indicator of eutrophication of the Oder River (Baltic Sea). Mar. Chem. 59, 35–49. https://doi.org/https://doi.org/10.1016/S0304-4203(97)00073-X

Wadia D N 1975 Geology of India, 4th edn. (New Delhi: Tata McGraw Hill).

Wagner, S., Brandes, J., Spencer, R.G.M., Ma, K., Rosengard, S.Z., Moura, J.M.S., Stubbins, A., 2019. Isotopic composition of oceanic dissolved black carbon reveals non-riverine source. Nature Communication. 10, 1–8. https://doi.org/10.1038/s41467-019-13111-7

Wagner, S., Jaffé, R., Stubbins, A., 2018. Dissolved black carbon in aquatic ecosystems. Limnology and Oceanography. Lett. 3, 168–185.

Walter, B.P., Heimann, M., 2000. A process-based, climate-sensitive model to derive methane emissions from natural wetlands: Application to five wetland sites, sensitivity to model parameters, and climate. Global Biogeochem. Cycles 14, 745–765.

Wang, S., Yeager, K.M., Lu, W., 2016. Carbon isotope fractionation in phytoplankton as a potential proxy for pH rather than for [CO 2 (aq)]: Observations from a carbonate lake. Limnology and Oceanography. 61, 1259–1270. https://doi.org/10.1002/lno.10289

Wang, S., Yeager, K.M., Wan, G., Liu, C., Wang, Y., Lü, Y., 2012. Carbon export and HCO3-fate in carbonate catchments: A case study in the karst plateau of southwestern China. Applied Geochemistry 27, 64–72.

Wang, X., Cui, L., Xiao, J., Ding, Z., 2013. Stable carbon isotope of black carbon in lake sediments as an indicator of terrestrial environmental changes: An evaluation on paleorecord from Daihai Lake, Inner Mongolia, China. Chem. Geol. 347, 123–134. https://doi.org/10.1016/j.chemgeo.2013.03.009

Watanabe, T., Naraoka, H., Nishimura, M., Kawai, T., 2004. Biological and environmental changes in Lake Baikal during the late Quaternary inferred from carbon, nitrogen and sulfur isotopes. Earth Planet. Sci. Lett. 222, 285–299. https://doi.org/10.1016/j.epsl.2004.02.009

Webb, M., Barker, P.A., Wynn, P.M., Heiri, O., Hardenbroek, M.V.A.N., Pick, F., Russell, J.M., Stott, A.W., Leng, M.J., 2016. Interpretation and application of carbon isotope ratios in freshwater diatom silica 31, 300–309. https://doi.org/10.1002/jqs.2837

Weber, M.E., Lantzsch, H., Dekens, P., Das, S.K., Reilly, B.T., Martos, Y.M., Meyer-Jacob, C., Agrahari, S., Ekblad, A., Titschack, J. and Holmes, B., 2018. 200,000 years of monsoonal history recorded on the lower Bengal Fan-strong response to insolation forcing. Global and Planetary Change, 166, pp.107-119.

Wilkes, E.B., Pearson, A., 2019. A general model for carbon isotopes in red-lineage phytoplankton: Interplay between unidirectional processes and fractionation by RubisCO. Geochimica et Cosmochimica Acta 265, 163–181.

Winiger, P., Andersson, A., Yttri, K.E., Tunved, P., Gustafsson, Ö., 2015. Isotope-Based Source Apportionment of EC Aerosol Particles during Winter High-Pollution Events at the Zeppelin Observatory, Svalbard. Environmental Science and Technology. 49, 11959–11966. https://doi.org/10.1021/acs.est.5b02644

Winiger, P., Barrett, T.E., Sheesley, R.J., Huang, L., Sharma, S., Barrie, L.A., Yttri, K.E., Evangeliou, N., Eckhardt, S., Stohl, A., Klimont, Z., Heyes, C., Semiletov, I.P., Dudarev, O. V, Charkin, A., Shakhova, N., Holmstrand, H., Andersson, A., Gustafsson, Ö., 2019. Source apportionment of circum-Arctic atmospheric black carbon from isotopes and modeling.

Wintle, A.G., 1997. Luminescence dating: laboratory procedures and protocols. Radiation measurements, *27*(5-6), pp.769-817.

Wolff, C., Plessen, B., Dudashvilli, A.S., Breitenbach, S.F.M., Cheng, H., Edwards, L.R., Strecker, M.R., 2017. Precipitation evolution of Central Asia during the last 5000 years. Holocene 27, 142–154. https://doi.org/10.1177/0959683616652711

Woolway, R.I., Weyhenmeyer, G.A., Schmid, M., Dokulil, M.T., de Eyto, E., Maberly, S.C., May, L. and Merchant, C.J., 2019. Substantial increase in minimum lake surface temperatures under climate change. Climatic Change, 155(1), pp.81-94.

Wright, J.D., 2000. Global climate change in marine stable isotope records. In Quaternary geochronology: Methods and applications (pp. 671-682). American Geophysical Union.

Wu, D., Chen, X., Lv, F., Brenner, M., Curtis, J., Zhou, A., Chen, J., Abbott, M., Yu, J., Chen, F., 2018. Decoupled early Holocene summer temperature and monsoon precipitation in southwest China. Quaternary Science Review. https://doi.org/10.1016/j.quascirev.2018.05.038

Wu, G., Liu, Y., Zhang, Q., Duan, A., Wang, T., Wan, R., Liu, X., Li, W., Wang, Z. and Liang, X., 2007. The influence of mechanical and thermal forcing by the Tibetan Plateau on Asian climate. Journal of Hydrometeorology, 8(4), pp.770-789.

Wünnemann, B., Demske, D., Tarasov, P., Kotlia, B.S., Reinhardt, C., Bloemendal, J., Diekmann, B., Hartmann, K., Krois, J., Riedel, F. and Arya, N., 2010. Hydrological evolution during the last 15 kyr in the Tso Kar lake basin (Ladakh, India), derived from geomorphological, sedimentological and palynological records. Quaternary Science Reviews, 29(9-10), pp.1138-1155.

Wünnemann, B., Hartmann, K., Janssen, M. and Hucai, C.Z., 2007. Responses of Chinese desert lakes to climate instability during the past 45,000 years. Developments in Quaternary Sciences, 9, pp.11-24.

Wünnemann, B., Mischke, S. and Chen, F., 2006. A Holocene sedimentary record from Bosten lake, China. Palaeogeography, Palaeoclimatology, Palaeoecology, 234(2-4), pp.223-238.

Wurtsbaugh, W.A., Vincent, W., Alfaro, R., Vincent, C. and Richerson, P., 1985. Nutrient limitation of algal growth and nitrogen fixation in a tropical alpine lake, Lake Titicaca (Peru/Bolivia). Freshwater Biology, 15(2), p.185.

Xu, B., Cao, J., Hansen, J., Yao, T., Joswia, D.R., Wang, N., Wu, G., Wang, M., Zhao, H., Yang, W., Liu, X., He, J., 2009. Black soot and the survival of Tibetan glaciers. Proceedings of the National Academy of Sciences of the United States of America. 106, 22114–22118. https://doi.org/10.1073/pnas.0910444106

Yanai, M., Li, C., Song, Z., 1992. Seasonal heating of the Tibetan Plateau and its effects on the evolution of the Asian summer monsoon. Journal of the Meteorological Society of Japan Ser. II 70, 319–351.

Yang, B., Shi, Y., Braeuning, A. and Wang, J., 2004. Evidence for a warm-humid climate in arid northwestern China during 40–30 ka BP. Quaternary Science Reviews, 23(23-24), pp.2537-2548.

Yang, X., Ma, N., Dong, J., Zhu, B., Xu, B., Ma, Z. and Liu, J., 2010. Recharge to the inter-dune lakes and Holocene climatic changes in the Badain Jaran Desert, western China. Quaternary Research, 73(1), pp.10-19.

Yang, X., Preusser, F. and Radtke, U., 2006. Late Quaternary environmental changes in the Taklamakan Desert, western China, inferred from OSL-dated lacustrine and aeolian deposits. Quaternary Science Reviews, 25(9-10), pp.923-932.

Yang, X., Scuderi, L., Paillou, P., Liu, Z., Li, H. and Ren, X., 2011. Quaternary environmental changes in the drylands of China–a critical review. Quaternary Science Reviews, 30(23-24), pp.3219-3233.

Yu, Z., Colin, C., Wan, S., Saraswat, R., Song, L., Xu, Z., Clift, P., Lu, H., Lyle, M., Kulhanek, D. and Hahn, A., 2019. Sea level-controlled sediment transport to the eastern Arabian Sea over the past 600 kyr: Clay minerals and SrNd isotopic evidence from IODP Site U1457. Quaternary Science Reviews, 205, pp.22-34.

Zachos, J., Pagani, M., Sloan, L., Thomas, E., Billups, K., 2001. Trends, rhythms, and aberrations in global climate 65 Ma to present. Science (80-.). 292, 686–693.

Zachos, J.C., Dickens, G.R., Zeebe, R.E., 2008. An early Cenozoic perspective on greenhouse warming and carbon-cycle dynamics. Nature 451, 279–283.

Zanchetta, G., Borghini, A., Fallick, A.E., Bonadonna, F.P., Leone, G., 2007. Late Quaternary palaeohydrology of Lake Pergusa (Sicily, southern Italy) as inferred by stable isotopes of lacustrine carbonates. Journal of Paleolimnology. 38, 227–239.

Zapata F (2002) Handbook for the Assessment of Soil Erosion and Sedimentation Using Environmental Radionuclides. Vienna: Kluwer Academic Publisher. pp 56-62

Zaz, N. S., Romshoo, S.A., Thokuluwa Krishnamoorthy, R., Viswanadhapalli, Y., 2019. Analyses of temperature and precipitation in the Indian Jammu and Kashmir region for the 1980-2016 period: implications for remote influence and extreme events. Atmos. Chem. Phys 19, 15–37. https://doi.org/10.5194/acp-19-15-2019

Zech, R., Zech, M., Kubik, P.W., Kharki, K., Zech, W., 2009. Deglaciation and landscape history around Annapurna, Nepal, based on 10Be surface exposure dating. Quaternary Science Review. 28, 1106–1118.

Zhang, H.C., Fan, H.F., Chang, F.Q., Zhang, W.X., Lei, G.L., Yang, M.S., Lei, Y.B. and Yang, L.Q., 2008. AMS dating on the shell bar section from Qaidam Basin, NE Tibetan Plateau, China. Radiocarbon, 50(2), pp.255-265.

Zhang, H.C., Peng, J.L., Ma, Y.Z., Chen, G.J., Feng, Z.D., Li, B., Fan, H.F., Chang, F.Q., Lei, G.L. and Wünnemann, B., 2004. Late quaternary palaeolake levels in Tengger Desert, NW China. Palaeogeography, Palaeoclimatology, Palaeoecology, 211(1-2), pp.45-58.

Zhang, M. and Liu, X., 2020. Climate changes in the Qaidam Basin in NW China over the past 40 kyr. Palaeogeography, Palaeoclimatology, Palaeoecology, 551, p.109679.

Zielhofer, C., Köhler, A., Mischke, S., Benkaddour, A., Mikdad, A., Fletcher, W.J., 2019. Western Mediterranean hydro-climatic consequences of Holocene ice-rafted debris (Bond) events. Climate of the Past 15, 463–475. https://doi.org/10.5194/cp-15-463-2019

List of Publications

Published

1. **Rahman, A**., Sarkar, S., & Kumar, S. (2020). Paleoenvironment of the central Himalaya during late MIS 3 using stable isotopic compositions of lacustrine organic matter occluded in diatoms and sediments. Quaternary International, 558,1-9. (https://doi.org/10.1016/j.quaint.2020.08.024)

2. **Rahman, A**., Khan, M. A., Singh, A., Kumar, S. (2021) Hydrological characteristics of the Bay of Bengal water column using $\delta^{18}O$ during the Indian summer monsoon. Coastal shelf research, (https://doi.org/10.1016/j.csr.2021.104491)

3. **Rahman, A**., Rathi, A., Nambiar, R., Mishra, P.K., Anoop, A., Bhushan, R. and Kumar, S., 2021. Signatures of natural to anthropogenic transition in lake sediments from the Central Himalaya using stable isotopes. Applied Geochemistry, *134*, p.105095. (https://doi.org/10.1016/j.apgeochem.2021.105095)

4. Sahoo, D., Saxena, H., Tripathi, N., Khan, M. A., **Rahman, A**., Kumar, S., Sudheer A.K., & Singh, A. (2020). Non-Redfieldian C: N: P ratio in the inorganic and organic pools of the Bay of Bengal during the summer monsoon. Marine Ecology Progress Series, 653, 41-55. (https://doi.org/10.3354/meps13498)

5. Shah, R. A., Achyuthan, H., Lone, A., Kumar, P., Ali, A., & **Rahman, A**. (2020). Palaeoenvironment shifts during last~ 500 years and eutrophic evolution of the Wular Lake, Kashmir Valley, India. Limnology, 1-10. (https://doi.org/10.1007/s10201-020-00639-7)

6. Khan, M.A., Rahman, A., Sahoo, D., Saxena, H., Singh, A. and Kumar, S., 2022. Nitrous oxide in the central Bay of Bengal during the summer monsoon. Regional Studies in Marine Science, p.102314. (https://doi.org/10.1016/j.rsma.2022.102314)

Under review

1. P. Ragavan; **Abdur Rahman**; Siddhartha Sarkar; Sangeeta Verma; C. Jeeva; P.M. Mohan, Sanjeev Kumar. Variability in soil organic carbon stock and isotopic signature in a tropical island mangrove forests of India (Under review in Regional Environmental Change)

2. Siddhartha Sarkar; Mohammad Atif Khan; Niharika Sharma; **Abdur Rahman**; Ravi Bhushan; A K Sudheer; Sanjeev Kumar. Lake Desiccation drives carbon and nitrogen biogeochemistry of a sub-tropical hypersaline lake (Under review in Hydrobiologia)

3. Rayees Ahmad Shah, Imran Khan, **Abdur Rahman**, Sanjeev Kumar, Hema Achyuthan, Anil D. Shukla, Pankaj Kumar, Chinmay Dash, Holocene climate events and associated land use changes in the eastern coast of India: inferences from the Chilika Lagoon (Under review in The Holocene)

4. Diptimayee Behera; Sharmila Bhattacharya; **Abdur Rahman**; Sanjeev Kumar; Ambili Anoop. Molecular tracers for characterization and distribution of organic matter in a freshwater lake system from the Lesser Himalaya (Submitted in Biogeochemistry)

5. **Abdur Rahman**, Rayees Ahmad Shah, Madhusudan G. Yadava, Sanjeev Kumar. Reconstruction of the late Holocene environment of the Kashmir Valley using stable isotopes in lake sediments (Submitted in Quaternary Research)

Presentations in Conference/Symposium

1. Poster presentation on Diatom oxygen isotopes: A potential tool for paleoclimate reconstruction in workshop on "Quantitative Reconstruction and Numerical Methods for Analysis of Past Climate Variability Using Diatoms" in NCAOR Goa (24.11.2017).

2. Rahman, A., Sarkar, S. and Kumar, S., 2020, December. Paleo-biogeochemistry of the central Himalayan region during late MIS 3 using stable isotopic composition of organic matter occluded in diatoms and lake sediments. In AGU Fall Meeting 2020. AGU (11 December 2020).

Publication attached with this thesis

1. **Rahman, A**., Sarkar, S., & Kumar, S., (2020). Paleoenvironment of the central Himalaya during late MIS 3 using stable isotopic compositions of lacustrine organic matter occluded in diatoms and sediments. Quaternary International, 558,1-9. (https://doi.org/10.1016/j.quaint.2020.08.024)

2. **Rahman, A**., Rathi, A., Nambiar, R., Mishra, P.K., Anoop, A., Bhushan, R. and Kumar, S., 2021. Signatures of natural to anthropogenic transition in lake sediments from the Central Himalaya using stable isotopes. Applied Geochemistry, *134*,   p.105095. (https://doi.org/10.1016/j.apgeochem.2021.105095)